AD A045679

AD

12

Technical Memorandum 25-77

DEVELOPMENT OF ADVANCED CONCEPTS FOR NOISE REDUCTION IN TRACKED VEHICLES

Thomas R. Norris
Anthony G. Galaitsis
Bolt, Beranek, and Newman, Inc.

Ronald B. Hare
FMC Corporation

Georges R. Garinther

DDC
OCT 26 1977
C

August 1977
AMCMS Code 672716.11.H7000

Approved for public release;
distribution unlimited.

AD No.
DDC FILE COPY

U. S. ARMY HUMAN ENGINEERING LABORATORY
Aberdeen Proving Ground, Maryland

Destroy this report when no longer needed.
Do not return it to the originator.

The findings in this report are not to be construed as an official Department of the Army position unless so designated by other authorized documents.

Use of trade names in this report does not constitute an official endorsement or approval of the use of such commercial products.

(18) HEL (11) TM-25-77

Unclassified

SECURITY CLASSIFICATION OF THIS PAGE (When Data Entered)

REPORT DOCUMENTATION PAGE

READ INSTRUCTIONS BEFORE COMPLETING FORM

1. REPORT NUMBER
Technical Memorandum 25-77

2. GOVT ACCESSION NO.

3. RECIPIENT'S CATALOG NUMBER

4. TITLE (and Subtitle)
(6) DEVELOPMENT OF ADVANCED CONCEPTS FOR NOISE REDUCTION IN TRACKED VEHICLES.

5. TYPE OF REPORT & PERIOD COVERED
(9) Final Report.

6. PERFORMING ORG. REPORT NUMBER
(14) FMC TR-3162

7. AUTHOR(s)
(10) Thomas R. Norris, Ronald B. Hare, Anthony G. Galaitsis, and Georges R. Garinther

8. CONTRACT OR GRANT NUMBER(s)
(15) DAAD05-76-C-0748

9. PERFORMING ORGANIZATION NAME AND ADDRESS
FMC Corporation, Ordnance Engineering Division,
1105 Coleman Ave, San Jose, CA 95108

10. PROGRAM ELEMENT, PROJECT, TASK AREA & WORK UNIT NUMBERS
AMCMS Code 672716.11.H7000

11. CONTROLLING OFFICE NAME AND ADDRESS
(11) U.S. Army Human Engineering Laboratory
Aberdeen Proving Ground, Maryland 21005

12. REPORT DATE
August 1977

13. NUMBER OF PAGES
~~79~~ 12 81 p.

14. MONITORING AGENCY NAME & ADDRESS (if different from Controlling Office)

15. SECURITY CLASS. (of this report)
Unclassified

15a. DECLASSIFICATION/DOWNGRADING SCHEDULE

16. DISTRIBUTION STATEMENT (of this Report)
Approved for public release; distribution unlimited.

17. DISTRIBUTION STATEMENT (of the abstract entered in Block 20, if different from Report)

18. SUPPLEMENTARY NOTES

19. KEY WORDS (Continue on reverse side if necessary and identify by block number)
Tracked vehicles
Noise reduction
Mechanical impedance measurement
Noise sources
Track and suspension

20. ABSTRACT (Continue on reverse side if necessary and identify by block number)

This investigation develops an understanding of the noise sources, the acoustical and vibratory paths through which energy enters the hull structure, and the mechanism by which noise arrives at personnel locations. A theoretical and experimental analysis of primary noise source of the vehicle, i.e. the track and suspension system, consisted of three phases:

(1) The design of a computer program to simulate the track and suspension;
(2) The isolation of the noise produced by the sprocket, idler and roadwheels to determine the contribution of each of these sources.

(cont'd on cover p. 14135)

DD FORM 1 JAN 73 1473 EDITION OF 1 NOV 65 IS OBSOLETE

Unclassified

SECURITY CLASSIFICATION OF THIS PAGE (When Data Entered)

402 012

(3) The measurement of vibration levels at the suspension system, and force-to-noise transfer functions for predicting interior noise levels.

This study indicates that at speeds above 10 mph the engine is not a major contributor to noise, and the roadwheels produce significantly less noise than the sprocket and idler. The study results indicate that the greatest potential for noise reduction lies in providing a softer compliance between the idler and the track. This should be followed by lowering the stiffness of the sprocket and finally by controlling roadwheel noise. The idler stiffness can be lowered either at the hub or at the rim, however rim compliance poses fewer design problems

ACCESSION for
NTIS
DDC
UNANNOUNCED
JUSTIFICATION
BY
DISTRIBUTION/AVAILABILITY CODES
Dist. AVAIL. and/or SPECIAL
A1

AMCMS Code 672716.11.H7000 Technical Memorandum 25-77

DEVELOPMENT OF ADVANCED CONCEPTS FOR NOISE REDUCTION IN TRACKED VEHICLES

Thomas R. Norris
Anthony G. Galaitsis
Bolt, Beranek, and Newman, Inc.

Ronald B. Hare
FMC Corporation

Georges R. Garinther

August 1977

APPROVED: _____
JOHN D. WEISZ
Director
U. S. Army Human Engineering Laboratory

U. S. ARMY HUMAN ENGINEERING LABORATORY
Aberdeen Proving Ground, Maryland 21005

Approved for public release;
distribution unlimited.

TABLE OF CONTENTS

	Page
INTRODUCTION	3
Objectives and Goals	3
General Discussion of Tracked Vehicle Interior Noise	3
Technical Approach	7
Summary of Results and Conclusions	7
EVALUATION OF NOISE SOURCE CONTRIBUTIONS	14
Test Vehicle	14
Data Acquisition for Suspension Noise and Vibration	15
Data Presentation	17
Noise Characteristics of Production M113A1	18
Idler Noise Contribution	19
Sprocket Noise Contribution	23
Roadwheel Noise Contribution	25
Analysis of High Speed Movies	30
IMPEDANCE AND TRANSFER FUNCTION MEASUREMENTS	32
Purpose of Hull Measurements	32
Measurements of Impedances and Transfer Functions	32
Results of Impedance and Transfer Function Measurements	34
NOISE REDUCTION ESTIMATES OF COMPLIANT IDLER RIMS AND HUBS	39
Background	39
Estimation of Noise Reductions	40
Conclusions Based on Noise Reduction Estimates	44
APPENDIX A LIST OF INSTRUMENTATION AND DATA DEVELOPED	45
APPENDIX B ANALYSIS OF ISOLATION EFFECTIVENESSES OF COMPLIANT RIMS AND HUBS	49
APPENDIX C TRACK SHOE IMPACT NOISE ANALYSIS	53

LIST OF ILLUSTRATIONS

Figure	*Page*
1 Sources and Paths Responsible for Interior Noise in Tracked Vehicles	4
2 Chordal Action	6
3 Speed Dependence of Track System Noise Sources at Crew Position	8
4 Crew Area Track System Noise Sources Compared at Various Speeds	9
5 Noise Source Spectra at 15 MPH at Center of Crew Compartment	10
6 Noise Source Spectra at 25 MPH at Center of Crew Compartment	11
7 Noise Source Spectra at 32 MPH at Center of Crew Compartment	11
8 Noise Source Spectra at 15 MPH at Driver's Position	12
9 Noise Source Spectra at 25 MPH at Driver's Position	12
10 Noise Source Spectra at 32 MPH at Driver's Position	13

LIST OF ILLUSTRATIONS (Continued)

Figure *Page*

11 Comparison of Idler and Sprocket Interior Noise Spectra at Driver's Position and In Crew Area at 32 MPH 13
12 Test Vehicle Towed by LVTP7 15
13 Microphone Locations for Measurements of Interior Noise 16
14 Accelerometer Locations for Roadarm Vibration Measurements 16
15 Idler and Sprocket Noise Test Stand 17
16 Speed Dependence of Production M113A1 Noise at the Crew Position 18
17 Speed Dependence of Production M113A1 Noise at the Driver Position 19
18 Idler Noise Test Set-Up 20
19 Speed Dependence of M113A1 Right Idler-Induced Noise at the Crew Position 21
20 Speed Dependence of M113A1 Right Idler-Induced Noise at the Driver Position 21
21 Right Idler-Induced Noise Spectra at 30 MPH for Two Values of Static Track Tension at the Crew Position 22
22 Right Idler Housing Vibration Spectra at 30 MPH with 2000 LBS Static Track Tension 22
23 Sprocket Noise Test Set-Up 23
24 Speed Dependence of M113A1 Left Sprocket-Induced Noise at the Crew Position 24
25 Speed Dependence of M113A1 Left Sprocket-Induced Noise at the Driver Position 24
26 Speed Dependence of Production M113A1 Vibration During Normal Operation 25
27 Vehicle in Roadwheels Only Configuration 26
28 Differences Between Roadarm Vibration During Normal and Roadwheel-Only Vehicle Operation 26
29 Roadarm Spindle Vibration at 20 MPH on Production M113A1 27
30 Speed Dependence of Roadwheel-Induced Noise at Crew Position 28
31 Speed Dependence of Roadwheel-Induced Noise at Driver Position 28
32 Crew Noise Caused by Track Guide Scrub at 25 MPH 29
33 Effects of Guide-Idler Contact on Track Engagement 31
34 Typical Shaker, Force Transducer, and Accelerometer Setup for Impedance and Transfer Function Measurement 33
35 Crew Area Force-to-Noise Transfer Function at Left Idler Wheel Rim with Tracks in Place 34
36 Driver's Position Force-to-Noise Transfer Function at Left Idler Wheel Rim with Tracks in Place 35
37 Driver's Force-to-Noise Transfer Function at Both Sprockets with Tracks in Place 35
38 Vibration Isolation Effect of M113 Inner Track Pad on Idler or Sprocket Rim 36
39 Track Impedance Magnitudes 37
40 Compliant Rim and Hub Concepts 39
41 Effect of Rim Stiffness on Isolator Efficiency with Infinitely Stiff Hub 41
42 Effect of Hub Stiffness on Isolator Efficiency with 14K LB_f/Inch Idler Rim Stiffness 42
43 Predicted A-Weighted Noise Levels for Compliant Idler or Sprocket Rims and Hubs at 30 MPH 43

INTRODUCTION

OBJECTIVES AND GOALS

The basic objective of this program was to develop vehicle interior noise reduction concepts that will result in light-weight tracked vehicles quiet enough so that crew members will not be required to use hearing protectors in addition to the DH132 Combat Vehicle Crewmen's Helmet.

Accordingly, the interior noise goal has been set at 100 dB(A) in conformance with the guidelines of MIL-STD-1474, Category B. Achievement of this goal requires a 15 dB(A) noise reduction, primarily at low frequencies. In a weight-critical machine designed for survivability in extreme environments, this represents a major technical challenge.

The U. S. Army Human Engineering Laboratory has recognized that practical design modifications required to achieve significant interior noise reductions do not exist at present, and that their development must be based on experimental and analytical evaluations of the noise sources and their transmission paths. Previous studies (e.g., References 2, 7, 12 and 13) have identified the major noise sources but have not quantified their contributions. An extensive review of available literature on the subject has yielded no general design guidance for noise reduction in tracked vehicles.

The specific objective of this investigation was to develop track system noise reduction concepts based upon a thorough understanding of tracked vehicle noise sources and transmission paths. The goals of this program may be stated as follows:

- to quantify the noise contributions of the idlers, sprockets and roadwheels
- to establish the potential noise reductions that might be obtained by suspension component modification
- to develop a digital computer program for use in conjunction with force-noise transfer function measurements in the evaluation of track noise source reducing concepts.

The M113A1 vehicle was chosen for this study because of its availability and relatively low cost of replacement parts for experimental modification. The M113A1 design is typical of lightweight high speed vehicles. Concepts based on M113A1 requirements are therefore readily adapted to other tracked vehicles in its class.

Noise sources other than the idlers, sprockets and roadwheels will be considered in future programs since suspension noise sources dominate at present.

GENERAL DISCUSSION OF TRACKED VEHICLE INTERIOR NOISE

Interior noise in tracked vehicles results from track interaction with the drive sprockets, idler wheels, and roadwheels. The engine and powertrain is a secondary noise source in most tracked vehicles. Some vehicles, such as the M60 and MICV, have track support rollers which may also produce significant interior noise. Figure 1 is a schematic representation of tracked vehicle noise sources and vibration paths.

Noise in moving tracked vehicles results from vibration of the hull which is excited by suspension and engine-powertrain components. The hull structure distributes vibration energy from each source to the remainder of the hull which, in turn, radiates noise. The interior noise levels at the driver and crew locations are established by the direct radiation of sound from the hull surfaces and by reverberant buildup.

Accordingly, noise control in lightweight tracked vehicles is more a matter of reducing hull vibration than installing barriers or absorbers. Consideration of "conventional" acoustic noise control barriers and absorbers showed that, because the entire hull radiates noise, the 100 dB(A) noise goal could not be met within practical weight, cost, durability and size limits. Therefore, the noise control concepts addressed in this study were: (1) the reduction of vibration at the various sources, and (2) attenuation of vibration energy paths between sources and the hull.

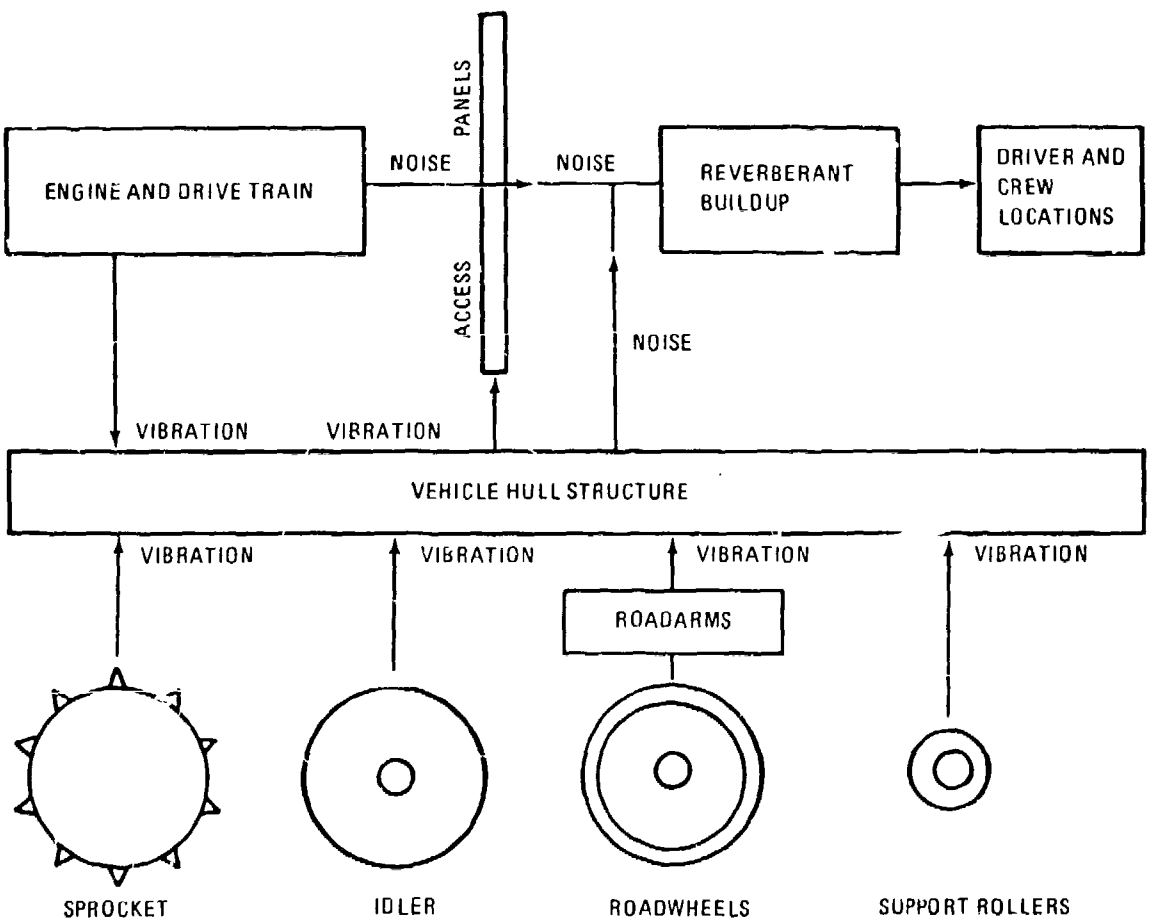

Figure 1. Schematic Diagram of Sources and Paths Responsible for Interior Noise in Tracked Vehicles

Only the major M113 suspension noise sources were examined in this study. Previous studies (Reference 7) have shown that other noise sources are secondary; such as the engine, powertrain, and final drive gearing. Further, suspension sources are specific tracked vehicle noise problems and the technology needed to successfully reduce the noise from these sources does not exist at present.

The basic phenomena responsible for tracked vehicle hull vibration at typical operating speeds are tension changes due to the geometry of track engagement with the idler and sprocket wheels, and forces resulting from impacts between track shoes and the idler and sprocket wheels. Both of these phenomena occur at track-laying rate.

Chordal action occurs as follows. As the track is carried around a wheel, it cannot form a smooth arc (as could a belt) because of the rigid track shoes. Instead, the shoes form part of a polygon, which is equivalent to a series of chords of a circle; hence the synonyms "chordal action" or "polygonal action".

Chordal action causes the velocities and accelerations of entering and exiting track pins to vary in a cyclical manner. In Figure 2a, as a track pin arrives directly above the wheel, its horizontal velocity is at a maximum and its vertical (radial) velocity is zero. One-half pitch cycle later (Figure 2b), the situation is changed. At this point, horizontal velocity is reduced, while vertical downward velocity is increased. (For a 10-tooth M113 sprocket, this downward velocity is about 10% of the vehicle's forward speed.) Because of the rapidity of the velocity changes and the massiveness of the track, considerable force is required to impose the necessary accelerations on entering (or exiting) track shoes. These imposed forces result in considerable reaction forces which, in turn, vibrate the hull.

The second major source of hull vibration is the impact which results from chordal action. Impacts occur only at the entering track shoe. As shown in Figure 2, the downward velocity of the entering track strand is suddenly interrupted by the idler wheel. The net result is a very powerful impact against the wheel causing the entire hull to vibrate. At present, data are not available that can be used to clearly separate impact noise from the noise generated by track tension changes. Also, the impacts and chordal action both cause the entire track to vibrate, so that all track shoes in contact with the wheel exert vibration forces.

Figure 2 represents the quasi-static case; i.e., the motion shown would correspond only to a near-zero vehicle speed. For track systems operating at high speed, track inertia may cause the impacts either to increase or to disappear and could cause the track shoes to slide or rock on the wheel. Centrifugal force, variable tension of both track strands, and rubber cushioning effects will combine to greatly modify chordal action and impact forces.

Further discussion of chordal action is available in the literature. Unfortunately, available works describe only power transmission chains and their dynamics. Such chains are comparatively light in weight for the power that they transmit; so the discussions do not directly apply to relatively heavy vehicle tracks.

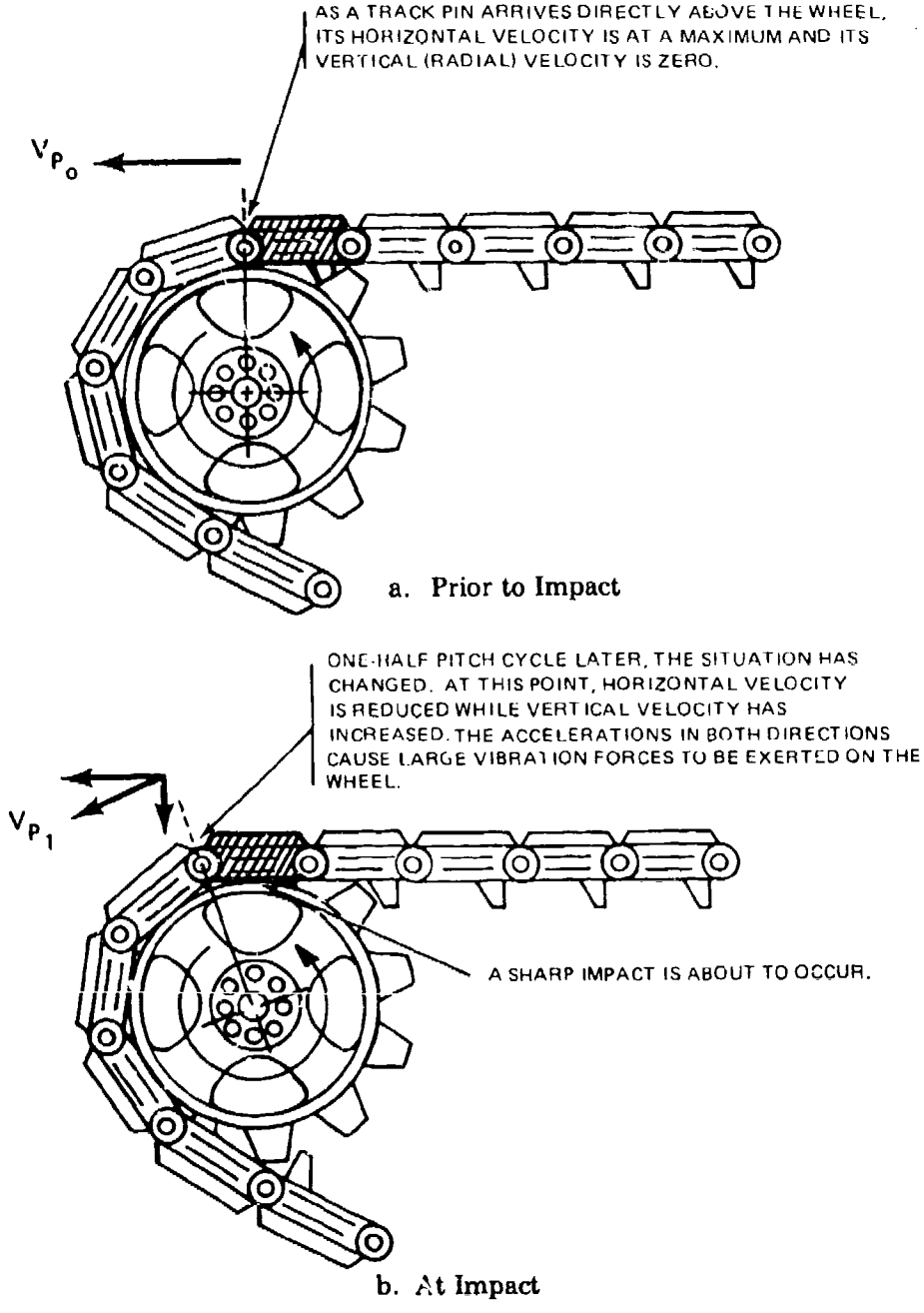

Figure 2. Chordal Action

Because of the complex dynamics involved in track engagement, a digital computer program was developed to aid in the evaluation of the effects of compliance on engagement geometry at the idler and sprockets. The computer program is described in detail in Appendix C.

In this report, no distinction is made between the rubber-on-metal impacts at the idler, and the impacts at the sprocket which might appear to be metal-on-metal. This is because in typical light-weight, high speed tracked vehicles, the track loads at the sprocket are carried primarily by a rubber cushion. Because the sprocket carrier rubber cushion impacts have been found in previous work to be more important to interior noise than the sprocket metal-on-metal tooth contact, the noise generating phenomena at the sprocket and idler are considered to be identical for purposes here.

TECHNICAL APPROACH

Only the major M113 suspension noise sources were examined in this study. Both analytical predictions and experimental measurements were employed. An analysis of track dynamics and the determination of potential noise reductions were partly accomplished by utilizing a computer program in conjunction with experimentally determined force-to-noise transfer functions. Noise reductions resulting from more compliant cushions between the track and sprocket wheel were also estimated by use of simplified linear impact theory and by calculations of track shoe impact velocity. These latter two calculations were separate from the computer program.

The dominant three track interaction noise sources (idler wheels, sprocket wheels, and roadwheels) were experimentally measured by making extensive mechanical changes to the test vehicle to enable the measurement of each noise source one at a time. The changes involved removal of all suspension components except for the one being investigated. Vehicle interior noise was measured with the vehicle in the following test configurations:

- Fully operational production M113A1 vehicle ("Production M113A1")
- Towed by another vehicle ("Towed")
- Towed with tracks removed ("No Tracks")
- Right idler only, vehicle on test stand ("Right Idler Only")
- Left sprocket only, vehicle on test stand ("Left Sprocket Only")
- Towed without sprockets and idlers ("Roadwheels Only")

SUMMARY OF RESULTS AND CONCLUSIONS

The summarized results and associated conclusions arrived at during this program are presented in the following order:

- Speed dependence of source contributions to interior noise
- Octave band spectra of noise source contributions at fixed speeds
- Noise reduction requirements

Speed Dependence of Noise Source Contributions to Interior Noise

Figure 3 summarizes the A-weighted noise levels at the crew microphone position produced by the right idler, left sprocket, and all ten roadwheels as track speed was varied. Production M113A1 self-powered and also towed measurements are shown. The 100 dB(A) noise goal is shown as a dashed horizontal line. Idler-dependent and sprocket-dependent noise (i.e., both right and left) should yield levels that are 3 dB higher.

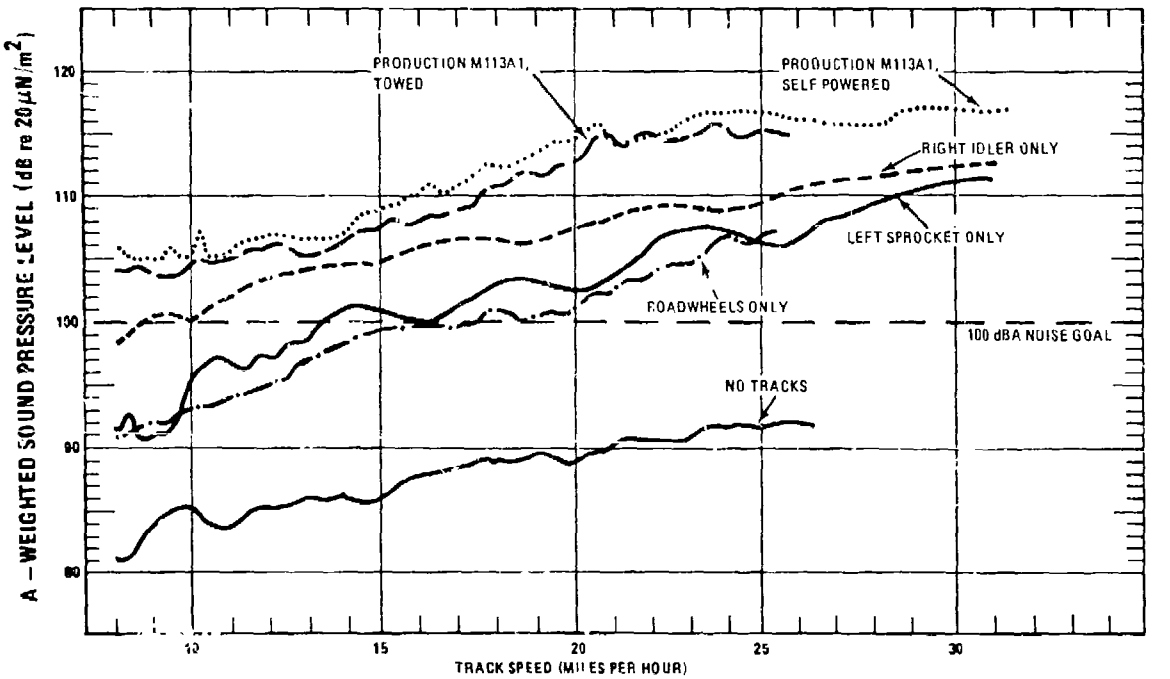

Figure 3. Speed Dependence of Track System Noise Sources at Crew Position

Figure 4 shows the same data at 15, 20, 25, and 30 miles per hour and more clearly shows the contributions of idlers, sprockets, and roadwheels to overall interior noise of the M113A1 vehicle.

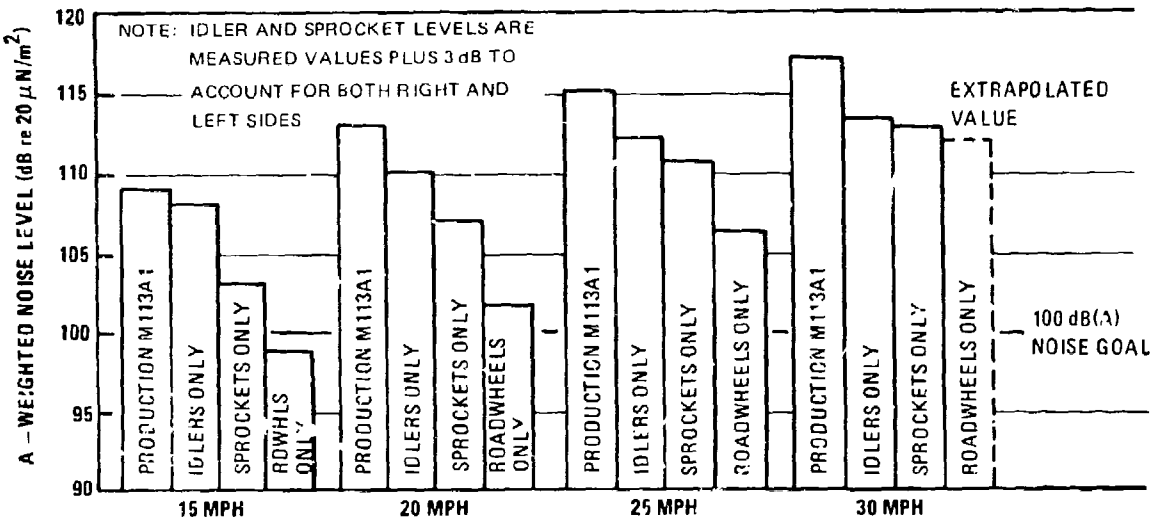

Figure 4. Crew Area Track System Noise Sources Compared at Various Speeds

Analysis of Figures 3 and 4 yields the following conclusions about track system noise sources:

- Significant reduction of any single suspension noise source will result in a relatively small overall noise reduction, especially at speeds above 25 miles per hour.
- Overall vehicle noise is dominated by the idlers at all measured vehicle speeds, especially at speeds below 20 miles per hour.
- At speeds above 20 miles per hour, the sprockets approach the idler in their contribution to overall noise.
- Straight-line extrapolation of the roadwheel noise level trend indicates that roadwheels may be significant contributors to overall noise at speeds of 30 miles per hour and above.
- Roadwheel dependent noise is significantly reduced when the tracks are removed, indicating that the interaction of the rough inner track surface and roadwheels is responsible for the majority of the vibration excitation and resulting interior noise.

Other conclusions resulting from this program are:

- The leading roadwheel produces more hull vibration and noise than any other roadwheel. However, to achieve significant roadwheel noise reduction, the noise from all roadwheels must be reduced.
- The engine is not an important contributor to interior noise above vehicle speeds of about 10 miles per hour (References 7 and 14).
- Idler, sprocket, and roadwheel noise reductions of 15 to 20 dB(A) are required for the 100 db(A) noise goal to be achieved at the 30 miles per hour vehicle speed.
- During normal operation, the driver position averages 1-4 dB(A) more noise than does the crew position.

- A softer cushion between the track and idler or sprocket rim offers the most potential noise reduction with a reasonable practicality risk.
- Horizontal and vertical force reactions at the idler and sprocket mounts produce approximately the same interior noise level in the 250 Hz octave band.
- Both horizontal and vertical forces exerted on the idler and sprocket must be controlled to achieve appreciable noise reduction.
- For idler and sprocket noise control, hub compliance is potentially more effective than rim compliance; but it poses serious design problems.
- Most or all of the required noise reduction for the idler and sprocket appears to be achievable with practical rim compliance concepts.
- If practical, reduction of the hull vibration force-to-noise transfer efficiency would provide a useful additional noise reduction.
- Selection of the vehicle operating speed for determination of vehicle interior noise performance is critical, owing to the presence of vibration response peaks within the normal speed range of the vehicle. Such peaks can reduce the repeatability of noise measurements.
- A track tension reduction from 3000 to 2000 pounds lowers interior noise by less than 2 dB. Practical track tension reductions, therefore, will not result in significant noise reduction.

Figures 5, 6, and 7 show the octave band spectra of the various noise sources in the crew area at vehicle speeds of 15, 25, and 32 miles per hour along with the 100 dB(A) noise goal spectrum given by MIL-STD-1474, Category B. Engine only noise levels (Reference 14) are shown for comparison purposes.

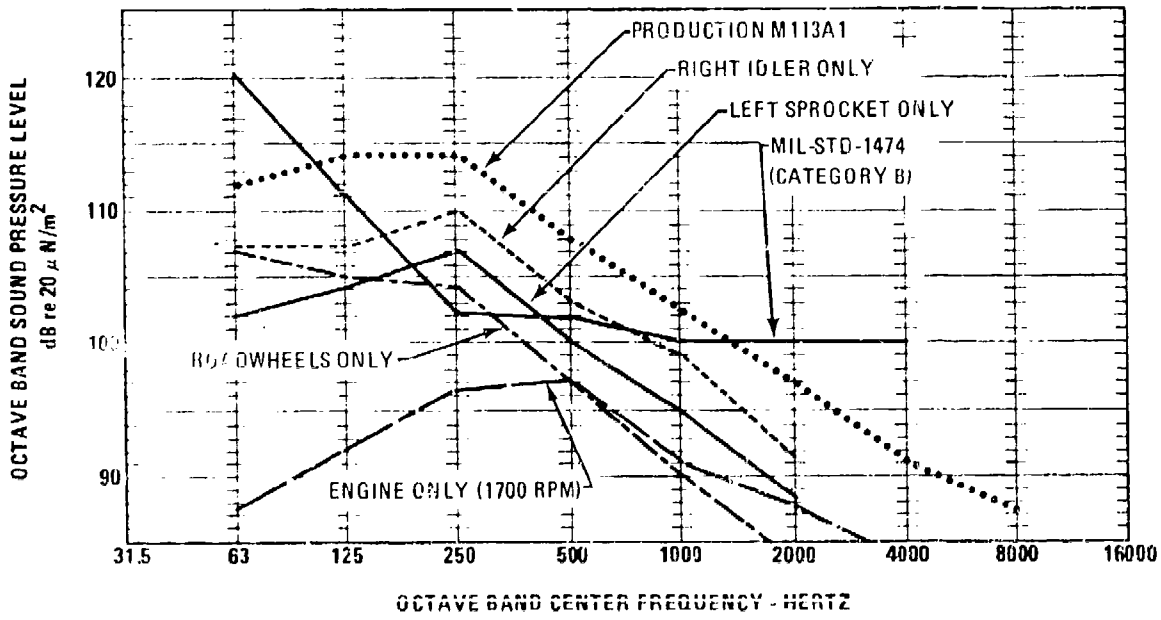

Figure 5. Noise Source Spectra at 15 MPH at Center of Crew Compartment

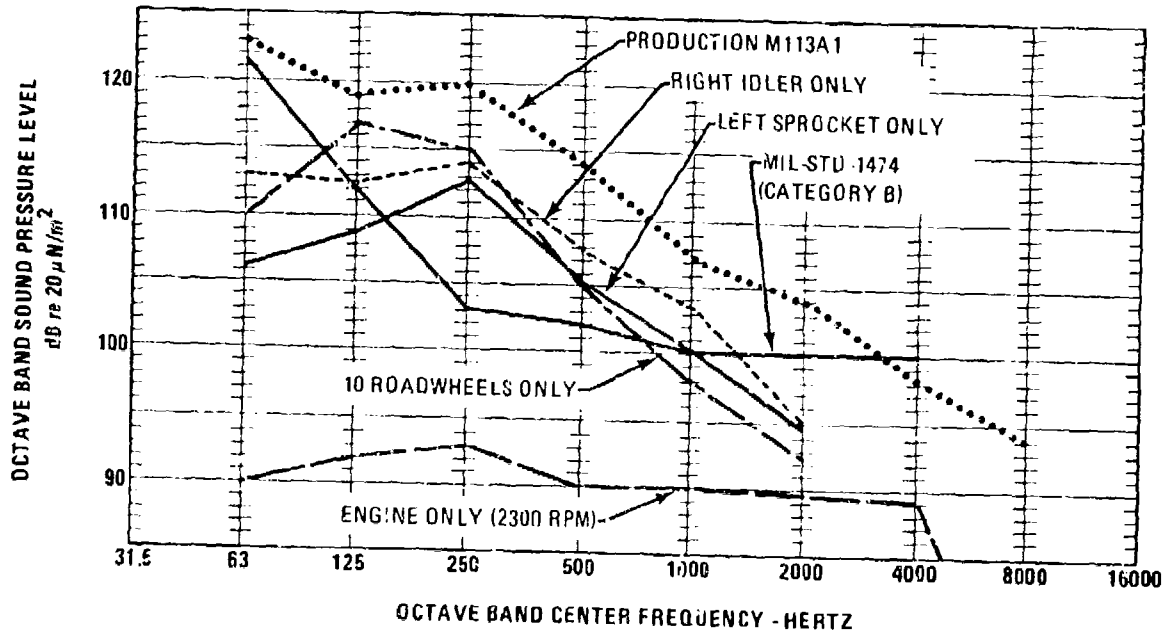

Figure 6. Noise Source Spectra at 25 MPH at Center of Crew Compartment

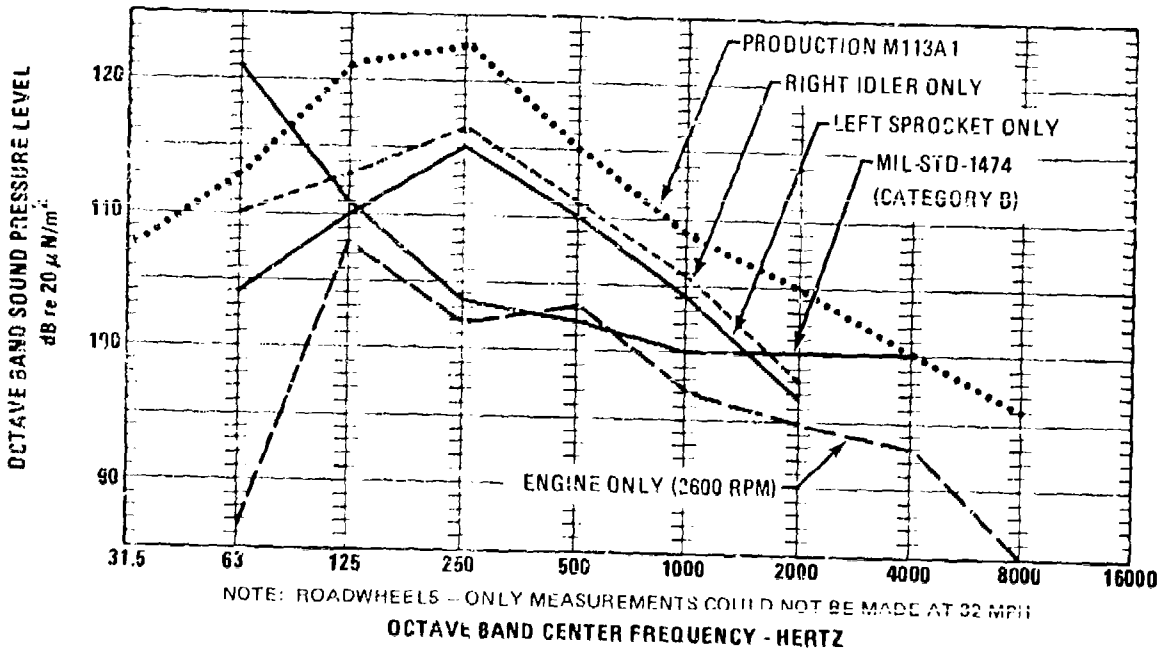

Figure 7. Noise Source Spectra at 32 MPH at Center of Crew Compartment

Figures 8, 9, and 10 show results similar to the above figures at the driver's microphone position.

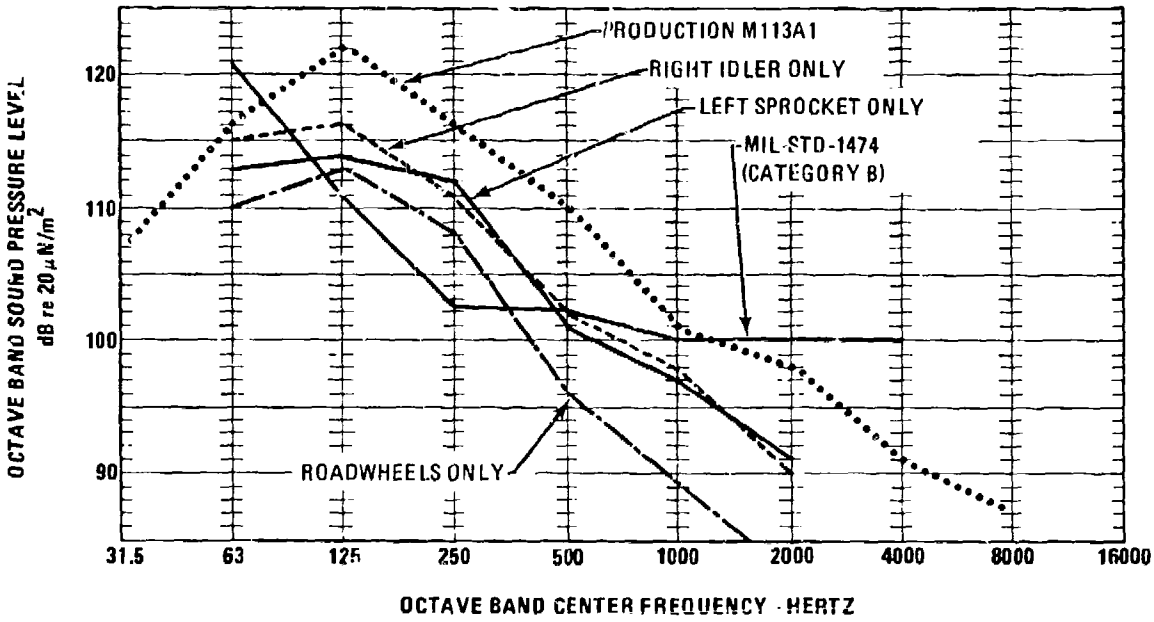

Figure 8. Noise Source Spectra at 15 MPH at Driver's Position

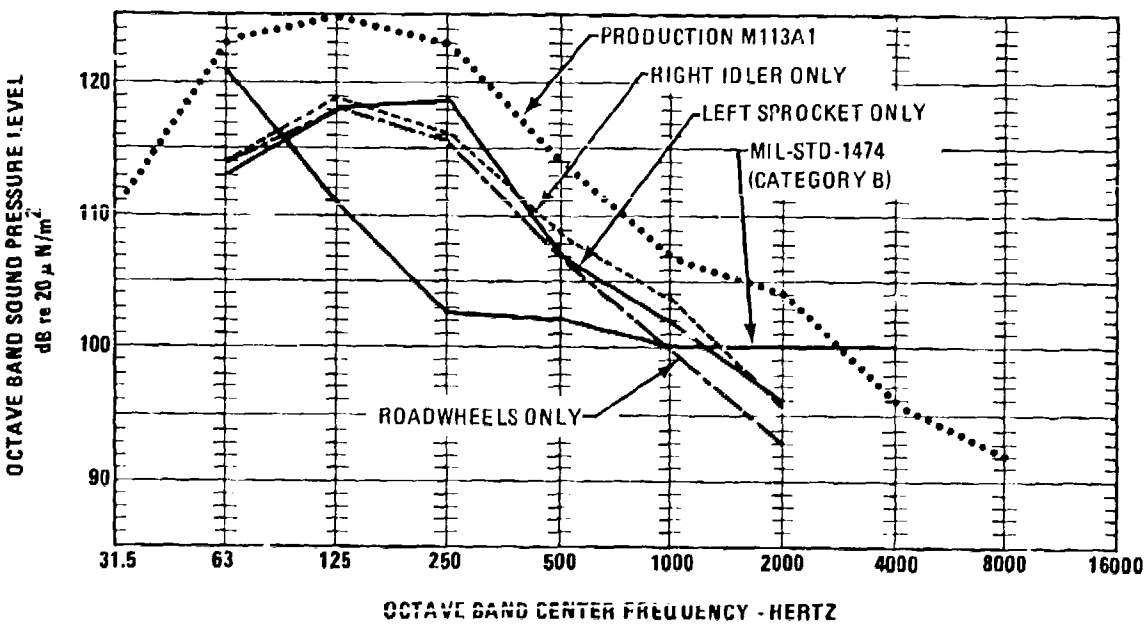

Figure 9. Noise Source Spectra at 25 MPH at Driver's Position

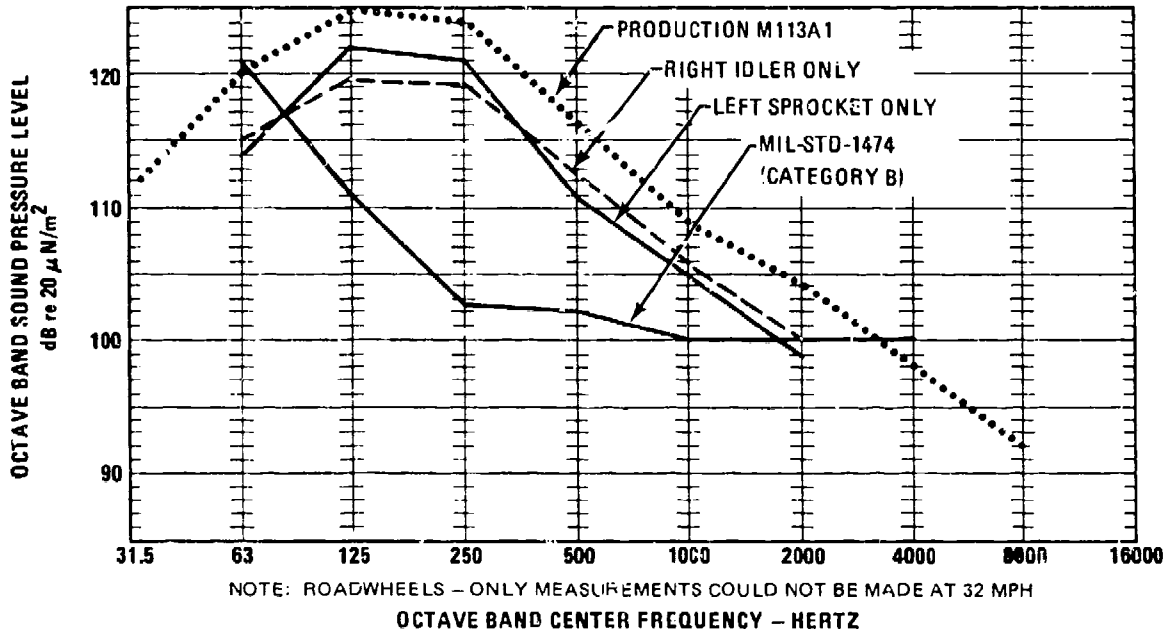

Figure 10. Noise Source Spectra at 32 MPH at Driver's Position

Figure 11 compares noise levels at the driver and crew microphone positions due to one sprocket or idler at 32 MPH.

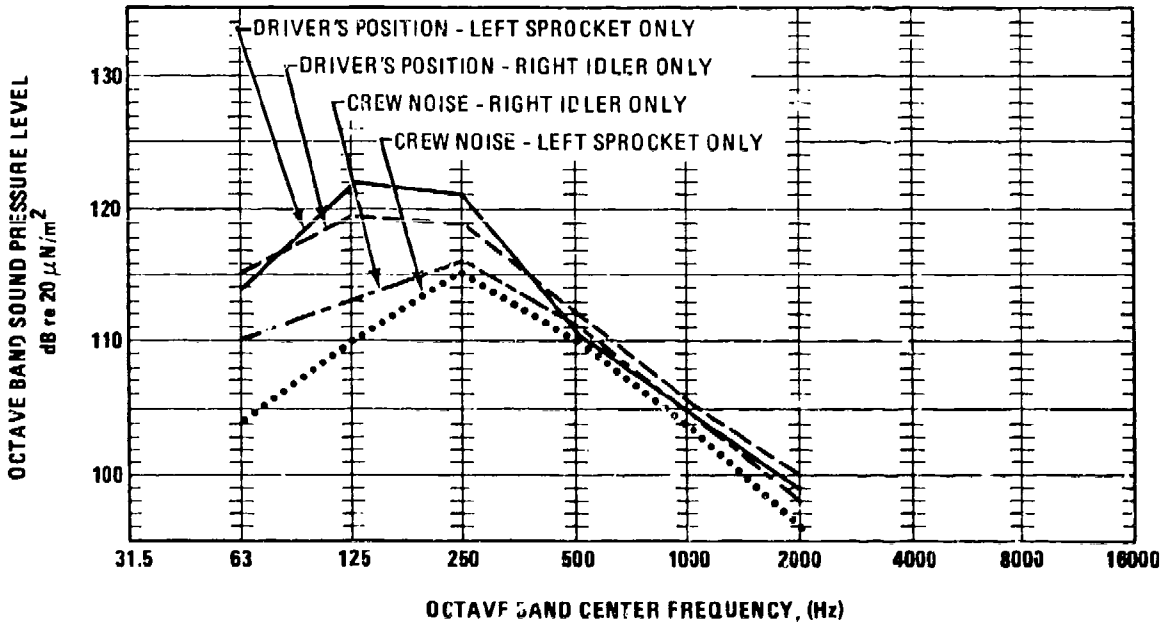

Figure 11. Comparison of Idler and Sprocket Interior Noise Spectra at Driver's Position and in Crew Area at 32 MPH

The shapes of the spectra show that overall A-weighted noise is dominated by 250 and 500 Hertz octave band energy at all speeds and at both microphone locations. Thus, reduction of tracked vehicle interior noise to the program noise goal requires a 15 to 20 dB reduction of sprocket and idler noise in the 250 Hertz octave band. Roadwheel noise must be reduced by at least 11 dB(A) at 25 MPH in order to meet the 100 dB(A) noise goal and, according to a straight line extrapolation must be reduced even more at higher speeds.

Noise Reduction Requirements

In order to achieve the 100 dB(A) noise goal in the crew area, idler, sprocket, and roadwheel noise each must be reduced to 95 dB(A) or below. The reductions required for a "balanced" (all noise sources contributing equal sound energy) noise control package are listed in Table 1.

Table 1. SOURCE NOISE REDUCTIONS REQUIRED TO ACHIEVE 100 dBA NOISE GOAL IN THE CREW AREA

Vehicle Speed (MPH)	15	20	25	30
Idler Reduction Required	13 dB(A)	15 dB(A)	17 dB(A)	18 dB(A)
Sprocket Reduction Required	8 dB(A)	12 dB(A)	15.5 dB(A)	17.5 dB(A)
Roadwheel Reduction Required	4 dB(A)	6.5 dB(A)	11 dB(A)	17* dB(A)

*Based on straight line extrapolation of roadwheel noise.

EVALUATION OF NOISE SOURCE CONTRIBUTIONS

TEST VEHICLE

All measurements were carried out on an M113A1 Armored Personnel Carrier, serial number SJ-136. This vehicle is standard, except as described below. To help reveal details of suspension noise and to help assure repeatability between tests, rattles were controlled by removing all seats, stowage equipment, floor plates, special panels, squad compartment fire extinguishers, the track shrouds and the trim vane. Both engine access panels were left in place. Figure 12 shows the test vehicle being towed on the paved track.

The driver's hatch was open for self-powered measurements and was closed for all other measurements.

All vehicle testing was done at FMC Corporation facilities in San Jose, California.

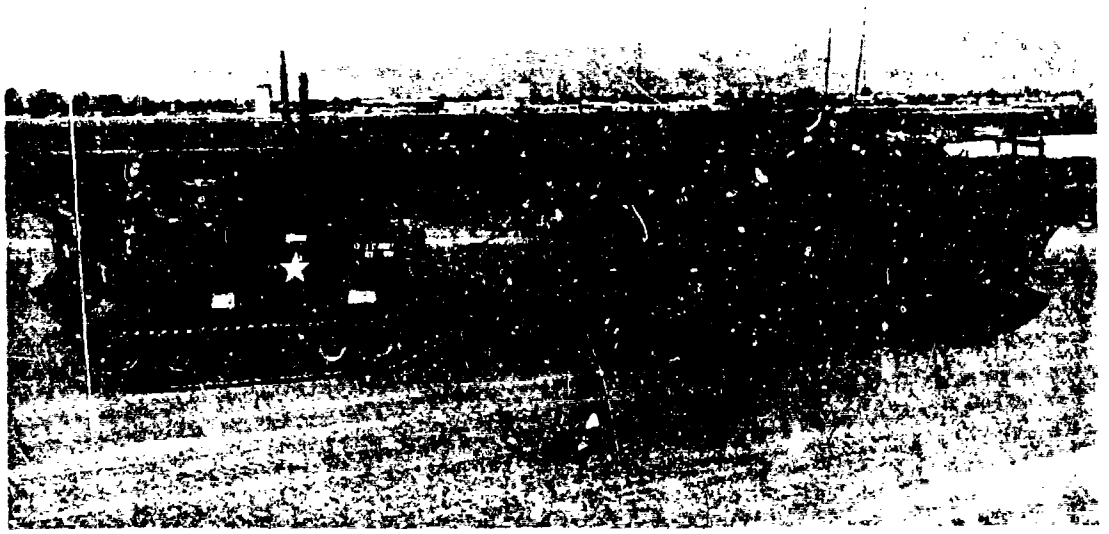

Figure 12. Test Vehicle Towed by LVTP7

DATA ACQUISITION FOR SUSPENSION NOISE AND VIBRATION

Vehicle interior noise measurements were made by means of two microphones; one located just behind the driver's head position, and the other in the crew compartment. The driver's position microphone was located 8-1/2 inches from the left upper side plate, 8-1/2 inches below the ceiling, and 1/2 inch aft of the rear engine access panel surface. During measurements, the crew compartment microphone was mechanically rotated in a horizontal 6-inch diameter circle about a point located 38 inches from the right upper side plate, 7 inches below the ceiling, and 44 inches aft of the rear engine panel. Rotation of the crew position microphone was employed in order to obtain a spatial averaging of the measured sound, and thus obtain a more representative sample.

The sound level meter and microphone used provided an "unweighted" (also sometimes called flat, over-all, linear, or all-pass) frequency pass band extending from 20 to 16,000 Hz. Figure 13 shows the microphones positioned in the test vehicle.

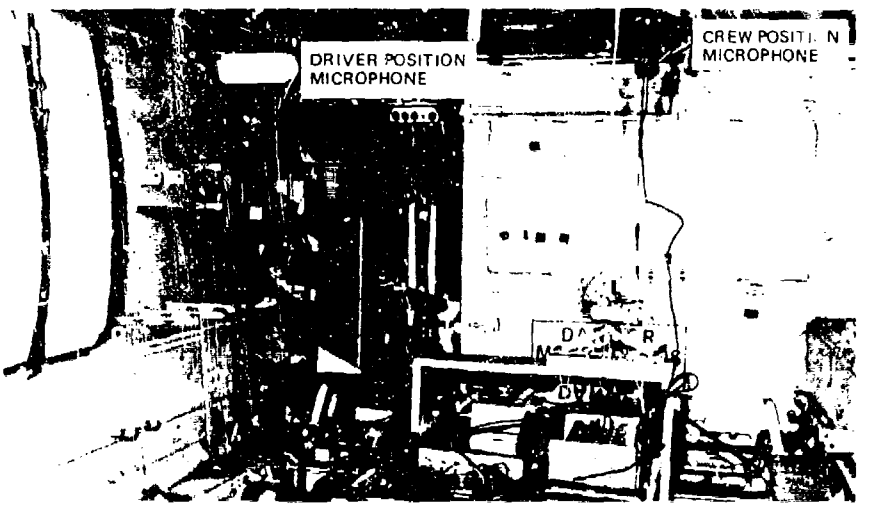

Figure 13. Microphone Locations for Measurements of Interior Noise

Two accelerometers were mounted to each of Roadarms #1, #3, and #5. As shown in Figure 14, one accelerometer measured acceleration parallel to the roadarm axis, and the other measured accelerations perpendicular to the same axis.

Figure 14. Accelerometer Locations for Roadarm Vibration Measurements

Running tests were conducted on FMC's paved track facility. Idler and sprocket tests were carried out with the vehicle mounted on the test stand shown in Figure 15.

Noise, vehicle speed, and vibration data were recorded on magnetic tape (four channels at a time) during gradual vehicle accelerations and decelerations. This test method was chosen over the planned series of fixed speeds because the vehicle drivers had difficulty in establishing accurate steady-state vehicle speeds, and also the continuous speed versus noise sweeps resulted in especially informative graphs.

High speed (2,000 frames per second) movies were taken of idler and sprocket engagement on the test stand at various vehicle speeds and track tensions. These films were used for a visual examination of track strand motion, engagement and disengagement geometries, wave motion, and impact characteristics.

DATA PRESENTATION

Most of the noise data in this report are presented as graphs of sound pressure level versus speed. This method yields information that is not readily apparent from steady-state spectral data. Slopes and cyclic variations of noise with speed, which are clearly shown on these graphs, have yielded valuable clues to the noise performance of the sprockets, idlers, and roadwheels.

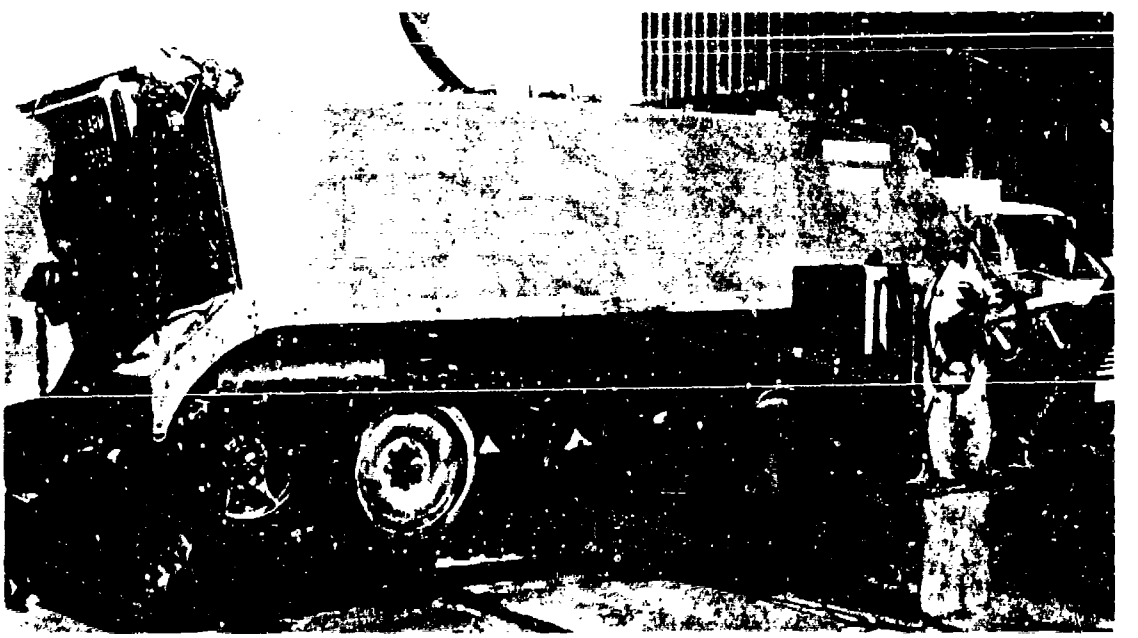

Figure 15. Idler and Sprocket Noise Test Stand

These curves are supplemented by octave band spectra corresponding to an average vehicle speed established during the gradual vehicle accelerations and decelerations. One-third octave band analysis was performed, but large momentary variations in the low frequency bands yielded results inconsistent with octave band and A-weighted data.

Although test stand measurements were made at track speeds up to about 42 mph, towing operations were limited to speeds below 30 mph owing to safety restrictions. The data presentations for all tests are thus limited to approximately 30 mph. Since this speed range also represents the major portion of tracked vehicle operating time, the data presented is representative. The 30 to 42 mph speed range on the test stand resulted in a 1 to 2 dB(A) increase in both idler and sprocket noise and showed no other significant trends.

The A-weighted and octave band sound level data are estimated to be accurate to within ± 2 dB, and the vehicle speed data are typically accurate to within ± 1 mph.

NOISE CHARACTERISTICS OF PRODUCTION M113A1

Figures 16 and 17 show the speed-dependence of the unweighted octave band, and A-weighted noise levels at the crew and driver microphone positions of the production M113A1 operating on the paved track.

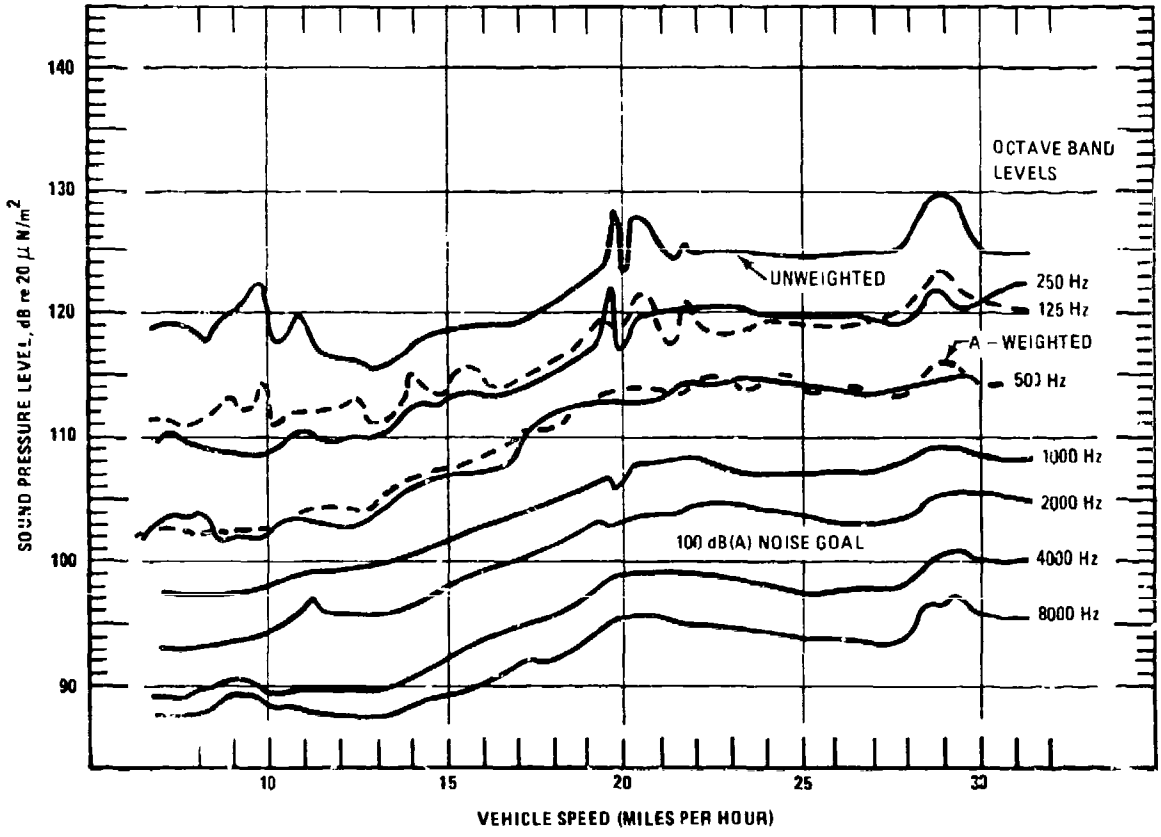

Figure 16. Speed Dependence of Production M113A1 Noise at the Crew Position

The octave band curves are more or less parallel to each other which indicates that the spectrum shape changes little with speed. The curves also show that the increase in vehicle speed from 20 to 30 miles per hour produced only a 2 dB(A) increase in the noise level. Also, noise at the driver's position averages 2 dB(A) higher than at the crew position.

Noise and vibration measurements of the unmodified M113A1 were made several times throughout the program. Four separate crew noise runs yielded unweighted noise versus speed curves which were within ± 2 dB of each [illegible] speeds. A maximum deviation of 6 dB occurred in the unweighted noise le[illegible] speeds near 28 miles per hour.

At 28 miles per hour, a speed deviation of only 1 mile per hour could vary the noise level by up to 6 dB, as shown on Figures 16 and 17. This result emphasizes the importance of checking noise measurements at various tracked vehicle speeds. Specification conformance noise tests for the M113A1 are presently run at a nominal vehicle speed of 28 miles per hour which, unfortunately, coincides with the least measurable point in the M113 speed range.

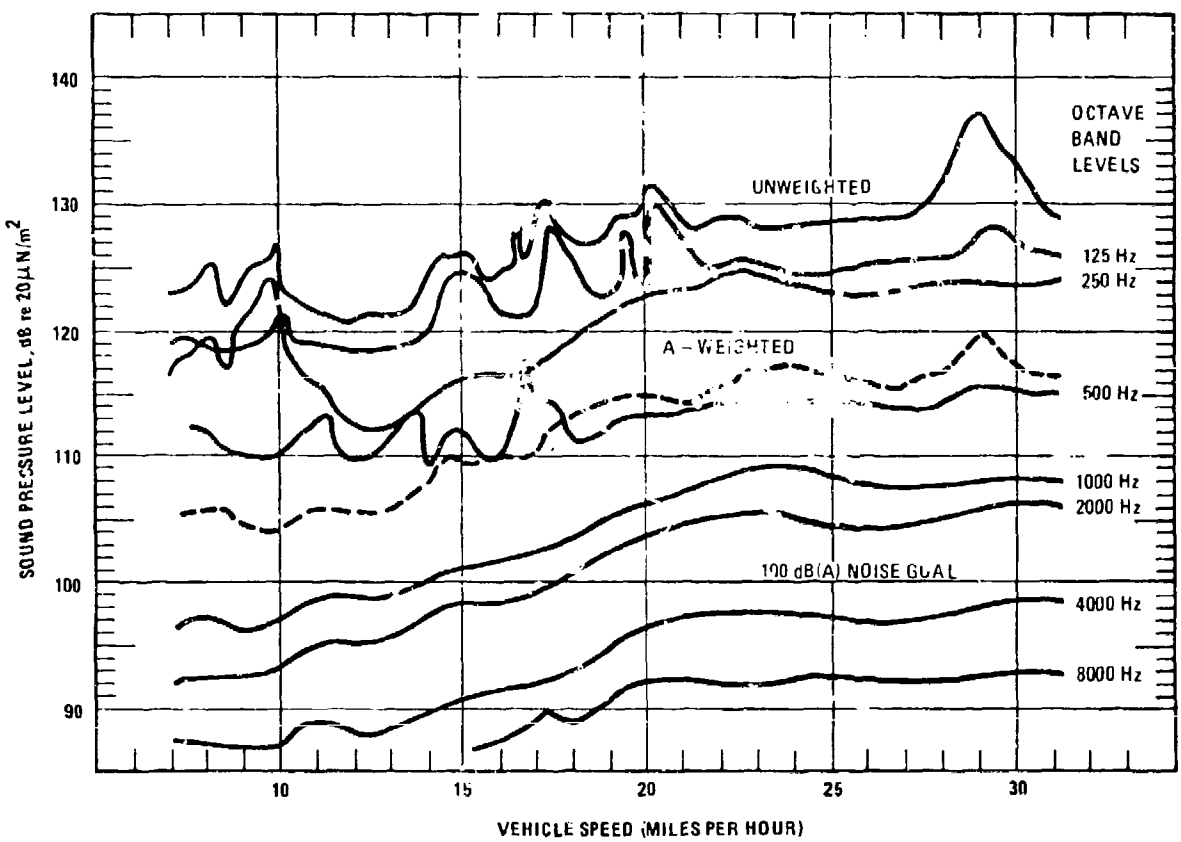

Figure 17. Speed Dependence of Production M113A1 Noise at the Driver Position

IDLER NOISE CONTRIBUTION

In order to evaluate the noise produced by the idler alone, the vehicle was set up on the idler test stand shown schematically in Figure 18. The shock absorbers, right side roadarm assemblies #2 and #4, right side torsion bars #1, #3, #5, and the right side final drive were removed. The track was driven by a separately supported, externally powered sprocket.

Noise measurements were made at static track tensions of 2000 and 3000 pounds. Tension was determined on the basis of static catenary sag measurements of the upper track strand between the idler and sprocket.*

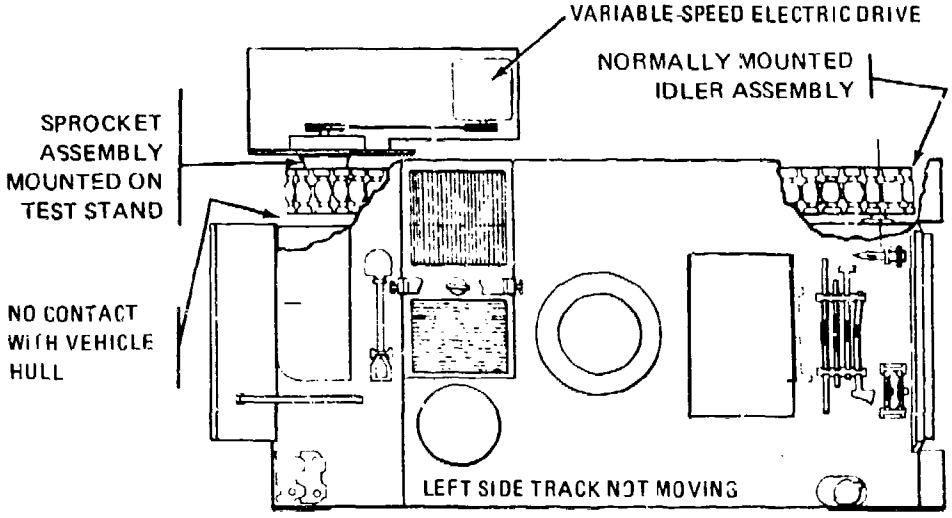

Figure 18. Idler Noise Test Set-Up

Figures 19 and 20 show the speed dependence up to 31 mph of idler-only noise at the crew and driver microphone positions. Measurements were also made at vehicle speeds up to 40 mph which show the same spectrum shape but increased steadily by 1 - 3 dB over the 31 mph levels. The essential parallelism of these speed dependence curves in the octave bands above 125 Hz indicates that the spectrum shape changes little with speed.

Comparison of Figures 19 and 20 shows that the right idler-induced driver's position noise levels are 1 to 2 dB(A) higher than crew area noise levels.

The effect of track tension on right idler-induced noise is evident from Figure 21, which shows idler noise one-third octave band spectra for static track tensions of 2000 and 3000 pounds. The 1000 pound increase in tension resulted in a 2 dB increase for most one-third octave bands and for the A-weighted sound level. The noise increase was similar at the driver's position and crew area. Because of this small dependence of noise on track tension, practical track tension reductions will not produce significant noise reductions (also see References 12 and 13 for similar results).

One-third octave band spectra of horizontal and vertical vibration measured on the right idler housing are presented in Figure 22. The horizontal vibration levels exceed the vertical levels by about 3 dB at the "frequency bands of primary concern" (125 to 500 Hz); that is, those frequencies requiring the most noise reduction.

---

*The static tension T(lb) is given by the common catenary equation $T = W(4S^2 + L^2)/8S$ where: W is the weight of track per unit length (3.5 lb/in.),
L is the length of unsupported track strand (150 in.), and
S is the measured static sag in inches

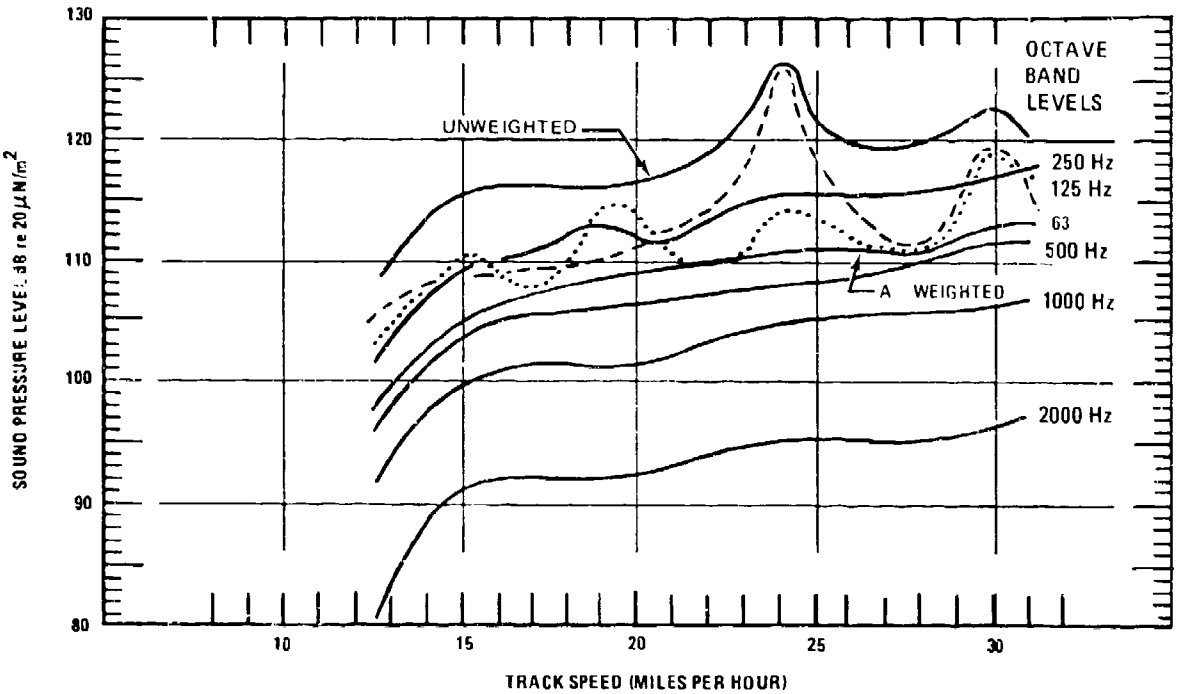

Figure 19. Speed Dependence of M113A1 Right Idler-Induced Noise at the Crew Position

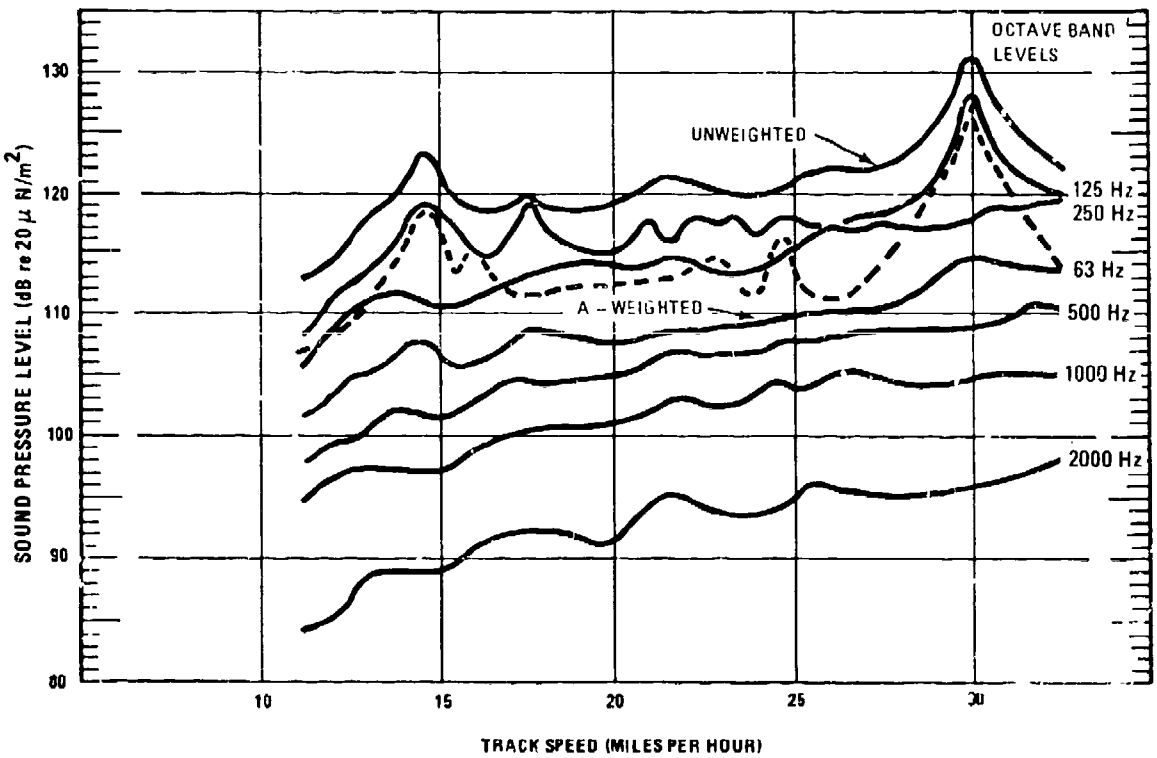

Figure 20. Speed Dependence of M113A1 Right Idler-Induced Noise at the Driver Position

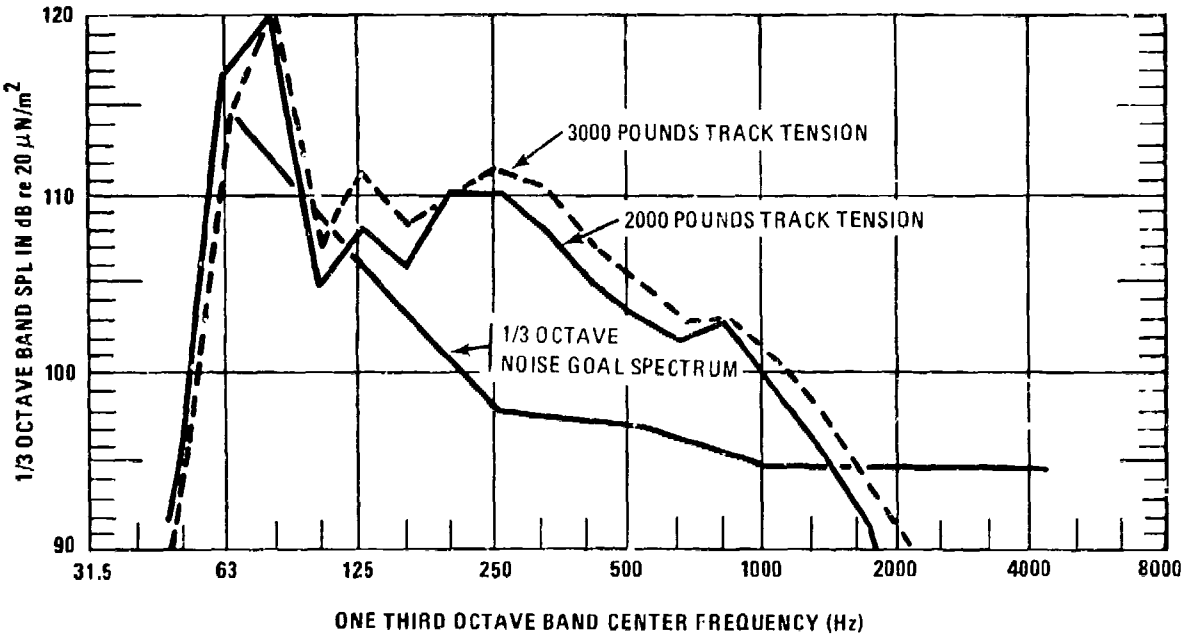

Figure 21. Right Idler-Induced Noise Spectra at 30 MPH for Two Values of Static Track Tension at the Crew Position

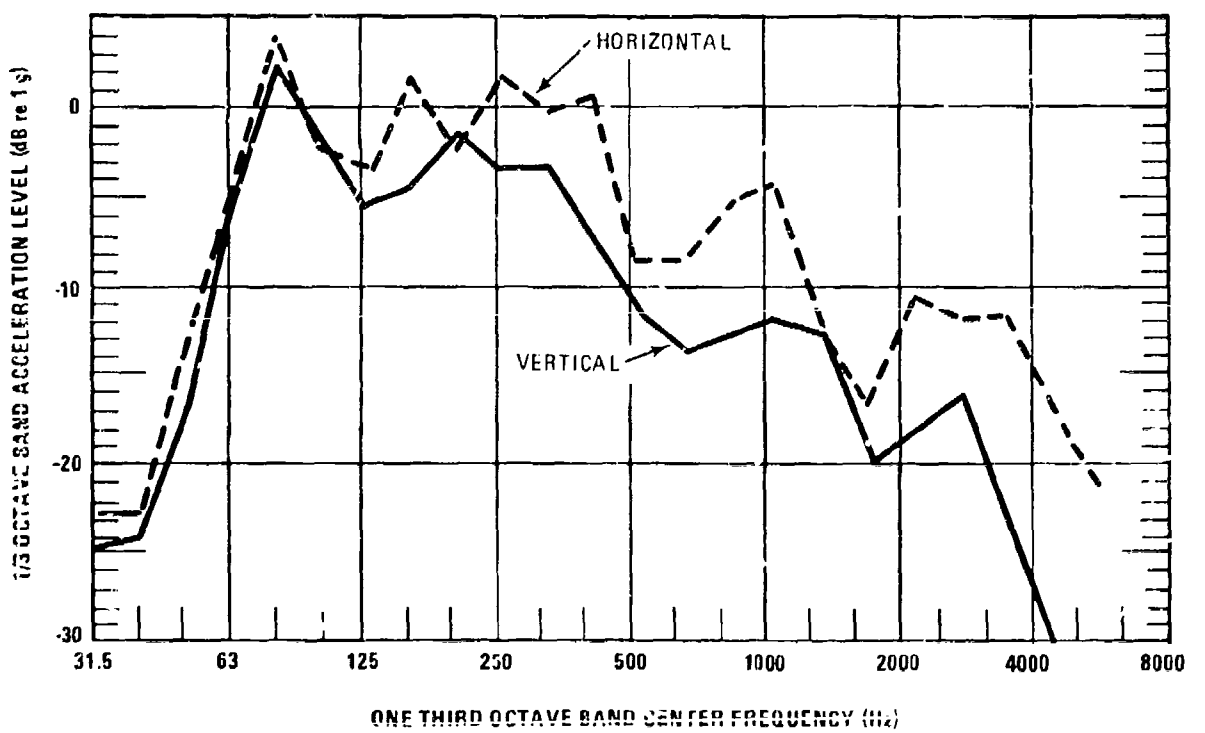

Figure 22. Right Idler Housing Vibration Spectra at 30 MPH with 2000 LBS Static Track Tension

The noise transfer function measurements (described later in Section 3) indicate that either horizontal or vertical vibration forces of the same level produce about the same interior noise level. Considering that 15 to 20 dB(A) of idler noise reduction is necessary to achieve the noise goal, it is clear that both vertical and horizontal vibration must be greatly attenuated.

SPROCKET NOISE CONTRIBUTION

Left sprocket-only measurements were made on a test stand consisting of two sprocket assemblies, as shown schematically in Figure 23. One sprocket assembly was mounted in its normal position on the hull. The idler assembly was replaced by a second sprocket assembly, which was supported independently of the hull. Three roadwheels remained attached to the vehicle to provide track guidance. These wheels imposed negligible forces on the track compared to the sprocket and, therefore, produced negligible hull vibration.

The variation with vehicle speed of left sprocket-induced noise measured at the crew and driver positions is shown in Figures 24 and 25. Driver position noise levels induced by the left sprocket were consistently 4 to 7 dB higher than left sprocket-induced crew position noise levels.

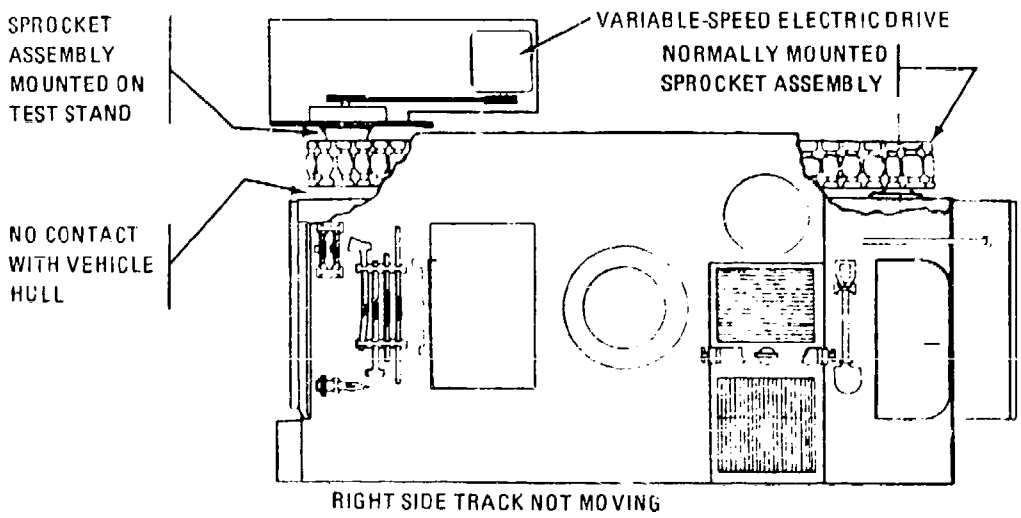

Figure 23. Sprocket Noise Test Set-Up

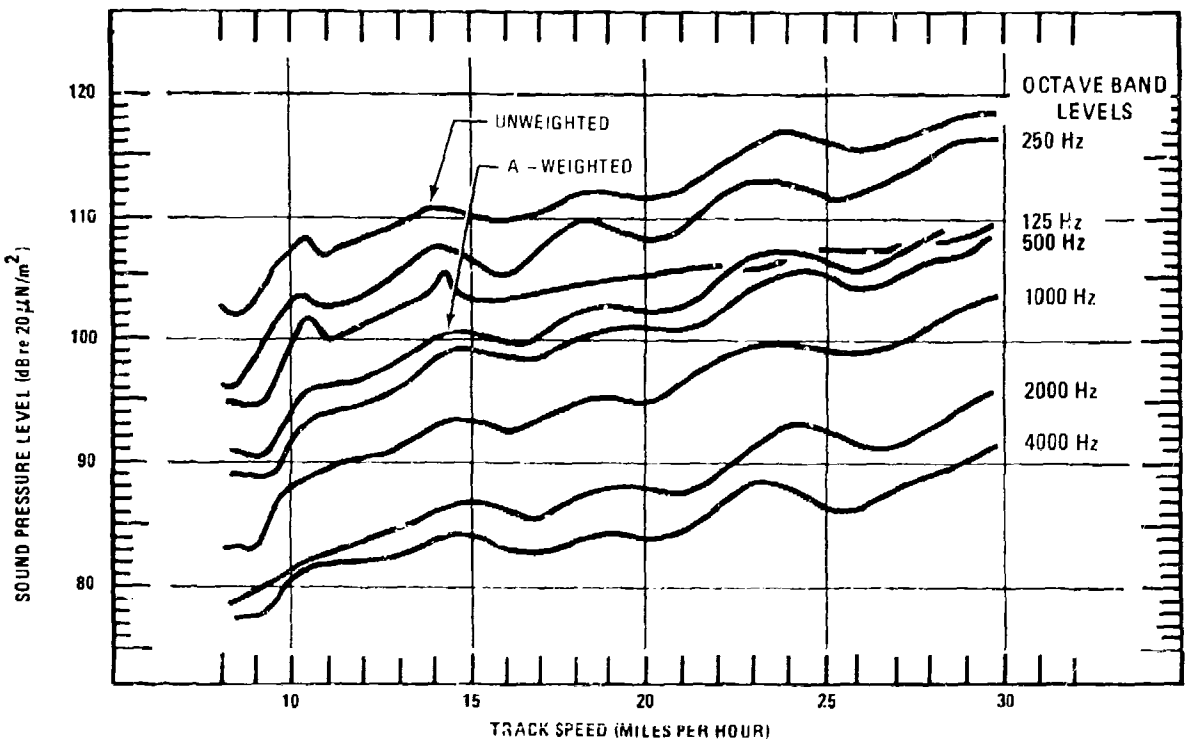

Figure 24. Speed Dependence of M113A1 Left Sprocket-Induced Noise at the Crew Position

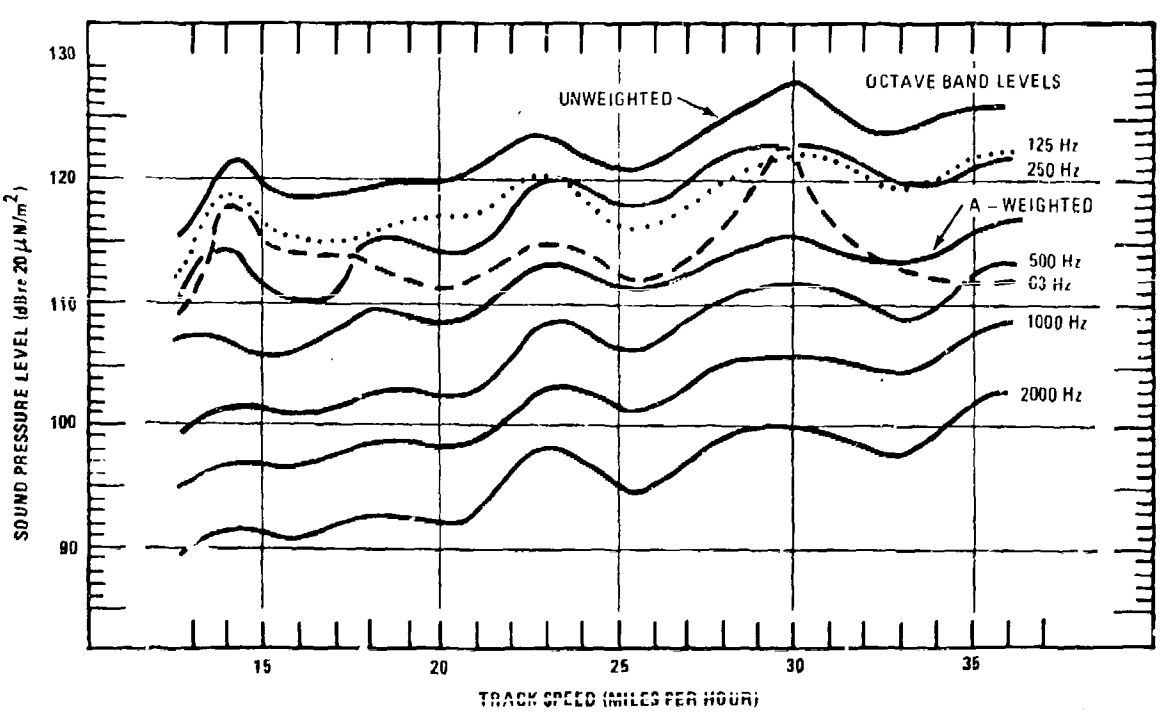

Figure 25. Speed Dependence of M113A1 Left Sprocket-Induced Noise at the Driver Position

Figure 26 shows the results of baseline final drive housing vibration measurements made during normal vehicle operation on the test track. Note that the horizontal and vertical vibrations are of similar magnitudes, implying that both vibration components must be attenuated to produce significant sprocket noise reduction.

The final drive housing vibration and some of the noise levels show a slight periodic variation with speed. This might be a force cancellation effect such as could occur between entering and exiting track shoes, vibration in the short exit track strand, or some similar phenomenon. Regardless, the lower noise portions of the undulations are only 3 dB below the average, which is not worth exploiting for noise control purposes.

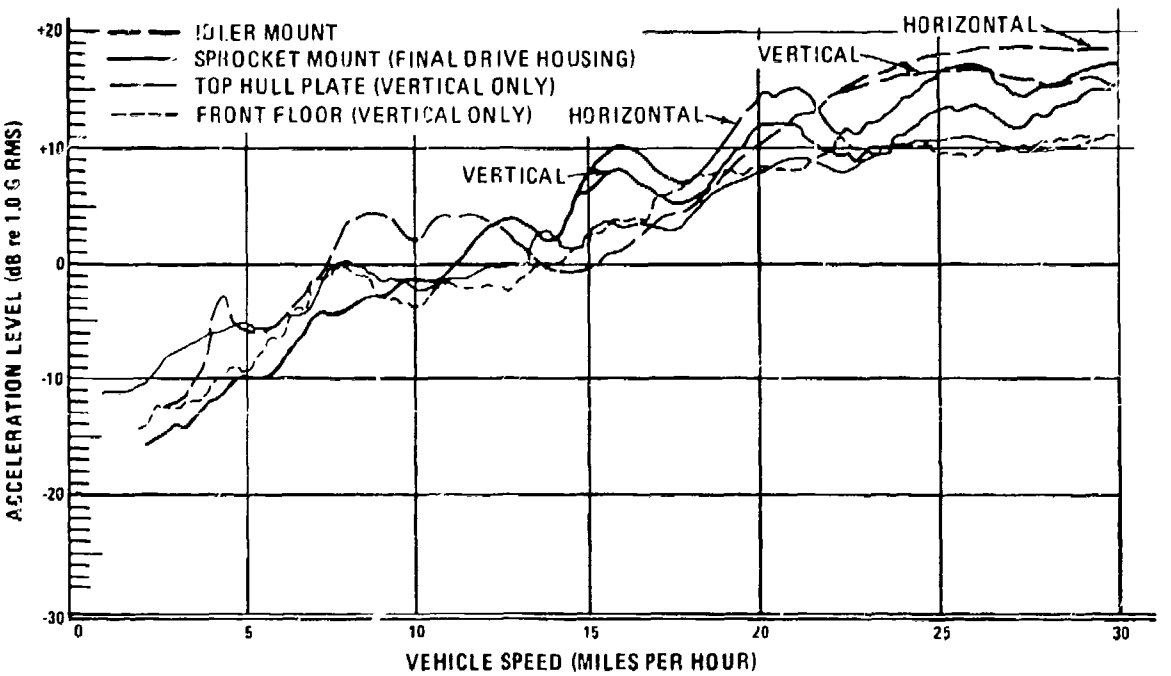

Figure 26. Speed Dependence of Production M113A1 Vibration During Normal Operation

ROADWHEEL NOISE CONTRIBUTION

To isolate the roadwheel noise contribution, the idler wheel assemblies, track tension adjusters, shock absorbers and final drives were removed. The track was shortened by removing an appropriate number of shoes, and vehicle weight was allowed to tension the track. Because of interference between the track and the torsion bar end of the roadarm, the #1 roadarm was installed in a leading, rather than in its usual trailing, position. Figure 27 shows the vehicle in its roadwheel noise test configuration.

There was concern that the changes in track tension and that the altered track entry to the leading roadwheel (as compared to normal operating conditions) would distort the results of the roadwheel noise tests. Therefore, two accelerometers and a strain gauge were mounted on each front, center, and rear roadarm. The outputs of these transducers were recorded during normal operation and also during roadwheel-only operation so that comparisons could be made.

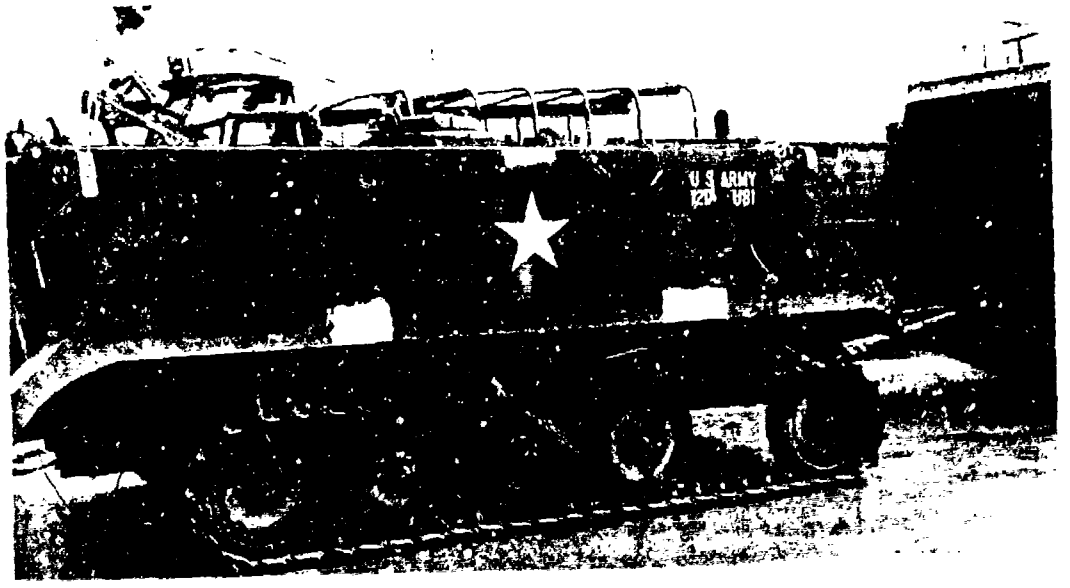

Figure 27. Vehicle in Roadwheels Only Configuration

Figure 28 shows the differences in roadarm vibration between normal and roadwheel-only operation. Vibration of the front and center roadarms are quite similar under both test conditions from 100 through 400 Hz, but the vibrations of the rear roadarm in the roadwheel-only configuration exceed those during normal operation by about 6 dB averaged in the frequency bands of primary concern (125-500 Hz).

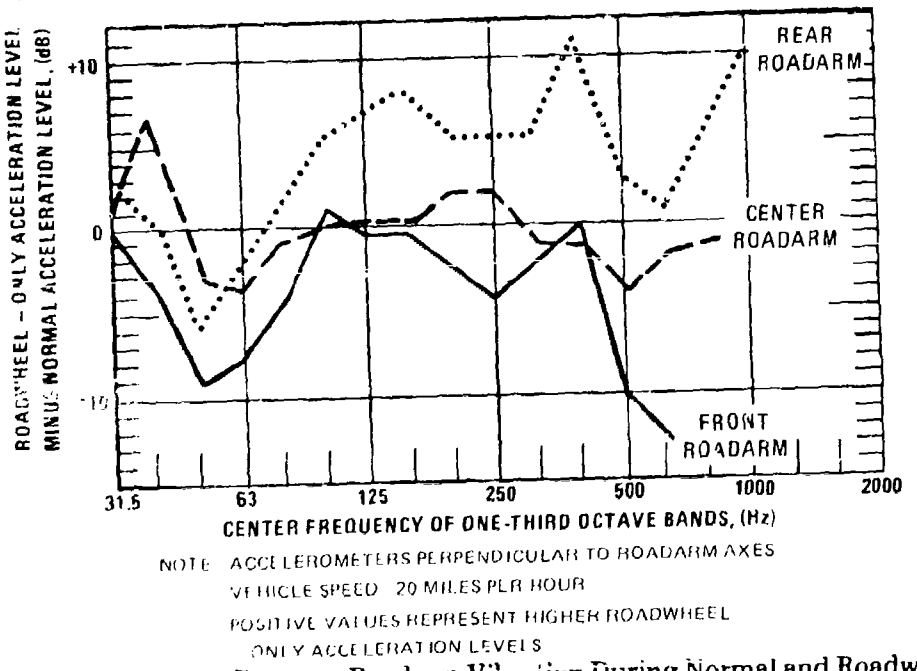

Figure 28. Differences Between Roadarm Vibration During Normal and Roadwheel-Only Vehicle Operation

Figure 29 illustrates that in normal operation the vibration of the leading roadarm exceeds that of the center roadarm by an average of 6 dB, and that of the trailing roadarm by an average of 10 dB. Therefore, even though the roadwheel noise test may exaggerate the contribution of the trailing roadwheel, and assuming that the noise contribution of a given roadarm is proportional to its acceleration, the increased trailing roadwheel noise is still too low to significantly affect the total noise level due to all roadwheels. From this, the roadwheel-only noise measurement technique appears to accurately represent roadwheel noise during normal vehicle operation.

The vibration data of Figure 29 also suggest that approximately one-half of the roadarm vibration energy during normal operation is due to the front roadwheel alone, assuming equal transfer functions between roadwheels. Hence, effective control of only the two front roadwheels would reduce roadwheel-induced noise by 2-3 dB. Further reduction would then require that the noise generated by the other roadwheels be reduced as well.

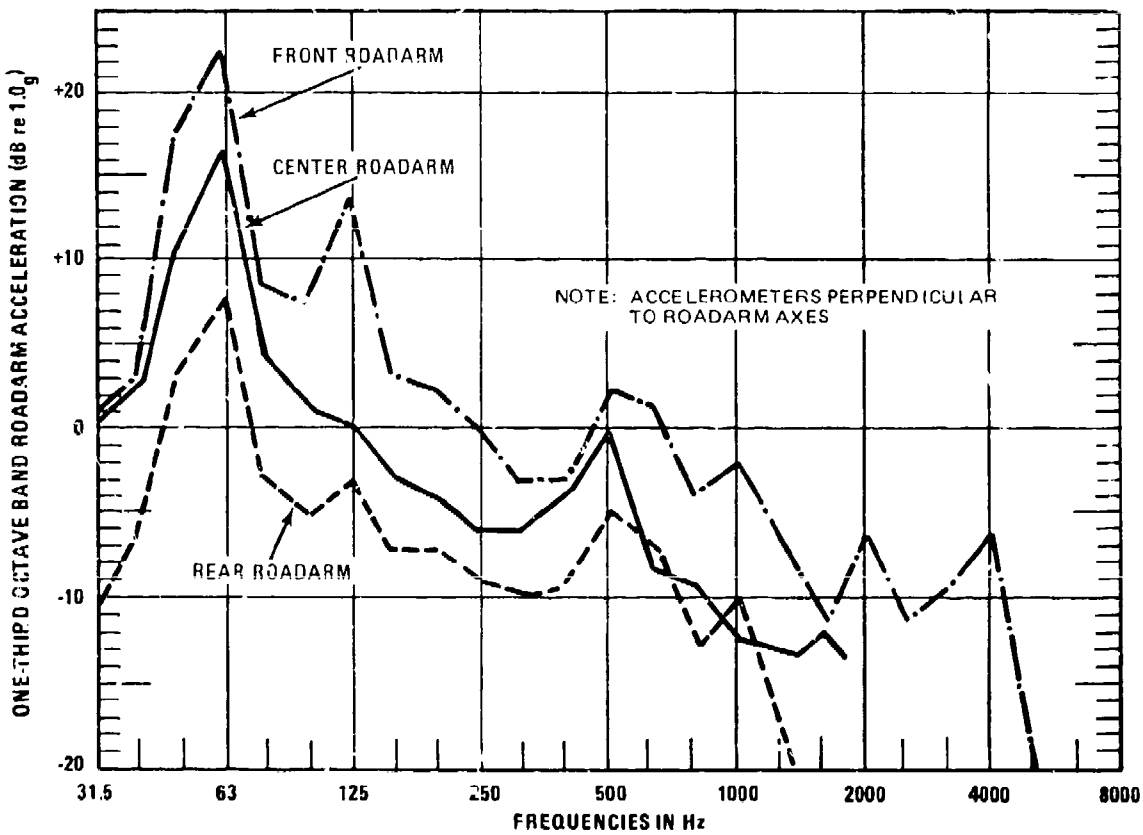

Figure 29. Roadarm Spindle Vibration at 20 MPH on Production M113A1

Figures 30 and 31 show the contribution of the roadwheels to the noise at the crew and driver positions measured during the roadwheels-only noise test.

Since Figure 30 shows noise level to increase with speed, straight line extrapolation to 30 mph indicates that the noise level would be 111 dB(A) in the crew area, and 112 dB(A) at the driver's position is expected at 30 mph.

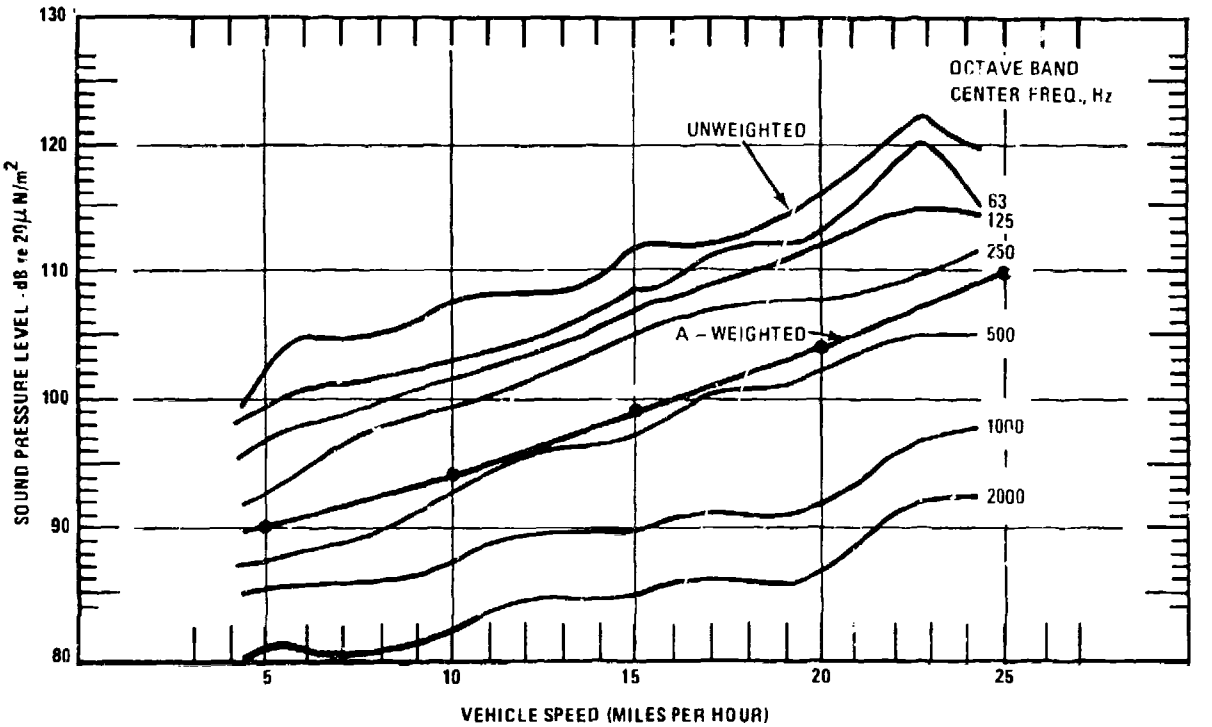

Figure 30. Speed Dependence of Roadwheel-Induced Noise at Crew Position

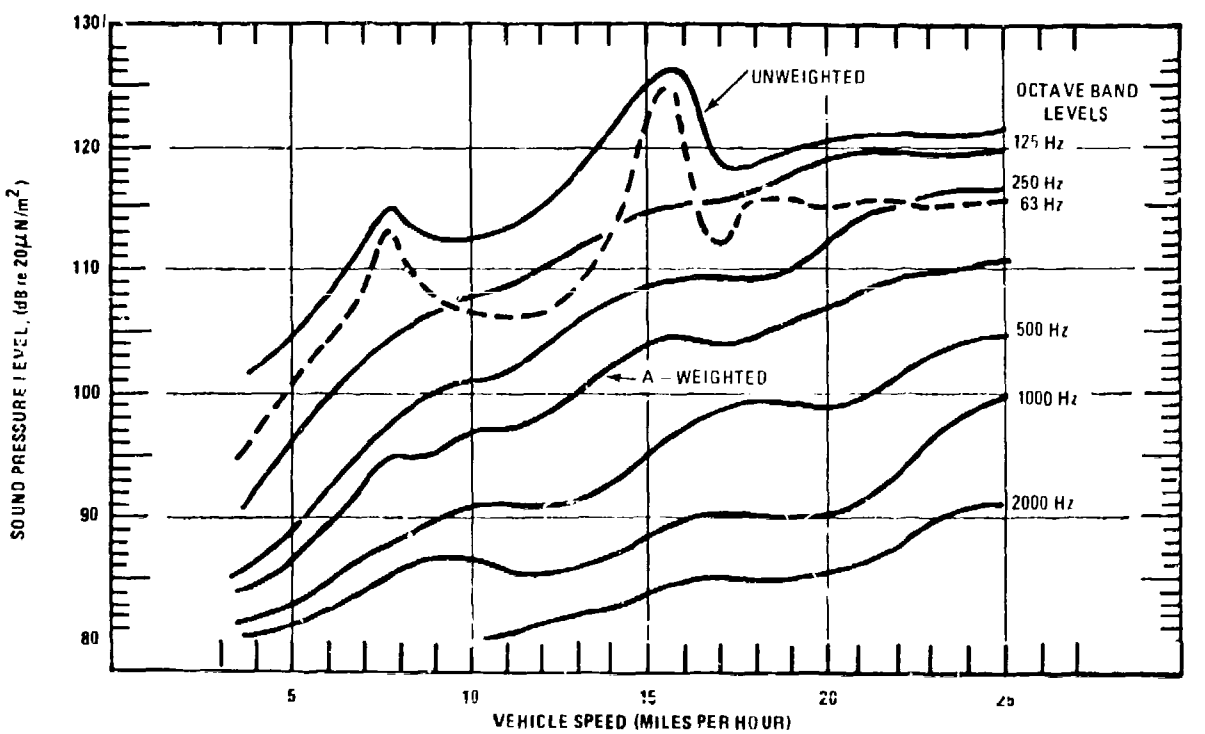

Figure 31. Speed Dependence of Roadwheel-Induced Noise at Driver Position

By the above extrapolation of the curves to 30 miles per hour, it can be seen that the noise due to the roadwheels at 30 mph is essentially as high as that due to a single idler or sprocket. To achieve a vehicle with an overall noise level of 100 dB(A) at 30 mph, the roadwheel noise alone must be reduced to approximately 95 dB(A), which would represent a challenging noise reduction of 17 dB(A). However, at lower speeds, the roadwheel noise has become much lower than that of the idler or sprocket, as can be seen from Figure 31. At 15 mph, the required noise reduction is only 4 dB(A) to achieve 95 dB(A) at the crew position due to the roadwheels alone. The required noise reductions at 15, 20, 25, and 30 miles per hour were summarized in Table 1.

During turns, the steel track guides scrubbed against the roadwheel metal wear plates, which produced a clearly audible noise. Figure 32 compares sound levels measured during turns and while on the straight-away. Comparison of the two spectra show that scrubbing noise is appreciable only in the 400 through 800 one-third octave bands, and is a comparatively minor interior noise source. Therefore, roadwheel metal-on-metal guide scrub noise is secondary to the noise produced due to hull vibrations caused by the rubber tires rolling over the inner track surface.

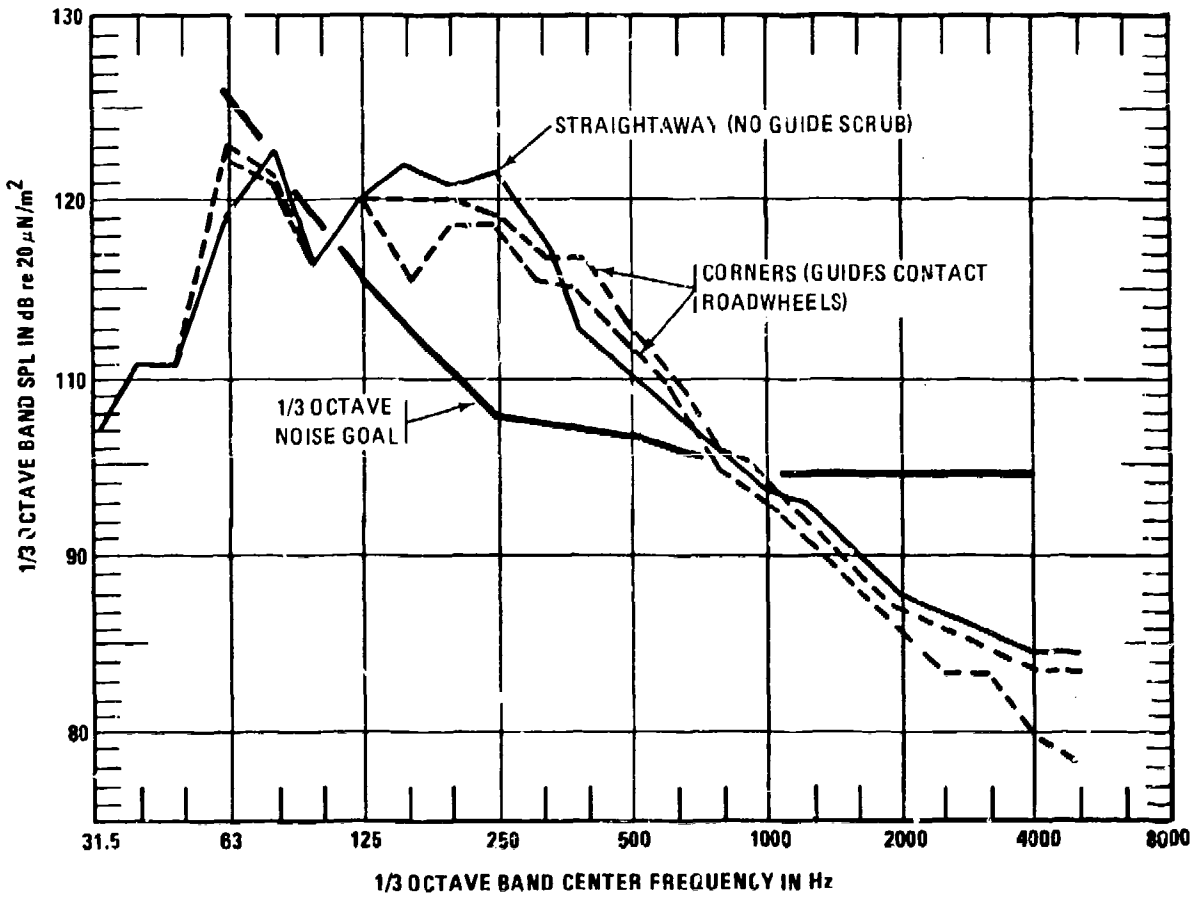

Figure 32. Crew Noise Caused by Track Guide Scrub at 25 MPH

It had been postulated that the right side roadwheel noise would be somewhat contained by the engine compartment, so that less noise reduction would be required for the right hand roadwheel mounts. However, separate right and left side roadwheel measurements showed that noise due to the right and left sides is approximately equal; therefore, noise reducing measures must equally involve roadwheels on both sides of the vehicle.

Towing tests made with both tracks removed (Figure 3) produced noise levels of only 92 dB(A) at 25 miles per hour. This is much lower than the noise produced when one or both tracks are in place. With the tracks removed, the wheel vibrations are due only to the hard rubber tires rolling on relatively smooth asphalt, which results in lower vibration and noise levels.

ANALYSIS OF HIGH SPEED MOVIES

Movies of the sprocket and idler with the vehicle track in motion yielded clues about the dynamic performance of track/sprocket and track/idler engagement. Sample photos (Reference 13) illustrate the track-idler engagement (Figure 33).

The photographs show that the path of the track pins at the idler engagement changes with track speed. Owing to the inertia of the approaching track, a high speed "overthrow" condition occurred at the point where the track engages the idler, as shown on the lower photos of Figure 33. At low speeds, instead of an "overthrow", a sharp impact occurred, as is shown on the upper left photo. A detailed analysis including development of equations relating track/idler impact forces to chordal geometry is developed in Reference 13.

The sprocket films showed the track pin path to be almost identical to that at the idler. In the M113 and similar light-weight tracked vehicles, sprocket carrier rubber tires, rather than the steel sprockets, support the track. Since track shoe position is almost totally governed by the carrier tires, the sprocket acts very much like the idler in its production of interior noise.

The track inertia which causes an overthrow condition at the idler was not apparent in the sprocket films. This appears to result from the different track entry conditions at the front and rear of the vehicle. In the photographs of Figure 33, above, it can be seen that gravity forces acting on the short section of track entering the idler pulls the track down and away from the idler. In contrast, at the sprocket the weight of the entire top track strand tends to force the entering track shoes downward and toward the sprocket, which apparently helps prevent track string overthrow at the sprocket.

In a front drive vehicle such as the M113, the sprocket carrier must cyclically lift each entering track shoe (and others coupled to it in the top strand) as a result of chordal action. The sprocket must also provide the tractive effort for the vehicle. Thus, the forces on the track at the front of the vehicle also tend to prevent overthrow of the entering track at the sprocket.

The changes in track entry geometry with track speed appear to have only a small effect on noise generation. However, it may explain the tendency of idler-dependent noise to increase more slowly with increasing track speed as compared to sprocket-dependent noise.

The overall usefulness of the high speed movies was to confirm that major track block bouncing or rocking motions were not present as well as to confirm the similarity between the idler and sprocket track engagement processes.

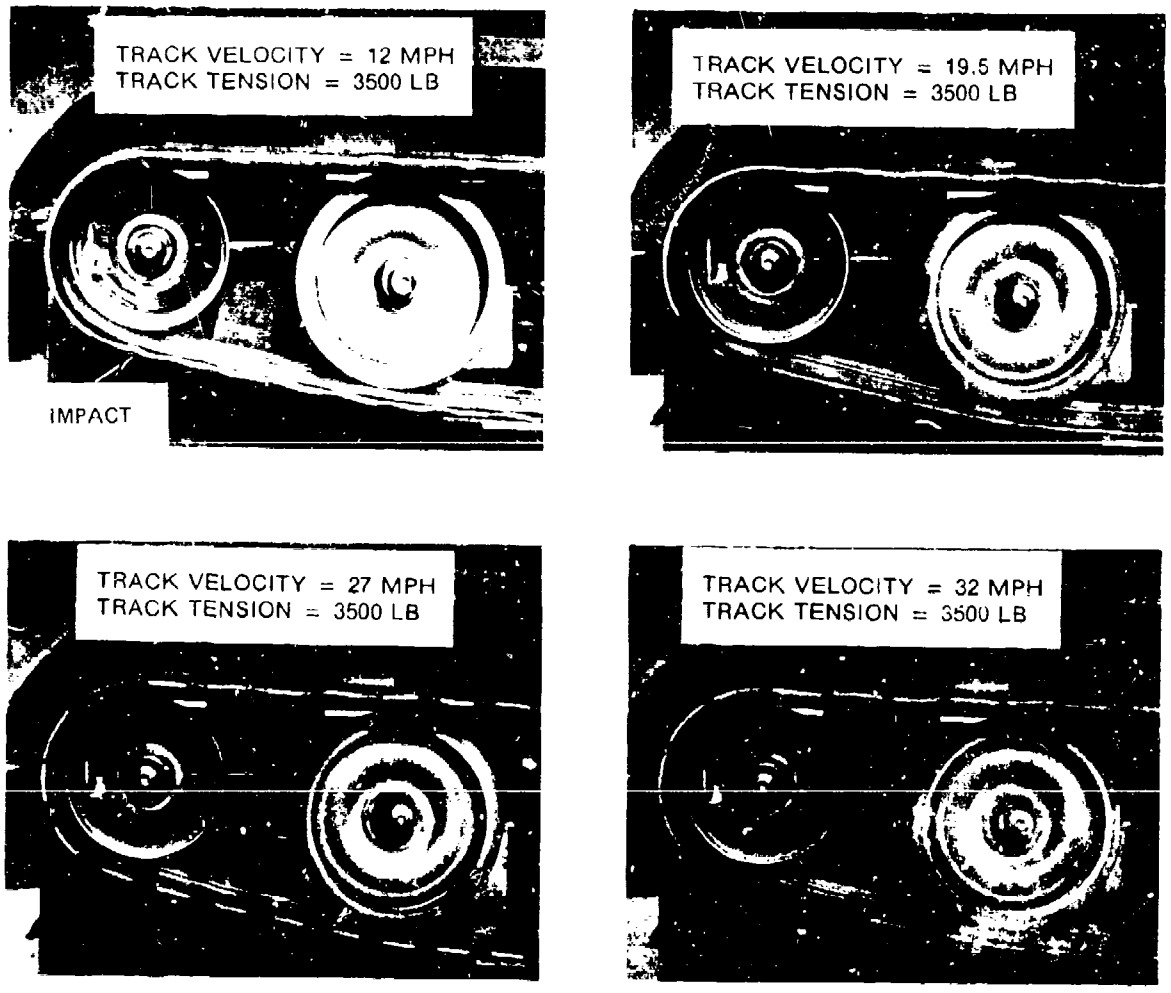

Figure 33. Effects of Track Velocity on Track Shoe Trajectory

IMPEDANCE AND TRANSFER FUNCTION MEASUREMENTS

PURPOSE OF HULL MEASUREMENTS

In this study, mechanical impedance is defined at a given frequency as the amplitude of the ratio of an applied force on the hull or suspension to the resulting velocity in the direction of the applied force.* This is a direct measure of how much vibration will result from a given force, such as may be exerted by an electrodynamic shaker, or by a track shoe impacting an idler wheel. The mechanical impedance is a fundamental tool that is useful in designing effective vibration isolation systems.

The force-to-noise transfer function is the ratio of the absolute value of an applied dynamic force to the resulting interior noise. In this study, the force-to-noise transfer function was used to determine how much M113 interior noise results from a given force caused by the track-sprocket and track-idler forces.

The specific purposes of impedance and transfer function measurements in this study were to:

(1) Establish the frequency dependent relationship between interior noise and forces applied at the idler or sprocket for use with the computer analysis.

(2) Establish relationships between interior noise and vibration velocity at the idler and sprocket mounts. These data, when combined with acceleration data measured during normal vehicle operation, helped determine if vibration control is required for both vertical and horizontal forces, or for one more than the other.

(3) Determine the impedances of the track, idler, and sprocket to estimate the noise reduction available by compliant idler or sprocket designs.

MEASUREMENTS OF IMPEDANCES AND TRANSFER FUNCTIONS

During all measurements reported here, the M113 interior configuration and microphone positions were as described in Data Acquisition. The crew position microphone was not rotated because the noise of the rotation mechanism would have contaminated the low-level sounds produced by the applied vibration. The track was in place for all measurements except during the idler and sprocket hub impedance and transfer function measurements. The vehicle was stationary with the engine "off" for all measurements reported in this section.

With the track removed for idler and sprocket hub measurements, static bearing loads are not present. Unloaded bearings could have different dynamic properties than the same bearings under the static track tension load. To compensate for this effect, the idler bearing was adjusted to a "snug" condition during trackless tests by tightening the adjustment nut. Adjustment was not practical at the sprocket, but the sprocket carrier's own weight adequately loaded the bearing. Acceleration measurements on both sides of both bearings revealed that

---

*To use an analogy, the mechanical impedances describe locations on the M113 hull or suspension in much the way that electrical impedances describe components in circuits.

in all cases the bearings behaved more-or-less as a solid unit below 1250 Hz, which eliminated the concern that the bearing dynamic properties during impedance measurements may not be typical of normal vehicle operation.

The idler track tension adjuster was restrained with steel bands, and the adjuster was pressurized during the idler hub "trackless" vibration measurements. While this certainly eliminated all slack in the adjuster, it may have slightly affected the horizontal measurements of impedance and transfer functions. For the longitudinal track impedance and for idler and sprocket transfer function measurements, a track shoe with the center removed was used. This arrangement provided access to the wheel for the shaker connection.

An electrodynamic shaker provided the vibration force for all impedance and transfer function measurements. The force was transmitted from the shaker via a turnbuckle, extension tube, force transducer, and a 10-32 brass screw (where required), to an aluminum coupling block that was bonded to the track or suspension component (Figure 34). This arrangement provided the adjustable mechanical connection required for application of known dynamic forces to the vehicle.

The relatively slender 3-inch long 10-32 brass extension screw provided a mechanically weak link to protect the force transducer and shaker should an abnormal force be developed. Buckling of the extension screw could have clouded the validity of the data. However, no obvious buckling of this screw was visible and vibration readings were stable when the brass screw was grasped, which is taken as evidence that significant buckling did not occur.

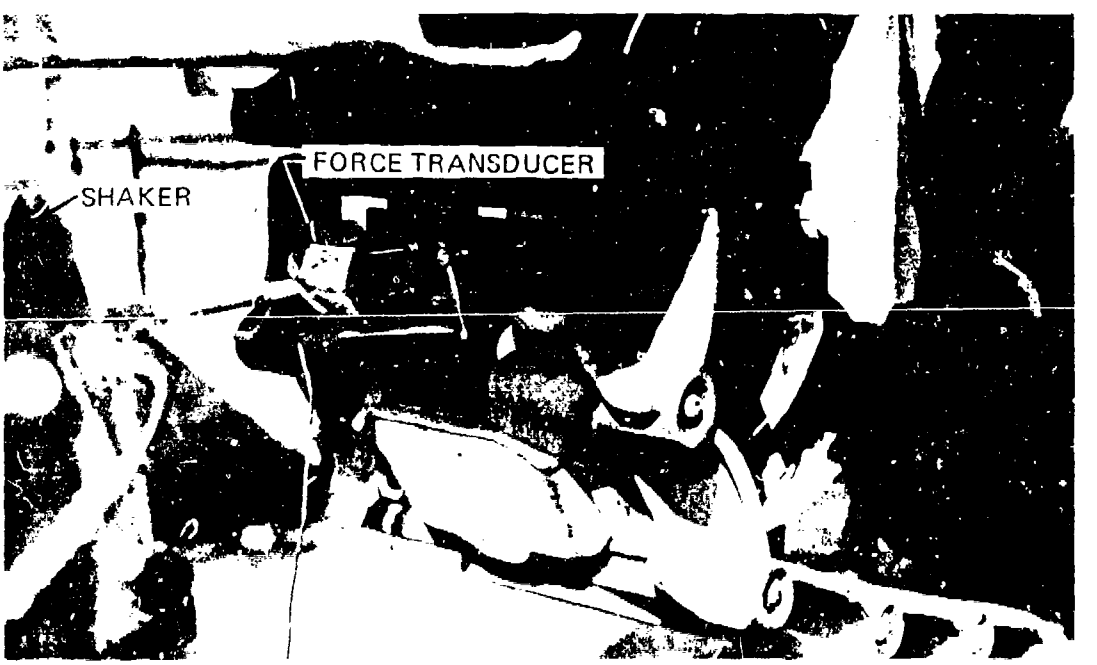

Figure 34. Typical Shaker, Force Transducer, and Accelerometer Setup for Impedance and Transfer Function Measurement

The input signal to the electrodynamic shaker was 1/3 octave pink noise. The nominal 5-pound RMS force produced by the shaker produced clearly audible noise inside the vehicle in each one-third octave band. Higher force levels were not used because the higher vibration levels produced occasional hull rattles of undetermined origin.

All acceleration, force and noise data used in this program were read on site and were also recorded on tape for future reference.

RESULTS OF IMPEDANCE AND TRANSFER FUNCTION MEASUREMENTS

The noise in the crew area produced by a 1-pound RMS 1/3 octave pink noise force acting on the left idler rim is shown in Figure 35. Except in the 250 Hz octave band, the vertical force produced from 1 to 16 dB more noise compared to the horizontal force. In the important 250 Hz octave band (where the most noise reduction is needed) the interior noise from the two directions was approximately equal.

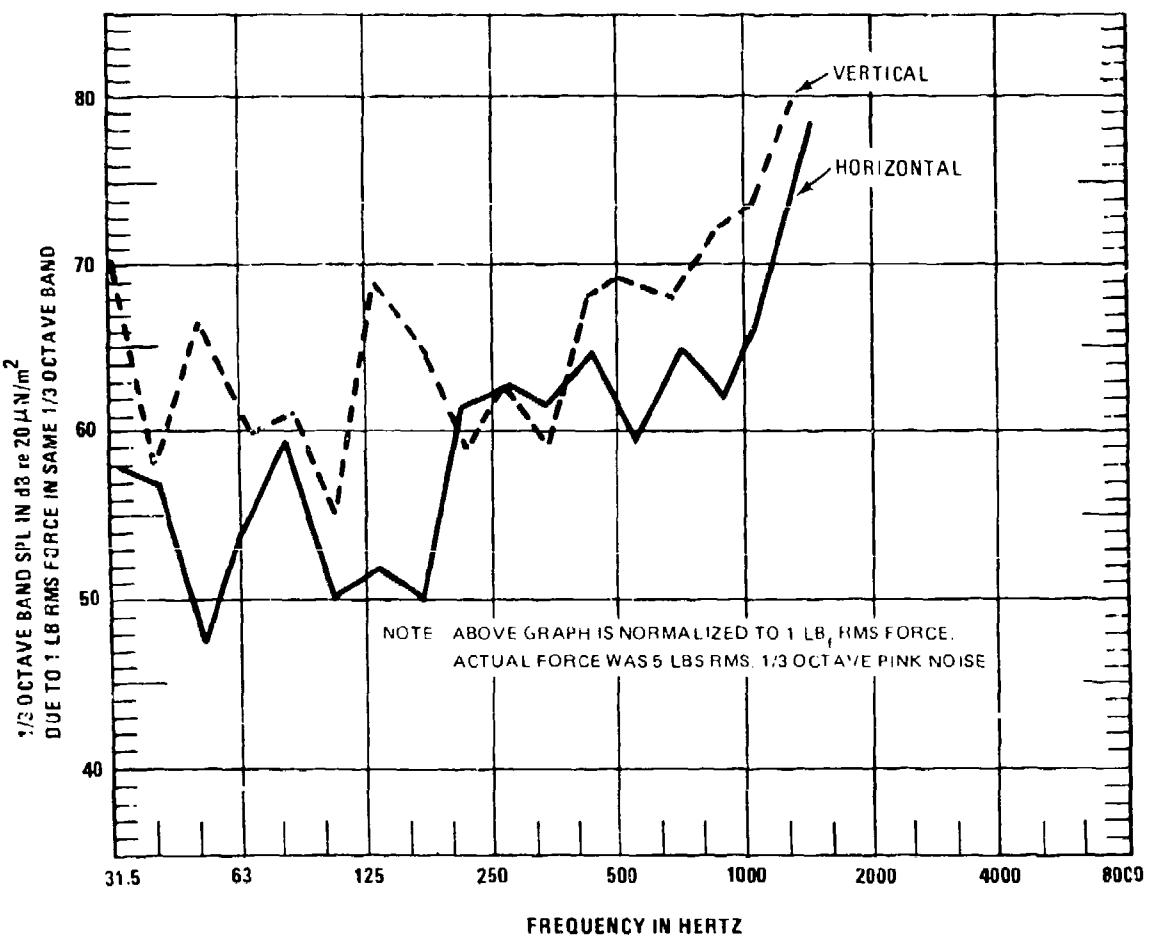

Figure 35. Crew Area Force-to-Noise Transfer Function at Left Idler Wheel Rim with Tracks in Place

Figure 36 shows the corresponding measured noise transfer function at the driver's position for a 1-pound RMS force acting on the left idler rim. At 250 Hz and above, the sound levels between the driver and crew positions are remarkably similar. In the 125 and 63 Hz octave bands, however, the driver's position noise levels are significantly higher. This may be an acoustic intensification due to the corner location of the driver's position, the close proximity of the driver's position to vibrating panels, or to a "small room effect." The latter phenomenon may occur when a cavity dimension is smaller than or comparable to the wave length of a sound.

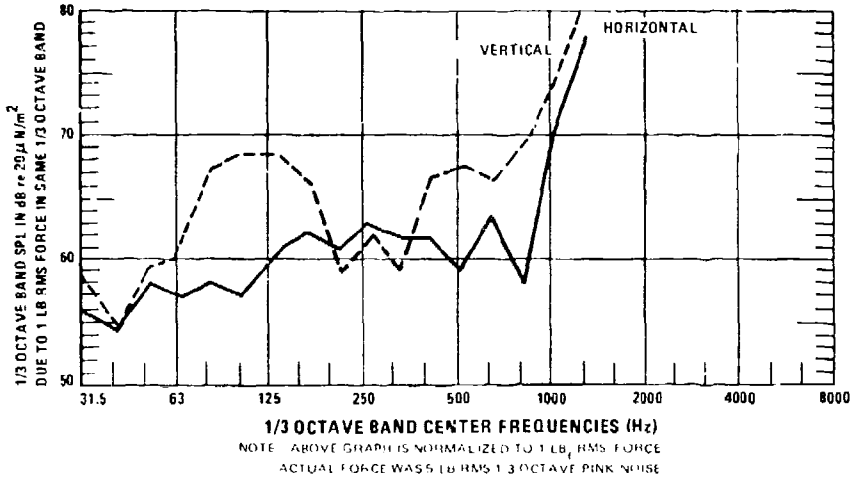

Figure 36. Driver's Position Force-to-Noise Transfer Function at Left Idler Wheel Rim with Tracks in Place

The noise levels produced by vibratory forces applied to the right and left sprockets are shown on Figure 37. At and above 250 Hz, the noise levels are nearly the same. However, where horizontal force was applied to the left sprocket, the resulting noise was, in general, slightly lower.

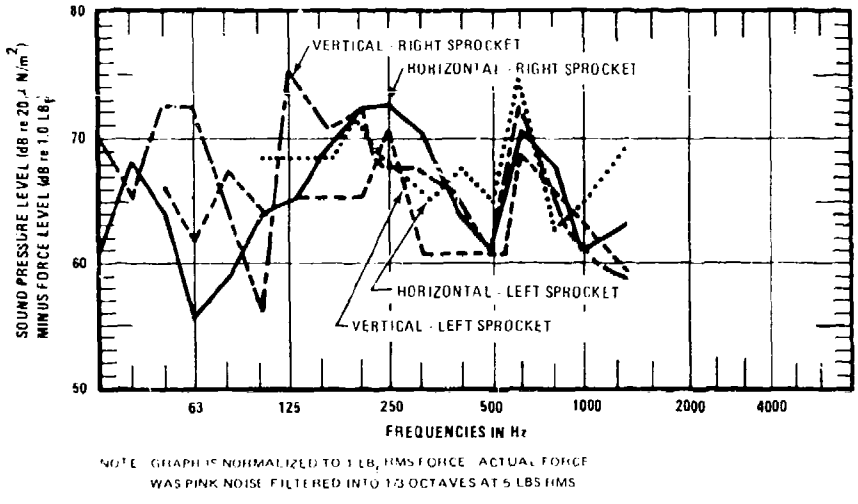

Figure 37. Driver's Position Force-to-Noise Transfer Functions at Both Sprockets with Tracks in Place

The dynamics of the M113A1 track-idler and track-sprocket systems were briefly investigated. Specifically, the vibration isolation properties of the rubber inner track pads and rubber sprocket carrier cushions were of interest. The track shoe resting vertically against the front of the sprocket or the rear of the idler was driven horizontally by the shaker. The setup was similar to that shown in Figure 34 above, except that the metal part of the track shoe was driven by the shaker while acceleration of the idler or sprocket carrier and track shoe were measured.

The curves of Figure 38 show the differences in acceleration response between the track shoe and the idler rim or the sprocket rim. This difference indicates that the compliant rubber track and sprocket components are capable of providing vibration isolation at above 500 Hz, at least in the radial direction for small vibration amplitudes.

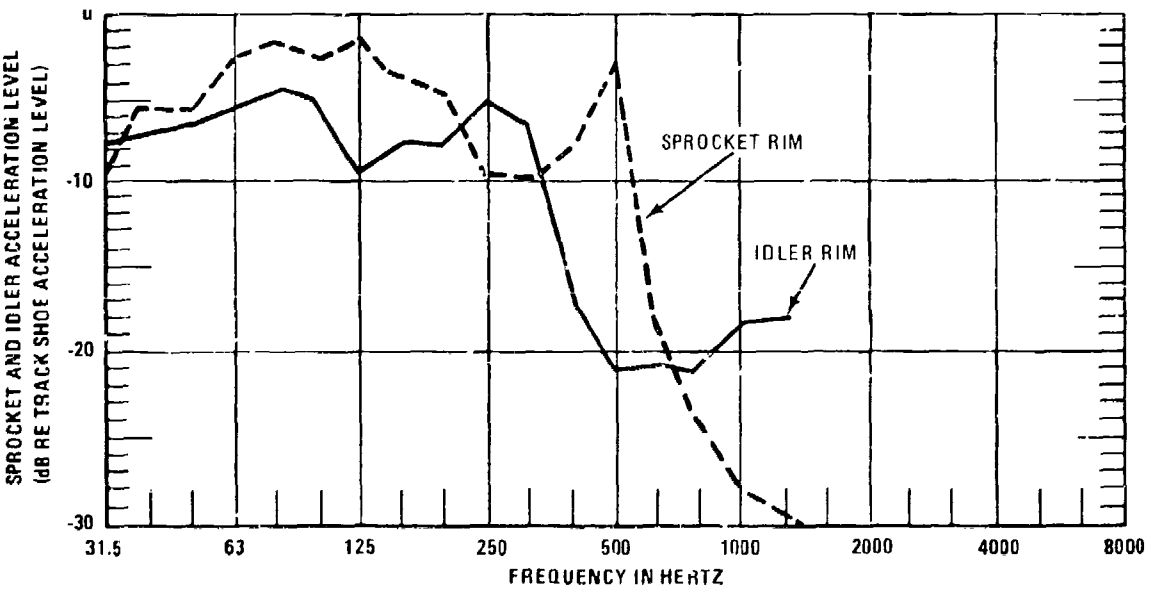

Figure 38. Vibration Isolation Effect of M113 Inner Track Pad on Idler or Sprocket Rim

The upper track strand impedance magnitudes are shown in Figure 39. In the frequencies of primary interest (between 125 and 500 Hz) the upper track strand behaves substantially as if it were a mass in response to forces perpendicular to its length.

The transverse impedance magnitude at the center of the track shoes is about 10 dB greater than that at the track pins at frequencies between 80 and 315 Hz. The impedance magnitudes are nearly the same above 315 Hz. At below 200 Hz, the longitudinal impedance exceeds the two measured transverse impedances.

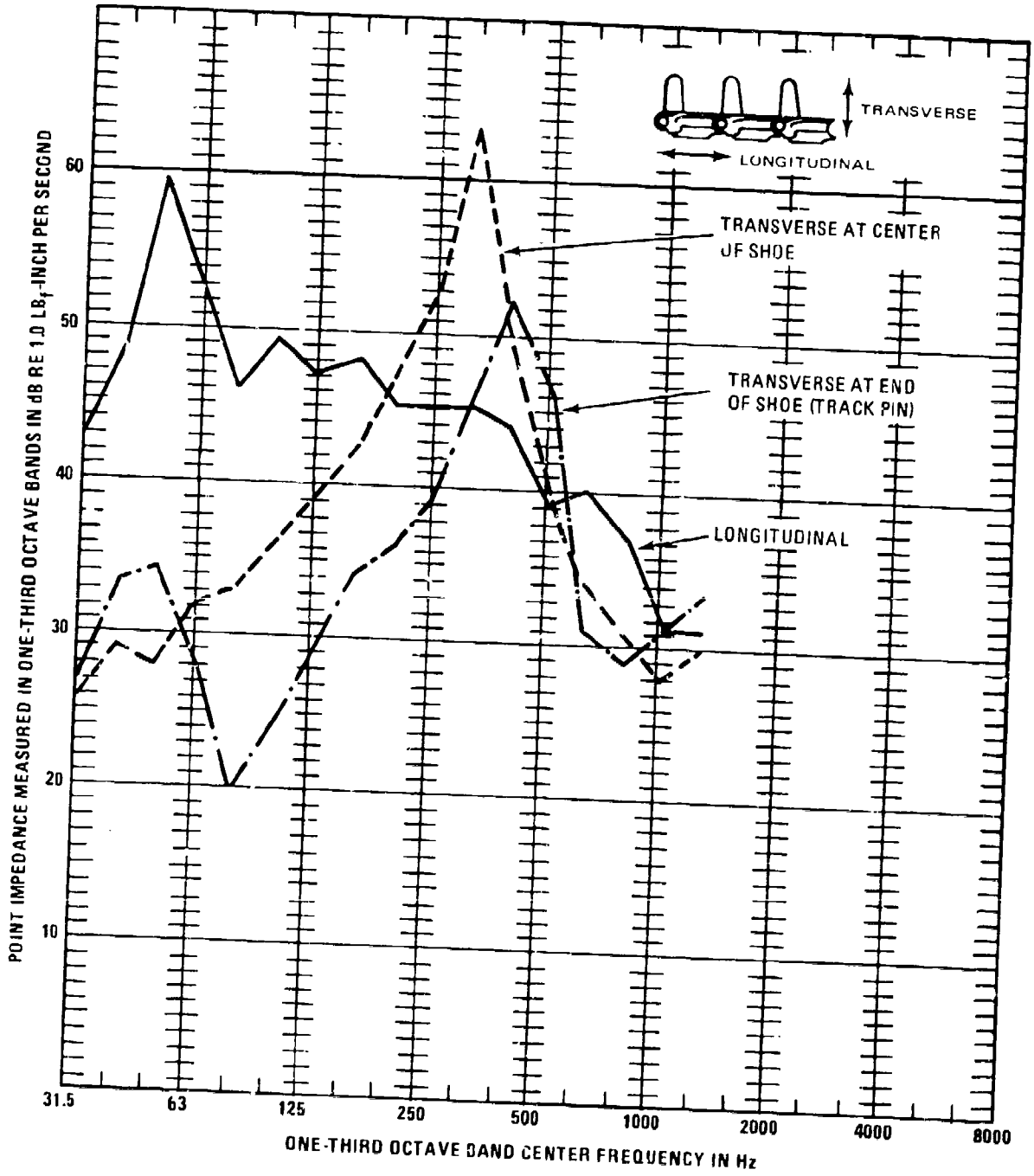

Figure 39. Track Impedance Magnitudes

One way to reduce the transmission of vibration into the hull is to insert a cushion between the hull and the idler or sprocket. From equations B-1 and B-2 of Appendix B, it can be deduced that these cushions, being of low impedance, should contact the track at the location of its highest impedance. Namely, this is at the center of the track shoes.

Significant conclusions based directly on the impedance and vibration measurements are below:

(1) For a given amplitude of horizontal and vertical force applied to the idler wheel rim, the resulting interior noise is approximately equal in the 250 Hz octave band; but the vertical force produced about 5 dB more noise in the 125 and 500 Hz bands.

(2) A given horizontal force at the sprocket rim, when averaged from 100 to 630 Hz, will produce only 2 dB less interior noise than will the same vertical force.

(3) A given vibratory force applied at either the left or right sprocket will result in approximately equal interior noise. Therefore, the engine compartment does not attenuate noise induced by the right sprocket.

(4) Idler or sprocket compliances should act on the center of each track shoe for the optimum vibration isolation effect.

(5) The track is quite "hard" (has high impedance) below 200 Hz to motion parallel to the track strand. Even small accelerations in this direction will be associated with relatively high forces on the idler or sprocket.

(6) Vibration along both horizontal and vertical axes must be controlled for effective noise reduction since significant horizontal and vertical accelerations are both present. An effective noise reducing compliant idler or sprocket should include both tangential as well as radial compliance.

(7) The present rubber track inner pads reduce idler noise at 400 Hz and above, while the rubber sprocket tires significantly attenuate vibration at 630 Hz and above.

NOISE REDUCTION ESTIMATES OF COMPLIANT IDLER RIMS AND HUBS

BACKGROUND

Recent research suggests that increased compliance at the idler or sprocket rims effectively reduces the hull vibration which causes interior noise (References 7, 12, and 13). Of particular interest is a practical noise reduction technique reported in Reference 13. The report documents a 5 dB unweighted noise reduction by giving the steel idler rim a rounded or crowned contour. This achieved an increased compliance by effectively utilizing the rubber inner track pads as a cushion. A sketch of two other compliant rim and hub concepts appears in Figure 40. It should be understood that in a practical design, the compliant elements would probably be recessed beneath the idler rim for protection.

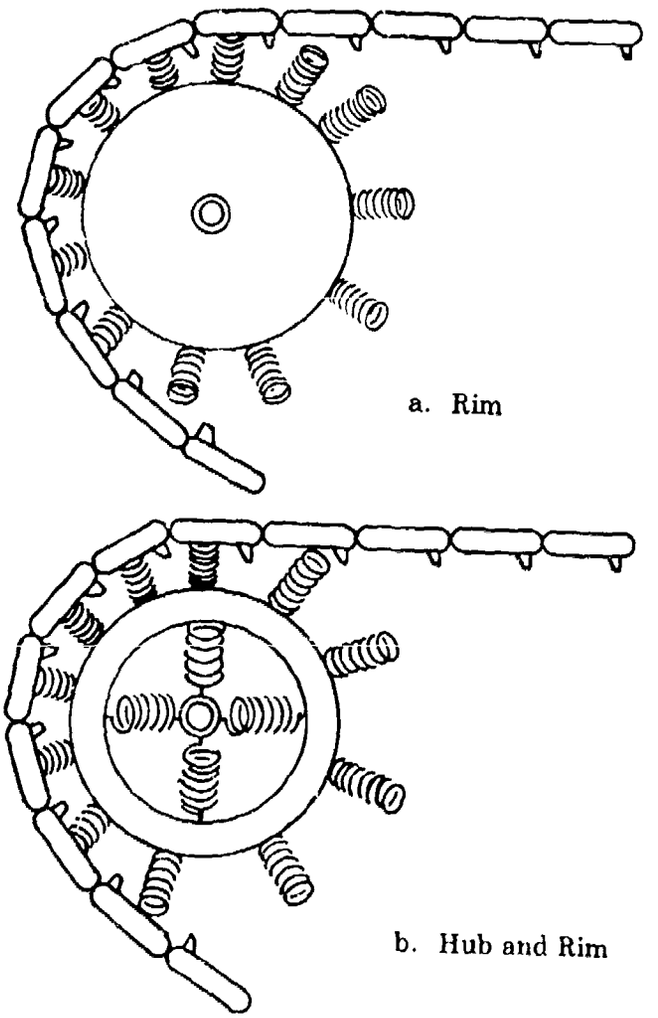

NOTE: THE EXPOSED COIL SPRINGS ARE SCHEMATIC REPRESENTATIONS OF COMPLIANT ELEMENTS FOR ILLUSTRATION PURPOSES ONLY

Figure 40. Compliant Rim and Hub Concepts

ESTIMATION OF NOISE REDUCTIONS

To develop a better understanding of how much wheel rim compliance would achieve the noise reduction goal, two separate analyses were made as a part of this program. In addition, the results are compared to the independent theory for predicting interior noise from velocity of impact developed in Reference 13. These analyses are reviewed below:

Simplified Vibration Isolator Analysis

For this analysis, the wheel rim compliance was considered to act as a simple vibration isolator or cushion acting in the radial direction. The vibration isolation effectiveness (Figure 41) in one-third octave bands was calculated by using the track and idler rim impedance data from Impedance and Transfer Function Measurement. Production M113 track-to-idler stiffness is 60,000 lb_f/inch. The 60K lb_f/inch curve of Figure 41 is the dynamic stiffness of the M113 idler.

The vibration isolator calculations were then repeated for an idler having both rim and hub compliance, this time utilizing both the hub and idler/track impedance measurements and assuming rim mass of 30 lbs and a rim compliance of 14,000 pounds per inch. The resulting isolator efficiency versus frequency values are plotted on Figure 42. The analysis procedures are presented in greater detail in Appendix B.

Vibration isolator theory predicts that reduction of M113 idler and sprocket noise to the noise goal is possible. However, the compliances required may not be achievable in practice.

Computer-Assisted Force Analysis

The computer graphics (Appendix C) show estimated noise levels for both vertical and horizontal forces. Horizontal and vertical forces were calculated in one-third octave bands for various rim compliances. The idler rim stiffnesses in the radial and tangential directions were assumed to be equal. Interior noise estimates were derived from these calculated forces by using the horizontal and vertical force-to-noise transfer functions from Impedance and Transfer Function Measurements. The separate noise estimates due to horizontal and vertical forces were A-weighted and combined on an energy basis to obtain a total noise estimate (Figure 43).

In the analysis of the two softest idler and sprocket rims, the computer generated a rather wide (20+ dB) scatter of data between track shoes. Therefore, the 23,000 and 3,000 pound per inch data in Figure 43 may not be accurate. Also, although the sprocket noise estimates agree very well with actual measurements, the idler data are 14 dB(A) too high at 30 mph. This could be due to the preliminary analysis, or to the transfer functions utilized.

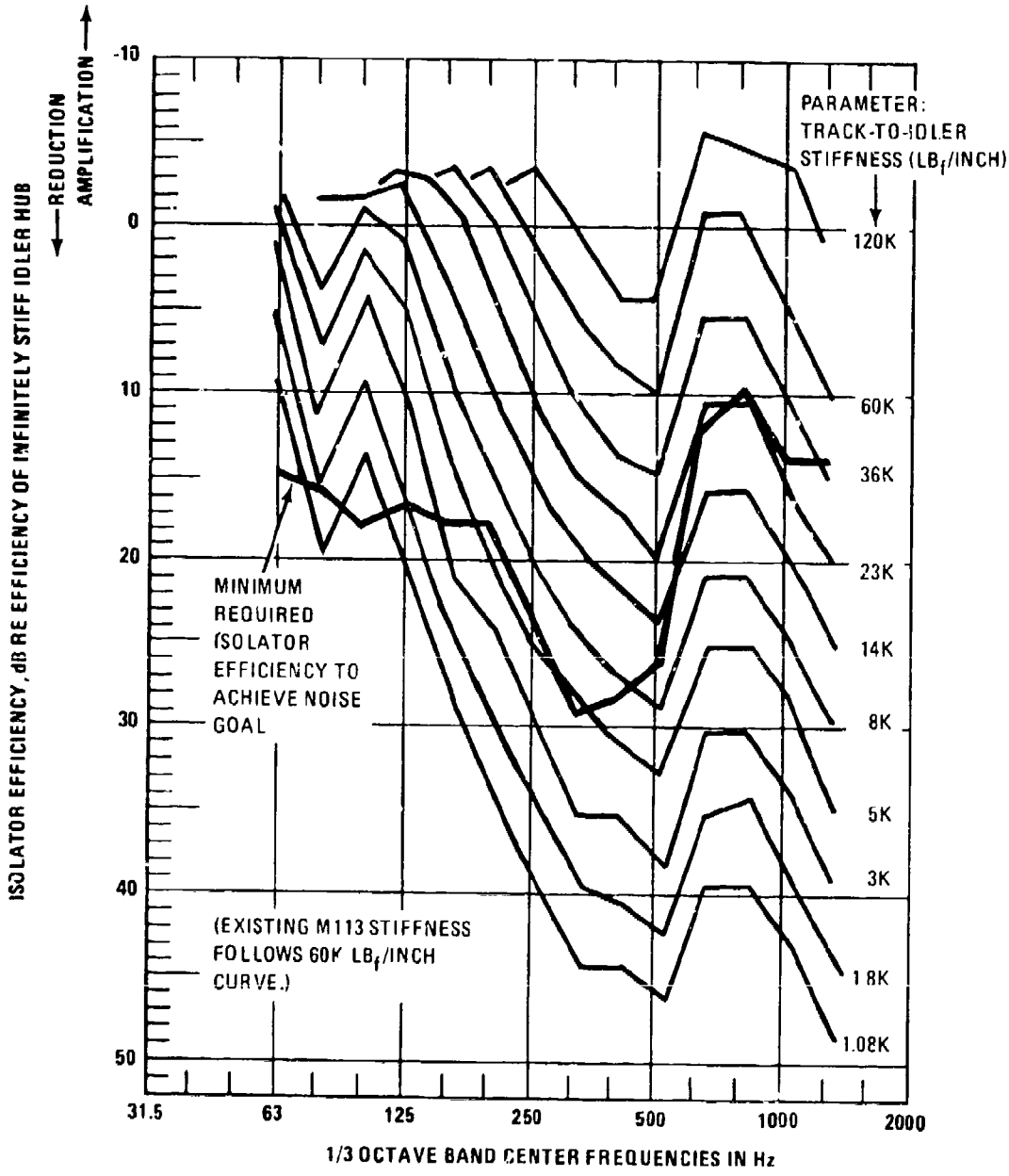

Figure 41. Effect of Rim Stiffness on Isolator Efficiency with Infinitely Stiff Hub

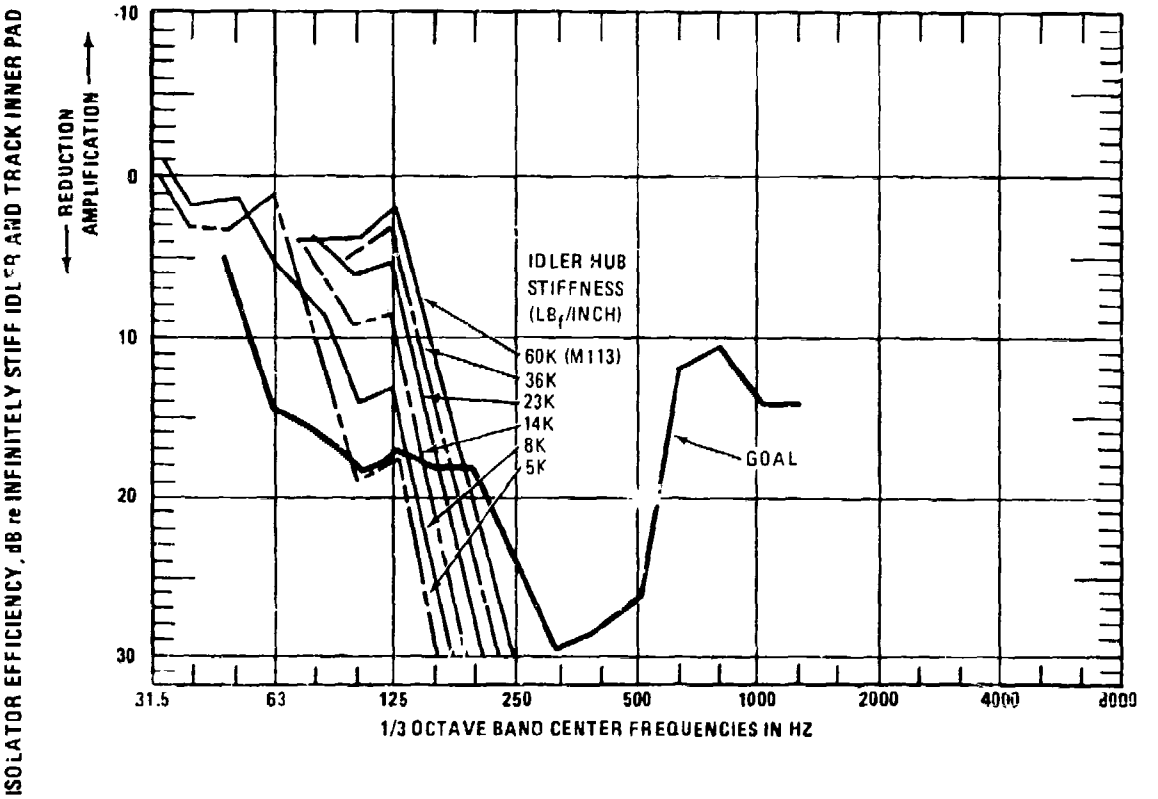

Figure 42. Effect of Hub Stiffness on Isolator Efficiency with 14K LB_f/Inch Idler/Rim Stiffness

Simplified Impact Force Analysis

The simplified impact force analysis is a third noise reduction estimate technique. At the present stage of development, this method will predict C-weighted noise level changes which would result from the design parameters which change the track block mass, idler-track interface compliance, or track block velocity of impact. The resulting relationship between noise level and compliance is 3 dB per halving of the total stiffness between the idler wheel and the track shoe effective mass. Details of the procedure and assumptions made are contained in Reference 13.

According to the impact force estimate, the benefit of improved compliance is cushioning of the track impacts on the idler. However, no noise reduction is assigned to other vibration isolation effects which may reduce higher frequencies more effectively than lower frequencies. An A-weighted noise reduction estimate would then be expected to increase more rapidly than 3 dB per halving of stiffness had these effects been considered.

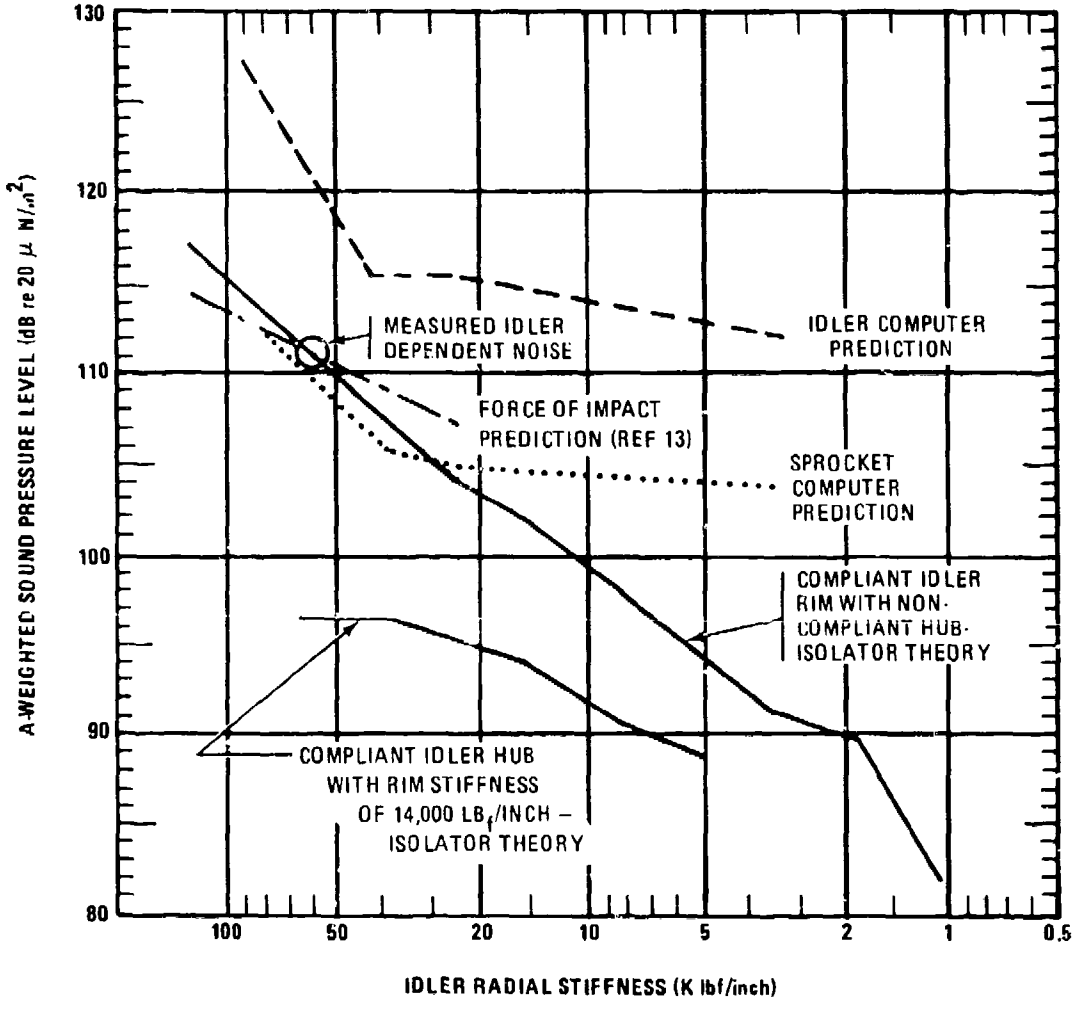

Figure 43. Predicted A-Weighted Noise Levels for Compliant Idler or Sprocket Rims and Hubs at 30 MPH.

Measured idler noise reductions correlate very well with the Impact Velocity Analysis predictions. Up to 5 dB C-weighted noise reduction was predicted, and then demonstrated, on an M113 APC by softening the effective idler rim compliance from 71,000 lbs/inch to 32,000 lbs/inch and increasing the idler diameter from 17.25 to 21.00 inches. Only C-weighted data were measured.

Figure 43 summarizes the predictions made by the simplified isolator analysis, the computer-assisted force analysis, and the impact velocity methods.

In all three of the above noise estimation techniques, no provision is made for possible steel-on-steel impacts at the sprocket. This omission is justified for the M113 because most of the track vibration forces are exerted on a rubber cushion mounted to the sprocket carrier, rather than on the steel sprocket teeth.

This fact was demonstrated in an experiment where the interior noise was not reduced after removal of the sprocket teeth. During these measurements, the vehicle was tethered to a test stand so that the tracks did not touch the ground (Reference 7). That the steel-on-steel impacts are relatively minor in the M113 and MICV was also confirmed by results of independent tests at FMC and in conversations with FMC track and suspension engineers. However, M113's with double pin tracks do not have such cushions and sprocket impacts may generate higher interior noise levels.

CONCLUSIONS BASED ON NOISE REDUCTION ESTIMATES

All three estimates show a noise reduction for decreased stiffness at the wheel rim. For stiffnesses above 25,000 pounds per inch, the force analysis and simplified vibration isolator analysis predict similar noise reductions of 4.5 dB(A) with halving of stiffness. The velocity of impact analysis predicts a 3 dB(C) noise reduction for the same stiffness change.

At the present stage of development, none of the three individual noise reduction estimates alone create a completely convincing prediction of the effects of increased compliance on interior noise. However, considered together, it is evident that increasing the compliance at the idler and sprocket rims can significantly reduce interior noise. These estimates, along with experimental results documented in Reference 13, yield the conclusion that interior noise will be reduced about 4 dB(A) for each halving of rim stiffness.

APPENDIX A

LIST OF INSTRUMENTATION AND DATA DEVELOPED

Running Tests

- Lockheed Electronics Store 4, 4-channel FM tape recorder
- Two General Radio Sound Level Meters, Model 1933, equipped with two General Radio Model 1962 1/2'' electret condenser microphones on extension cables
- General Radio Microphone Calibrator, Model 1562
- Six CEC Accelerometers, Model 4-281-001
- Four Endevco Type 2221D Accelerometers, with Type 2641 Charge Followers
- General Radio Vibration Calibrator, Model 1557A
- Ectron Model 418 Strain Gage Signal Conditioner
- Weston Model 750 DC Tachometer Generator, driven by a Track Test 5th Wheel
- DC Tachometer Generator, driven by final drive input member
- Esterline Angus X-Y Recorder, Model 2411 TB
- Hewlett-Packard 1/3 Octave Band Analyzer

Impedance and Transfer Function Measurements

- Two Bruel & Kjaer 1'' Microphones, Type 4131, with random incidence correctors
- Two Bruel & Kjaer Sound Level Meters, Type 2209
- Two Bruel & Kjaer Octave Band Filters, Type 1613
- Goodman 50 lb Shaker
- Wilcoxon Impedance Head, Model Z-602
- General Radio Pink Noise Generator Model 1382
- B&K 1/3 Octave Band Filter, Type 1616
- General Radio 1/3 Octave Band Analyzer, Type 1564A
- Nagra IV-SI Magnetic Tape Recorder
- Honeywell SAI-2 Real Time Analyzer/Digital Averager

DATA DEVELOPED

Source Definition Recordings

Table A-1 lists the measured parameters and vehicle operating conditions which were recorded during gradual vehicle accelerations and decelerations. The data format is analog (FM) magnetic tape conforming to IRIG Standard Document 106-66, Intermediate Band, 4-Channels on 1/4-inch tape, recorded at 30-inches per second. The passband was DC to 10,000 Hz.

TABLE A1. RECORDED DATA

	VIBRATION (ACCELERATION)												NOISE		
	HULL TOP PLATE	FRONT LEFT FLOOR	REAR LEFT FLOOR	REAR RIGHT FLOOR	IDLER MOUNT HORIZONTAL	IDLER MOUNT VERTICAL	FINAL DRIVE HOUSING HORIZONTAL	FINAL DRIVE HOUSING VERTICAL	ROADARMS NOS. 1, 3, 5 (PARALLEL)	ROADARMS NOS. 1, 3, 5 (PERPENDICULAR)	ROADARM BENDING STRAIN	FINAL DRIVE OUTPUT TORQUE	DRIVER NOISE	CREW NOISE	VEHICLE SPEED
BASELINE-SELF POWERED	X	X	X		X	X	X	X	X	X	X		X	X	X
BASELINE-TOWED	X								X	X	X		X	X	X
ROADWHEELS ONLY-TOWED	X								X	X	X		X	X	X
SPROCKET ONLY-ON STAND		X					X	X				X	X	X	X
IDLER ONLY-ON STAND	X			X	X	X							X	X	X

Source Definition Analysis

Octave band and one-third octave band data were developed from the tape recordings for most of the runs and are in the form of graphs of octave band level versus vehicle speed (octave band data) or numerical listings (one-third octave band data).

Impedance and Noise Transfer Function Data

Impedance and noise transfer function values were developed from measurements of force, acceleration, and sound pressures. Transducer signals were recorded on tape (2-channel, direct, at 7-1/2 inches per second) for possible future reference.

High Speed Movies

Approximately 4,400 feet of 16-mm Ektachrome EF film was used to record idler and sprocket track engagement at various track tensions and vehicle speeds. This footage was edited into a 400-foot reel containing sections of each run.

Computer Program

A digital computer program was developed to predict the motion of and the forces exerted by a single track shoe as it engages a wheel. The compliance between the wheel and track may be varied to determine the effect on noise. Inputs are the speed, track pitch, track bushing spring rates, wheel radius, track shoe mass, track shoe moment of inertia, and the measured horizontal and vertical vibratory force-to-noise transfer functions. In the present form, the outputs are graphs of instantaneous forces exerted on the wheel and one-third octave band noise levels.

REFERENCES

1. "T91E3 Type Rubber Mounted Sprockets with Harris Products Co. #69001 Rubber Bushings," G. L. Benson, Cadillac Motor Car Division — General Motors Corporation, Cleveland Tank Plant (Test and Development Department TE-20), Report No. 137, June 17, 1952.

2. "Rubber Tired Sprocket Hub (International Harvester Company Design) Effect on T 141 Vehicle Vibration," Warren J. Young, Cadillac Motor Car Division — General Motors Corporation, Cleveland Tank Plant (Test and Development Department TE-20), Report 1201, March 11, 1954.

3. "Vibration Comparison of Four Types of Tracks," J. R. Prior, Cadillac Motor Car Division — General Motors Corporation, Cleveland Tank Plant (Test and Development Department TE-20), Report 1203, January 12, 1956.

4. "Durability Test of International Harvester Rubber Tired Hub and Sprocket Assemblies," L. W. Hoberecht, Cadillac Motor Car Division — General Motors Corporation, Cleveland Tank Plant (Test and Development Department TE-20), Report No. 850, Test Requested by International Harvester Company for M75 Vehicle, May 20, 1954.

5. "Engineering Testing Division Automotive Branch Report on Noise and Vibration Test of M113 Armored Personnel Carrier with Standard and Short Pitch Tracks," Ronald P. Lenert, Ordnance Test Activity, Development and Proof Services, Aberdeen Proving Ground, Maryland, Report No. DPS/OTA-166, September 1962.

6. "Automotive Division Report on Component Development Test of Wire-Link Track, Tested in Comparison with Standard T130 Forged Track," John P. Sobczyk, Development and Proof Services, Aberdeen Proving Ground, Maryland, Report No. DPS-850, DA Project No. 548-12-001, February 1963.

7. "Development of Measurement Techniques for the Analysis of Tracked Vehicle Vibration and Noise," Charles L. Bates and Cecil R. Sparks, Southwest Research Institute, SWRI Project No. 04-1421, Contract DA 23-072-AMC-144 (T), October 1964.

8. "MICV XM723 Test Report: Internal Noise Survey of the Prototype Vehicle," R. B. Hare, Ordnance Engineering Division, FMC Corporation, FMC OED Technical Report 2762, Contract DAA E07-73-C-0100, October 1964.

9. "High-Frequency Vibration Isolation," E. E. Ungar and C. W. Dietrich, Journal of Sound and Vibration, April 1966, Volume 4, Part 2, page 224.

10. "XM 551 Noise Reduction Program — Phase I," J. R. Wiley, General Motors Proving Ground, Milford, Michigan, MPG 187, P.O. No. NEP-63571-KM and NEP-63570-KM, June 13, 1966.

11. "Return Idler Wheels: Various Designs Compared for Durability and Effect on Vehicle Noise and Vibration Levels," R. N. Bibbens, Ordnance Engineering Division, FMC Corporation, FMC OED Technical Report 722, October 1969.

12. "Tracked Vehicles: Noise and Vibration Control Study Using a Reduced Scale Model," Thomas R. Norris, Bolt Beranek and Newman Inc., San Francisco, California, BBN Technical Report No. 3031, prepared for Mr. Donald Rees, U. S. Army Tank Automotive Command, Warren, Michigan, Report 12099.

13. "Study of Track-Idler Engagement and Its Effect on Interior Noise," T. B. Van Wyk, FMC Corporation, San Jose, California, Technical Report 2976, April 1976.

14. "Noise Levels in the Passenger Areas of a Standard and a Product Improved M113A1 Armored Personnel Carrier," Howard H. Holland, Jr., U. S. Army Human Engineering Laboratories, Aberdeen Proving Ground, Maryland, Letter Report No. 124, October 1970.

APPENDIX B

ANALYSIS OF ISOLATION EFFECTIVENESSES OF COMPLIANT IDLER RIMS AND HUBS

Calculation of Noise Reduction of Compliant Rim

In this appendix, the noise reduction of compliance at the idler or sprocket rim is estimated by a simple linear analysis based on the vibration isolation effectiveness of the compliance, and on impedance measurements. The noise reduction of an idler or sprocket wheel with an additional compliance at the hub is also calculated, again based on impedance measurements. For purposes here, the idler and sprocket are considered identical, as sprocket tooth contact is not a major noise source. Only the idler noise reduction is estimated; the sprocket noise reductions would, in general, be similar.

The simplified linear analysis described below was used to calculate the noise reductions of the compliant rim design. The formulae for isolator effectiveness are taken from Ungar and Dietrich (Reference 9). The simplified physical model used is shown in Figure 40. To simplify the calculations, the entering track shoe is the only one in contact with the idler wheel, and only vertical forces are considered. Tangential forces are assumed to be zero. In this simplified model, the track shoe impact velocity against the wheel is assumed to be constant, regardless of compliance changes.

The required inputs to this noise level estimate are:

(1) Impedance magnitudes measured on an M113 idler rim and track, and

(2) Idler noise levels measured in an M113 vehicle.

For a simple conceptual model, where motions along only one line are considered and where the mass of the compliant element has no significant effect, the isolation effectiveness obeys

$$E = 1 + \frac{M_I}{M_S + M_R}$$

where M_I denotes the mobility (i.e. the complex ratio of vibration velocity to force) of the resilient element (the "isolator"), M_S the mobility of the track (the vibration source), and M_R the mobility of the idler spindle (the receiver) (Reference 9). The vibration amplitudes of the idler spindle are considered to be proportional to those of the hull. In general, all of the mobilities are complex numbers. However for purposes here, the mobility of the resilient element is taken to be that of an undamped massless spring:

$$M_I = iw/k$$

which is purely imaginary, where k denotes the stiffness of the resilient element, w represents the radian frequency, and $i = \sqrt{-1}$.

In addition, the idler spindle impedance is assumed to be purely real, and was determined by experimental measurements shown in Figure B-1. The assumption of a real impedance at the idler spindle is plausible because at frequencies above 100 Hz, the frequency interval be-

tween hull modes is expected to be smaller than the bandwidth associated with a modal response (for an estimated hull loss factor of 0.02). In other words, the hull responds as if it were an infinite plate which has a purely real mobility (Reference 9).

The absolute value of the track mobility was taken from the data presented in Figure 39, which was derived from measurements made at the track pins. The real component of track impedance taken as $Re\{M_S\} = 0.01$ in/sec-lb_f, corresponding to the lowest damping measured, and the imaginary component was calculated so that the absolute value corresponds to Figure 39.

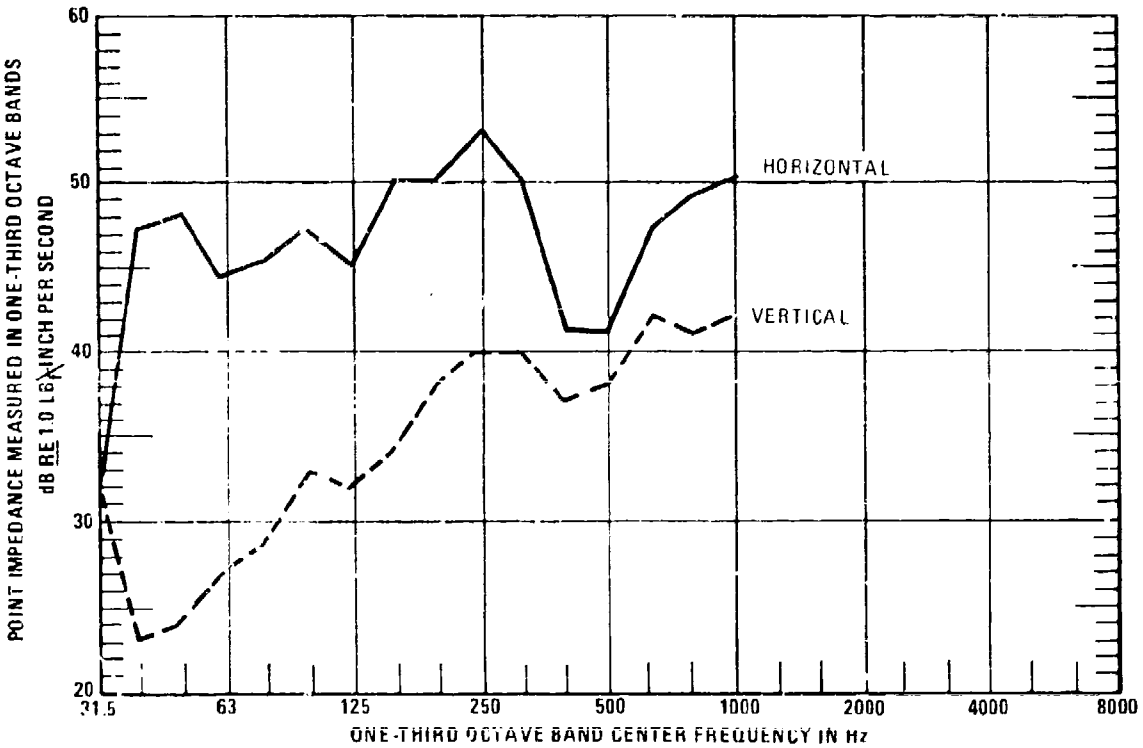

Figure B1. Vertical and Horizontal Left Idler Spindle Impedance Measured with Idler Wheel Removed

This model is naive in several respects, especially in that the measured impedance is for a straight track section, while the actual track in the region of interest is curved around the idler. Also, for very soft compliances, the amount of impacting against the idler may vary in unpredictable ways.

The simplified model is conservative in that the track mobility value used in calculations is the greatest measured, which is at the track pins. If an actual design can support the track at the center of each block rather than at the pins, the mobility is an average of 10 dB lower, and a greater isolator effectiveness is obtained.

The predicted noise reduction of this model was shown in Figure 43 in Section 4. A rim compliance of 5000 lbs_f/inch gives 20 dB(A) which would be a very significant noise reduction if achieved in a producible idler. A very soft idler rim may not be achievable in practice owing

to track retention, debris ingestion, and durability tradeoffs. Preliminary concepts show that materials are available which satisfy the application; however, only field experience can provide a certain answer. In an actual idler design, it is unlikely that over 20 dB will be achieved because of wave effects in isolators, track guide scrub, and other effects.

Idler Noise Reduction by Compliance at the Idler Hub or Spindle

To achieve large noise reductions, rather than further increase the idler rim and track inner pad compliance as described above, the center of the idler wheel is an alternate compliance location that offers several advantages. First, the present track-idler rim might be basically unchanged, thus retaining a simple, proven mechanical system. Second, the noise reduction is more predictable than for compliance at the rim because the track trajectory will be unchanged. Third, the isolated mass of the idler wheel itself greatly enhances high frequency vibration reduction.

A possible compliant idler hub (or spindle) concept was shown on the lower portion of Figure 40. The compliant element could be attached to the wheel or to the spindle. If attached to the wheel, it is reverse stressed by track tension forces with each revolution. Alternately, if the compliance is attached to the spindle so that it does not rotate, it is not reverse stressed by track tension with each revolution. In this case, it is subject to much less fatigue and heating.

The compliant hub efficiency was calculated by using the two stage isolator formula presented by Ungar and Dietrich in Reference 9:

$$E = \left| 1 + \frac{1}{M_S + M_R} (M_{I_1} + M_{I_2}) + \Delta E \right|$$

$$\Delta E = \frac{(M_{I_1} + M_S)(M_{I_2} + M_R)}{M_m (M_S + M_R)}$$

where M_{I_1} is the track-rim compliance mobility, M_{I_2} is the hub compliance mobility, M_m is the idler mass mobility, and ΔE represents the increase in noise reduction due to two, instead of one, compliance elements separated by a mass. For present purposes, both compliances are assumed to have no damping. Other terms and approximations are the same as given earlier for idler rim formulae.

The A-weighted predicted noise reduction was shown in Figure 43 which compares rim compliance to hub compliance predictions. The compliant hub design offers a great deal more high-frequency noise reduction than the compliant rim alone, but is about equal to the rim concept in the 63 and 125 Hz octave bands for the same total compliance. The abrupt "corner" of the attenuation curves is the resonance between the track and idler rim. This corner could be moved to a lower frequency by increasing the compliance at the idler rim or hub.

The soft hub noise reduction was calculated assuming that the track pad and rim could be modified to achieve 14,000 lbs_f/in. compliance, which is much softer than the present 60,000

lbs_f/in. This lower rim compliance appears to be practical from materials considerations, but considerable development may be required to achieve acceptable durability parameters.

The very large vibration reductions shown for 250 Hz and above are due to the idler wheel mass, which is assumed to be rigid. Any practical idler, however, is only rigid at below perhaps 250 Hz, and will resonate at a number of higher frequencies. The net effect of the resonances is to increase high frequency vibration transmitted. This is not serious since the major problem will be in the 125 Hz octave band, which will not be effectively isolated.

The baseline for all compliant idler noise reduction estimates is for the existing M113 60,000 lbs_f/in idler-track compliance. For practical purposes, sprocket noise reductions are practically identical, except the baseline is 49,000 lbs_f/inch owing to the rubber impact tire.

APPENDIX C:

TRACK SHOE IMPACT NOISE ANALYSIS

Approach

Impacts and vibration of track shoes against the sprocket and idler wheel cause the wheels to vibrate. These vibrations are transmitted to the hull, and vibrations of the hull produce noise in the vehicle interior. The first step toward understanding and predicting this interior noise is determining the track shoe/wheel interaction forces. Once these forces are known, they can be combined with force-to-noise transfer functions to calculate the resulting noise.

Analysis of the track shoe/wheel interaction forces is complicated, not only because of the intricate geometry, but also because of the nonlinearity in these forces due to the track shoes losing contact with the wheel during parts of their motion. (The compliance at the wheel rim may be modeled as a linear spring when it is in compression, but it can provide no restoring forces when contact is lost.) Because of this complexity, computer-assisted numerical analysis of the interaction forces is indicated. The previously mentioned transfer functions can best be determined experimentally.

Dynamical Model

In the present analysis, which is intended to include only the major features of the dynamic system, the wheel of radius R is assumed to rotate with constant angular velocity ω and to vibrate only by a negligible amount compared to the track shoes.

The present analysis investigates the track/wheel interaction forces that are generated as a finite length of track (made up of 60 shoes) moves over the wheel. The midpoint of the first shoe is taken to be rigidly fixed to the wheel rim, and the last shoe is taken to move uniformly at the vehicle speed V along a line tangential to the wheel. The remaining shoes are permitted to move under the influence of their inertias, shoe-to-shoe interaction forces, and shoe/wheel interaction forces.

In the present analysis, initial conditions are imposed on the system, and the subsequent motions of the system are calculated for a finite time period. Although one would ideally like to determine what happens when steady state is reached, this calculation would require an expenditure of considerable more computer time and associated costs.

The present analysis is limited to periods of motion that are short enough so that waves reflected from the last track shoe (Figure C-1) do not return to the wheel during the period considered. Therefore, damping effects in the system (as analyzed here) play no significant role and have been omitted from consideration. However, this omission restricts the maximum duration of the simulation.

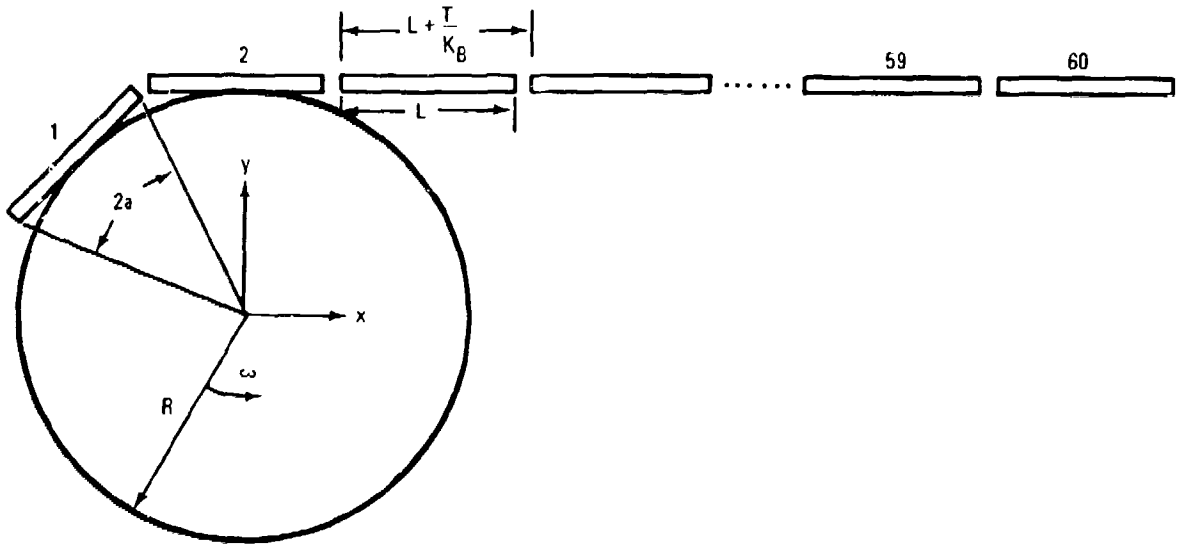

Figure C-1: Basic Features of Dynamic Model at t = 0

Equations of Motion

The equations of motion are readily obtained by Lagrange's method, which uses the Lagrangian function L defined as

$$L = T(\dot{q}_1, \dot{q}_2, \ldots, \dot{q}_s; t) - V(q_1, q_2, \ldots, q_s; t) \tag{C-1}$$

where T denotes the kinetic energy and V the potential energy of the system, the q_s represent the generalized coordinates used to describe the system, and the dot indicates differentiation with respect to time. The S differential equations of motion then are obtained from References C-1 and C-2.*

$$\frac{d}{dt}\left(\frac{\partial L}{\partial \dot{q}_s}\right) = \frac{\partial L}{\partial q_s}, \qquad s = 1, 2, \ldots, S. \tag{C-2}$$

The generalized coordinates are comprised of the spatial coordinates $x_n(t), y_n(t)$ of the center of the N shoes and of the angular coordinates $\phi_n(t)$ of the shoes (Figure C-2). The total kinetic energy of the system then may be written as

$$T = \frac{1}{2}\sum_{n=2}^{N}\left[m(\dot{x}_n^{\,2} + \dot{y}_n^{\,2}) + I\dot{\phi}_n^{\,2}\right] \tag{C-3}$$

*References are given at the end of this appendix.

where m and I denote the mass and the mass moment of inertia of a shoe. Note that the first shoe makes no contribution to the vibrational kinetic energy, because this shoe is assumed to be rigidly connected to the wheel.

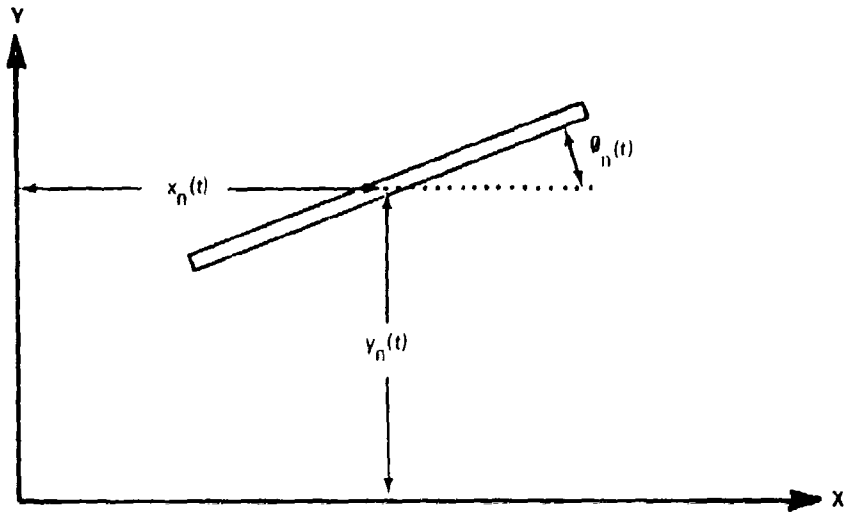

Figure C-2: Coordinates of Nth Shoe

If one neglects the contribution due to gravity, one may consider the potential energy V as made up of a contribution V_B from compression of the bushing springs, of a contribution V_Q from torsion of these springs, and of a contribution V_C from compression of the compliant layer between the track and the wheel:

$$V = V_B + V_Q + V_C \tag{C-4}$$

The displacement of the left end of shoe n with respect to the right end of the shoe n-1 may be taken as equal to the elongation ΔS_n of the elastic element of the bushing between these shoes, if this displacement (and the elongation) is zero under zero tension. In view of the definition of the link coordinates,

$$(\Delta S_n)^2 = \left[x_n - x_{n-1} - \frac{L}{2}(\cos\phi_n + \cos\phi_{n-1})\right]^2 + \left[y_n - y_{n-1} - \frac{L}{2}(\sin\phi_n + \sin\phi_{n-1})\right]^2 \tag{C-5}$$

One thus may evaluate

$$V_B = \frac{1}{2} K_B \sum_{n=2}^{N} (\Delta S_n)^2 \tag{C-6}$$

where K_B denotes the extensional stiffness of a bushing.

One may write the torsional potential energy stored in the bushing between the nth and (n-1)th shoe in terms of the relative rotation $(\phi_n - \phi_{n-1})$ of the two shoes as

$$V_Q = \frac{1}{2} Q \sum_{n=2}^{N} (\phi_n - \phi_{n-1})^2 \quad , \tag{C-7}$$

where Q denotes the rotational stiffness of a bushing.

For the present analysis it is convenient to assume that the compliant layer between the track and wheel acts only at the center of each shoe and has the same stiffness K_C, no matter in what direction the shoe is displaced relative to the wheel's rim, provided that the shoe's center is pushed inside the rim radius R. If the shoe center is outside this radius, the shoe is assumed to have lost contact, and the effective interface stiffness is zero. Then one may write

$$V_C = \frac{1}{2} K_C \sum_{n=2}^{N} \left[(x_n - R\cos\theta_{n0})^2 + (y_n - R\sin\theta_{n0})^2\right] \delta_n \tag{C-8}$$

where

$$\delta_n = \begin{cases} 0 & \text{for} \quad x_n^2 + y_n^2 > R^2 \\ 1 & \text{otherwise} \end{cases} \tag{C-9}$$

and

$$\theta_{n0} = \frac{\pi}{2} + 2\alpha(n-2) + \omega t \ . \tag{C-10}$$

Here $x_{n0} = R\cos\theta_{n0}$ and $y_{n0} = R\sin\theta_{n0}$ are the coordinates of a shoe in contact at the rim at equilibrium (i.e., with the compliant layer not displaced), with θ_{n0} representing the angular position of this shoe along the wheel, and $\alpha = \arctan(L/2R)$.

One may then obtain an expression for V by substituting Eqs. C-6, C-7, and C-8 into Eq. C-4, and one may determine the Lagrangian function L by substituting this result and Eq. C-3 into Eq. C-1. Finally, one may apply Eq. C-2 to obtain the equations of motion:

$$\ddot{x}_n = -\omega_C^2(x_n - R\cos\theta_{n0}) - \omega_B^2\left[2x_n - x_{n-1} - x_{n+1} - \frac{L}{2}(\cos\phi_{n-1} - \cos\phi_{n+1})\right]$$

$$\ddot{y}_n = -\omega_C^2(y_n - R\sin\theta_{n0}) - \omega_B^2\left[2y_n - y_{n-1} - y_{n+1} - \frac{L}{2}(\sin\phi_{n-1} - \sin\phi_{n+1})\right]$$

$$\ddot{\phi}_n = -\omega_Q^2(2\phi_n - \phi_{n-1} - \phi_{n+1}) - \frac{K_B L}{2I}\Big[\sin\phi_n(x_{n+1} - x_{n-1})$$

$$-\cos\phi_n(y_{n+1} - y_{n-1})\Big] - \frac{K_B L^2}{4I}\Big[\sin\phi_n(2\cos\phi_n + \cos\phi_{n-1} + \cos\phi_{n+1})$$

$$-\cos\phi_n(2\sin\phi_n + \sin\phi_{n-1} + \sin\phi_{n+1})\Big] \tag{C-11}$$

where the frequency parameters ω_C, ω_B, and ω_Q are related to the stiffness and inertia parameters through $\omega^2_C = K_C/m$, $\omega^2_B = K_B/m$, and $\omega^2_Q = Q/I$. These equations apply for all shoes, except the first and the last, whose motions are prescribed.

Initial Conditions and Constraints

For all but the first shoe the initial conditions are taken as

$$\phi_n(0) = 0 \ , \qquad x_n(0) = (n-2)L + (N-1)\Delta L \ , \qquad y_n(0) = R$$

$$\dot{\phi}_n(0) = 0 \ , \qquad \dot{x}_n(0) = -V \ , \qquad \dot{y}_n(0) = 0 \qquad \text{(C-12)}$$

where

$$\Delta L = P/K_B \qquad \text{(C-13)}$$

denotes the axial displacement of one shoe relative to the next due to the applied tension P, with K_B representing the previously mentioned bushing stiffness. The average vehicle speed V is related to the track pitch L, wheel radius R, and angular speed ω, through

$$V = \frac{\omega L}{2\alpha} \qquad \text{(C-14)}$$

The constraint imposed on the first shoe is that it remains rigidly connected to the wheel, so that for all values at t,

$$\phi_1(t) = \frac{\pi}{2} + 2\alpha + \omega t \ , \qquad x_1(t) = R\cos\phi_1 \ , \qquad y_1(t) = R\sin\phi_1 \qquad \text{(C-15)}$$

The last (i.e., the 60th) shoe is taken as constrained to move tangentially to the wheel, so that

$$\phi_{60}(t) = 0 \ , \qquad x_{60}(t) = 58L + 59\Delta L - Vt \ , \qquad y_{60}(t) = R \ . \qquad \text{(C-16)}$$

Computational Considerations

The differential equations of motion may be solved by use of finite difference techniques (References C-3 and C-4), which require one to select time steps and the total time to be considered.

In order to provide an accurate solution, the time step Δt must be small; its corresponding frequency $f = 1/\Delta t$ must be at least three times the highest frequency of interest. Thus, if this frequency is 2500 Hz, the time step must be no greater than 1.33×10^{-4} sec. In order to insure stability of the solution, the frequency f must also be several times larger than the highest resonance frequency of the system. For a resonance frequency of 520 Hz (that can result from 20 lb shoe masses oscillating between 140 Klbs/in. bushing springs), the foregoing choice of $\Delta t = 1.33 \times 10^{-4}$ sec provides a more than adequate margin.

The total time $T_0 = N_0 \Delta t$ for which the computation is carried out is limited by accuracy and computation time (cost) considerations. Accuracy requires that the interval T_0 be long enough so that $f_0 = 1/T_0$ is less than one half of the lowest frequency of interest. If the latter frequency is 32 Hz, then T_0 must be at least 60 msec, and the required number of steps $N_0 > T_0/\Delta t = 451$. Computation system (Fast Fourier Transform) considerations require N_0 to be chosen as an integral power of 2; we therefore choose $N_0 = 512$, and take $\Delta t = T_0/N_0 = 0.117$ msec.

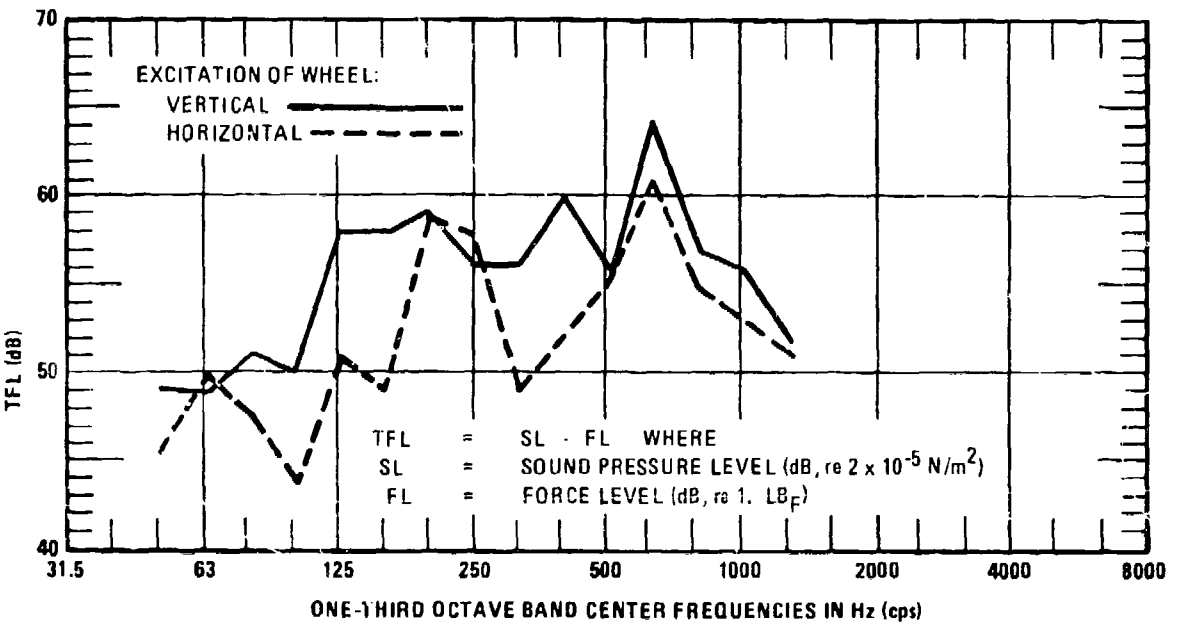

Figure C-3: Transfer Function for Sprocket Wheel Vibration to Noise in Crew Compartment

Since the computation time and cost increase with the number N of track shoes, it is advantageous to minimize the number of shoes included in the calculation. On the other hand, the track length must be selected sufficiently great so that waves reflected from the last shoe will not affect the motions of the first few shoes that are to be studied in detail. Since the phase velocity of longitudinal waves in the M113 track may be estimated to be 818 ft/sec, such a wave would in 60 msec traverse (818) (0.060) = 50 ft or about 100 half-foot long shoes. In this same time interval, about 5 shoes interact with a wheel on a vehicle travelling at 30 mph. Thus, selection of N = 60, corresponding to a 120 shoe round-trip length for a wave beginning at the wheel, ensures that the motions of shoes 2 through 6 are unaffected by the returning reflected wave.

Computed Results

In accordance with the foregoing discussion a 60 shoe track string was considered for a total observation time of 60 msec. A time step of $\Delta t = 0.117$ msec was used, and calculations were carried out for 512 time points.

The calculated displacements were multiplied by the appropriate stiffness K_C to yield the forces acting on the wheel, and the noise levels produced by these forces were determined on the basis of corresponding measured crew area force-to-noise transfer functions (Figure C-3). Note that these calculations yield the noise due to each shoe individually acting on the wheel; additional interpretation and computation is needed in order to account for the effects of a multitude of shoes.

The results of the calculations are presented in Figures C-4 through C-18. The upper part of each figure shows the time-dependences of the x and y components of the force exerted on the wheel by a particular shoe. The lower part of each figure shows the 1/3-octave band spectrum of noise due to the x and y components of force separately, together with the result of an addition of these two noise contributions. The addition shown corresponds to a worst case condition, that is, the x and y forces cause noise that is in phase. For example, adding 90 dB due to the x force and 90 dB due to the y force yields a total of 96 dB. (The noise estimates on all other figures are based on energy additions, i.e. 90 dB + 90 dB results in 93 dB.)

The figures are divided into three sets, each set corresponding to a different value of the stiffness K_C of the compliant layer between track and wheel. Each set consists of five individual figures, one for each shoe from number 2 through number 6.

The parameter values for which these calculations were carried out are listed below:

Track pitch	L	0.5 ft.
Wheel radius	R	9.5 in.
Average vehicle speed	V	30 mph
Track shoe mass	m	0.625 slug
Track shoe moment of inertia	I	0.0130 slug · ft^2
Track tension	P	3000 lb
Bushing extensional stiffness	K_B	140 klb/in.
Bushing torsional stiffness	Q	0
Compressional and tangential stiffness of track shoe/ wheel compliance	K_C	3, 23, 36, and 77 klb/in.

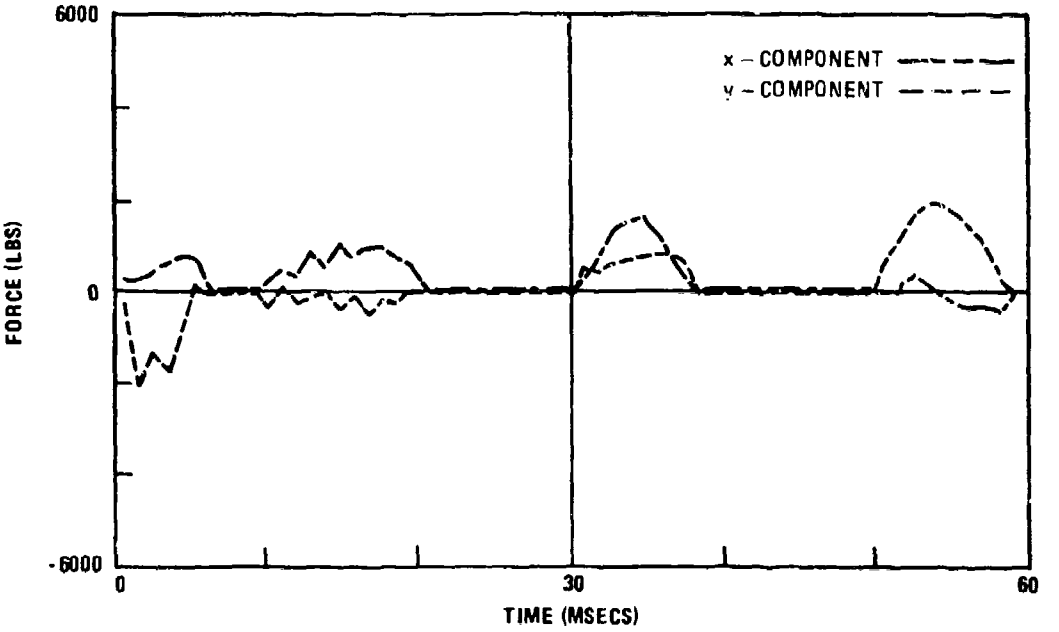

Figure C-4a: Time Histories of Forces Exerted on Wheel by Track Shoe Number 2 (23,000 lb_f/inch)

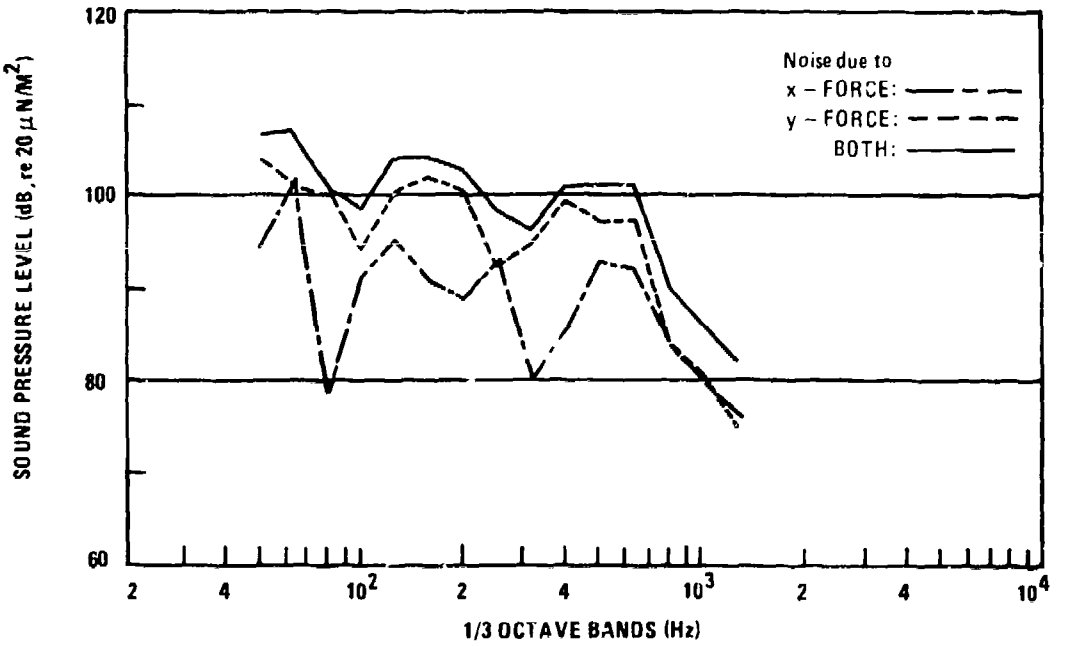

Figure C-4b: Interior Noise Spectra Associated with Forces of Figure C-4a

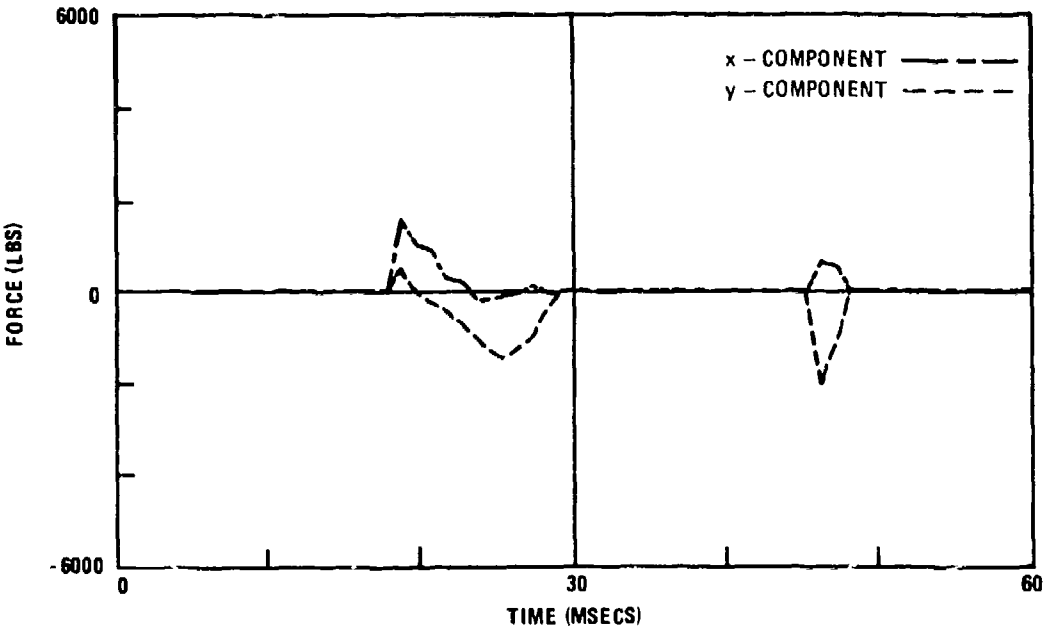

Figure C-5a: Time Histories of Forces Exerted on Wheel by Track Shoe No. 3 (23,000 lb_f/inch)

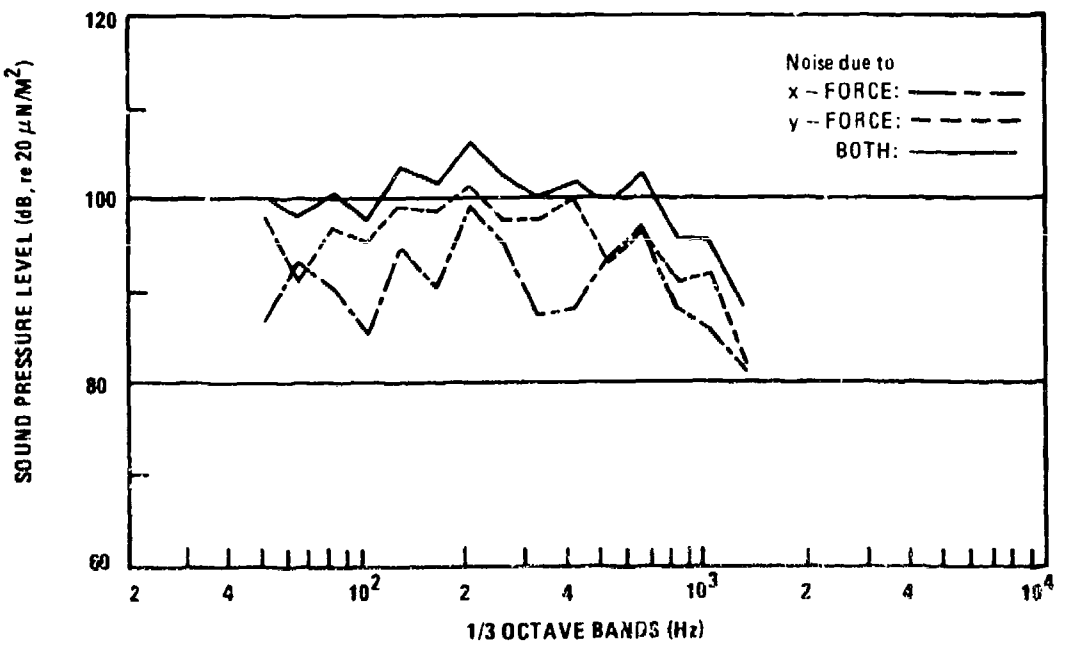

Figure C-5b: Associated Noise Spectra

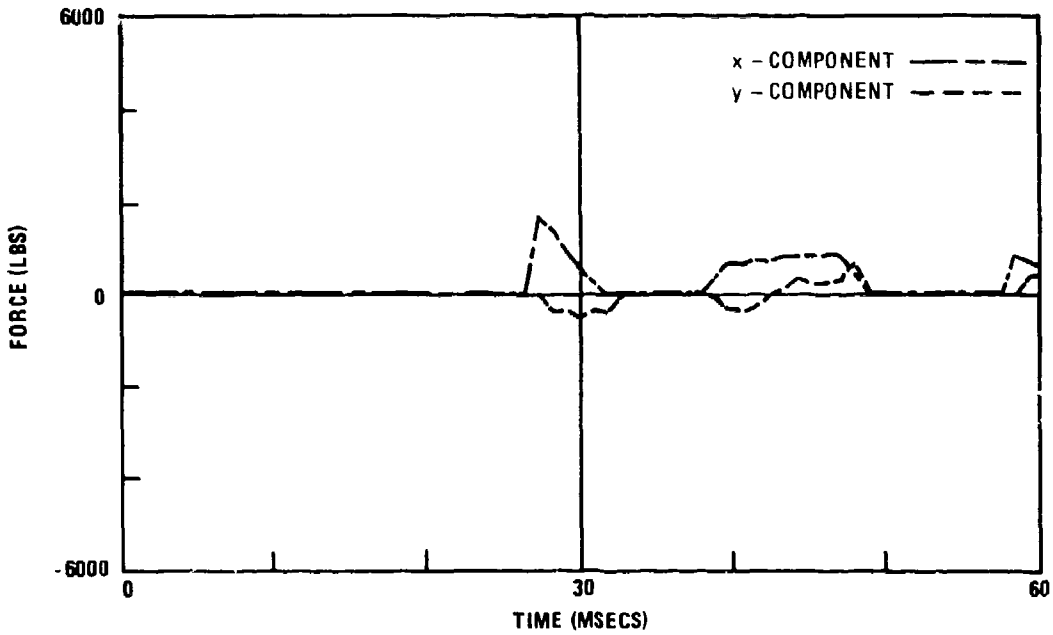

Figure C-6a: Time Histories of Forces Exerted on Wheel by Track Shoe No. 4 (23,000 lb_f/inch)

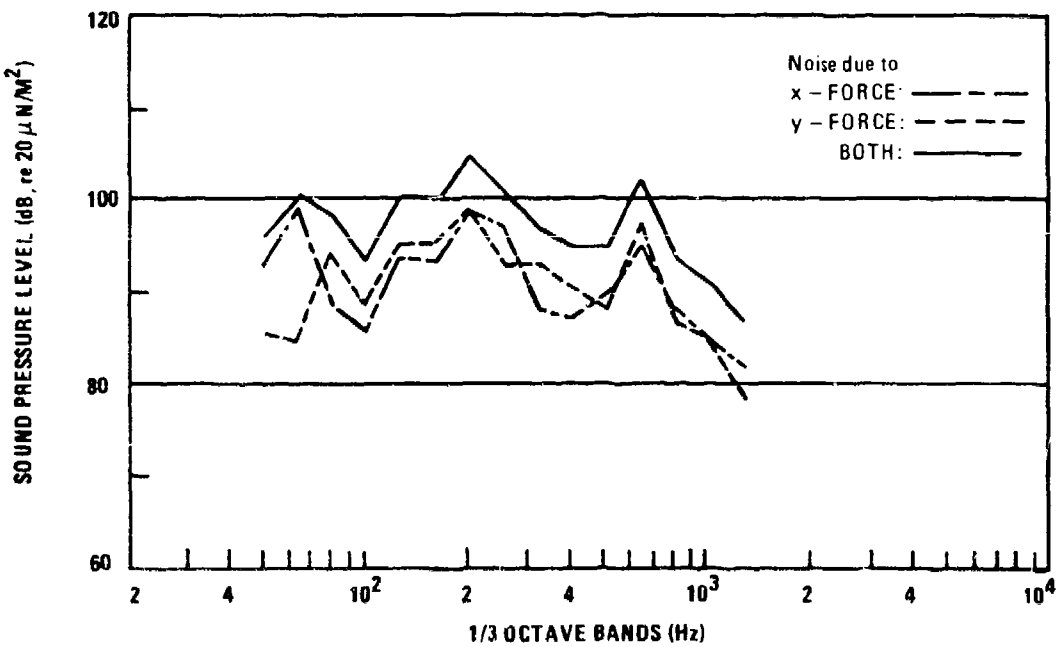

Figure C-6b: Associated Noise Spectra

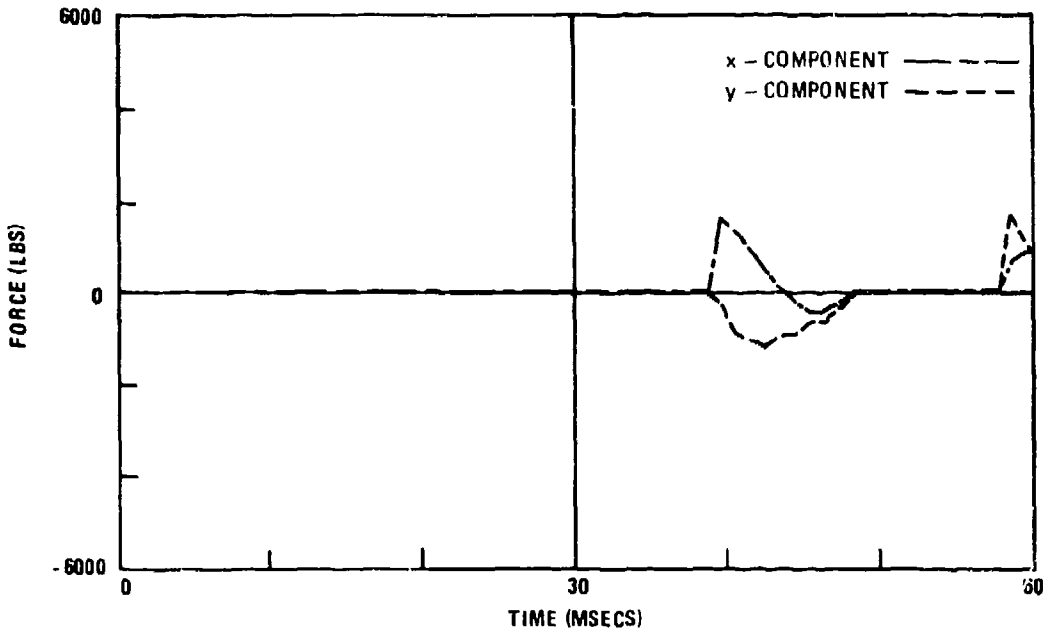

Figure C-7a: Time Histories of Forces Exerted on Wheel by Track Shoe No. 5 (23,000 lb_f/inch)

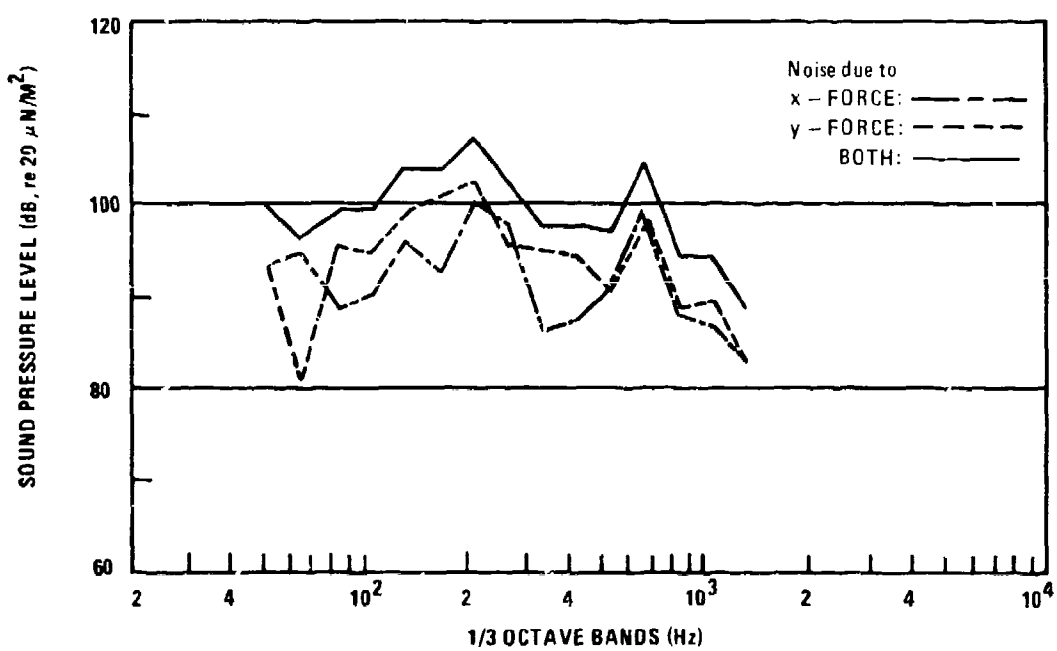

Figure C-7b: Associated Noise Spectra

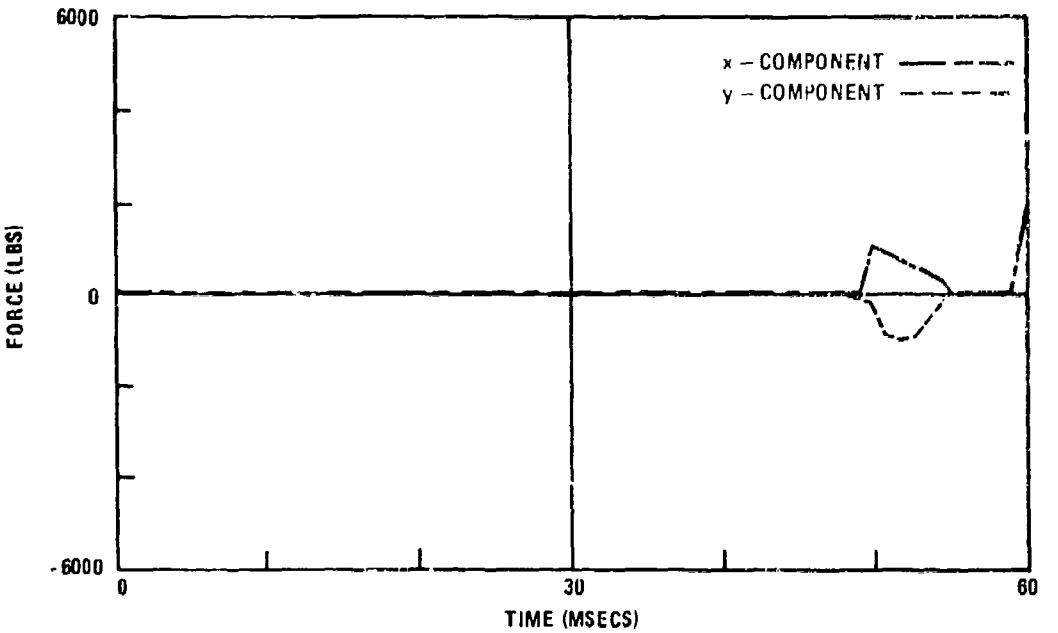

Figure C-8a: Time Histories of Forces Exerted on Wheel by Track Shoe No. 6 (23,000 lb_f/inch)

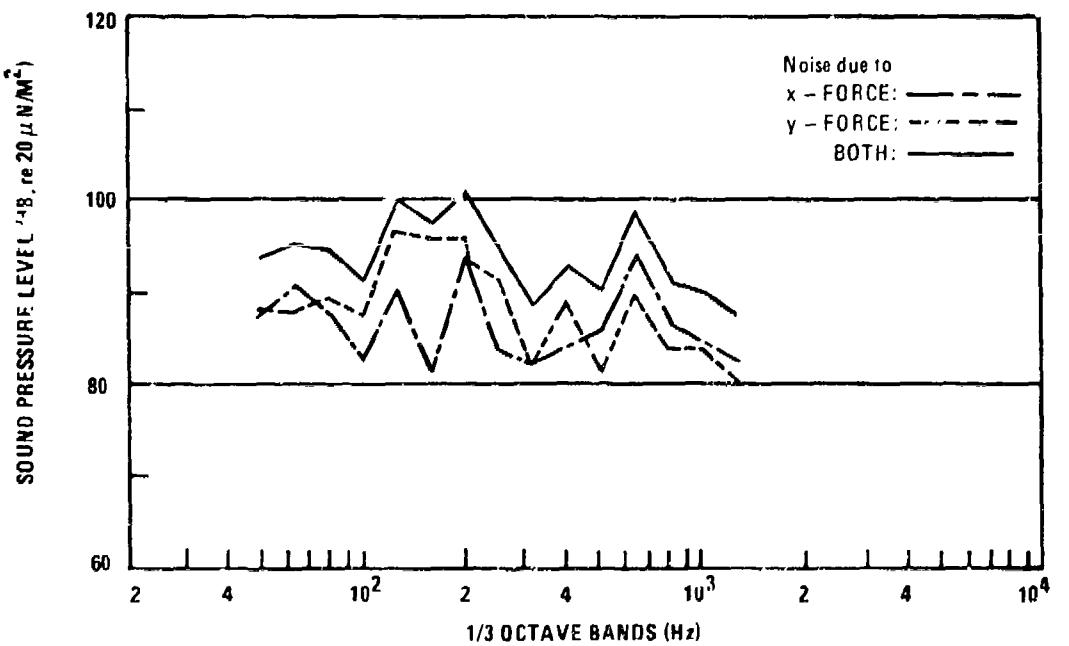

Figure C-8b: Associated Noise Spectra

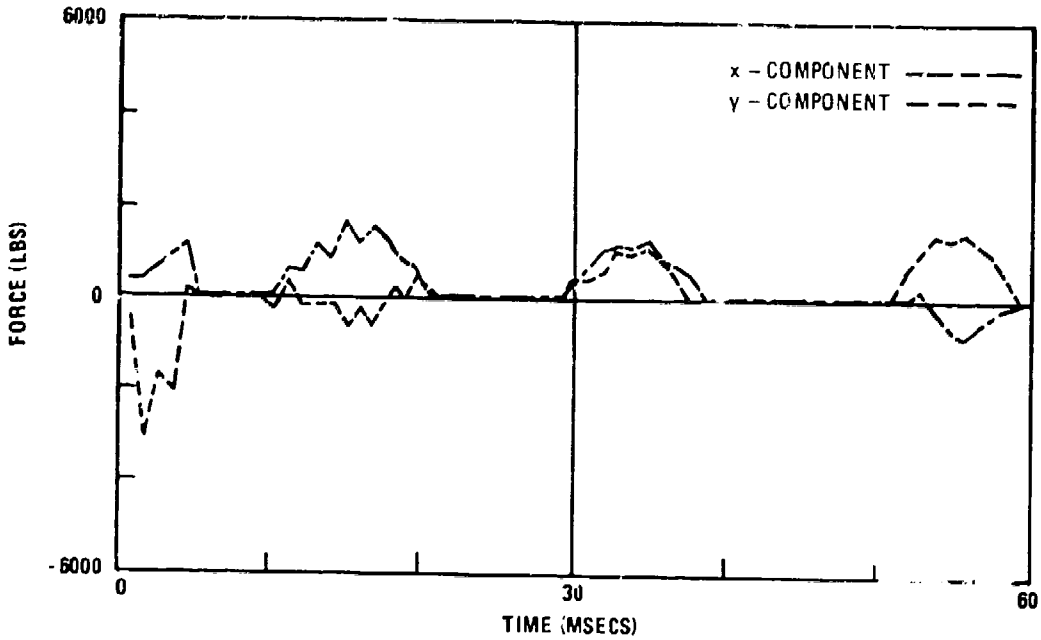

Figure C-9a: Time Histories of Forces Exerted on Wheel by Track Shoe No. 2 (36,000 lb_f/inch)

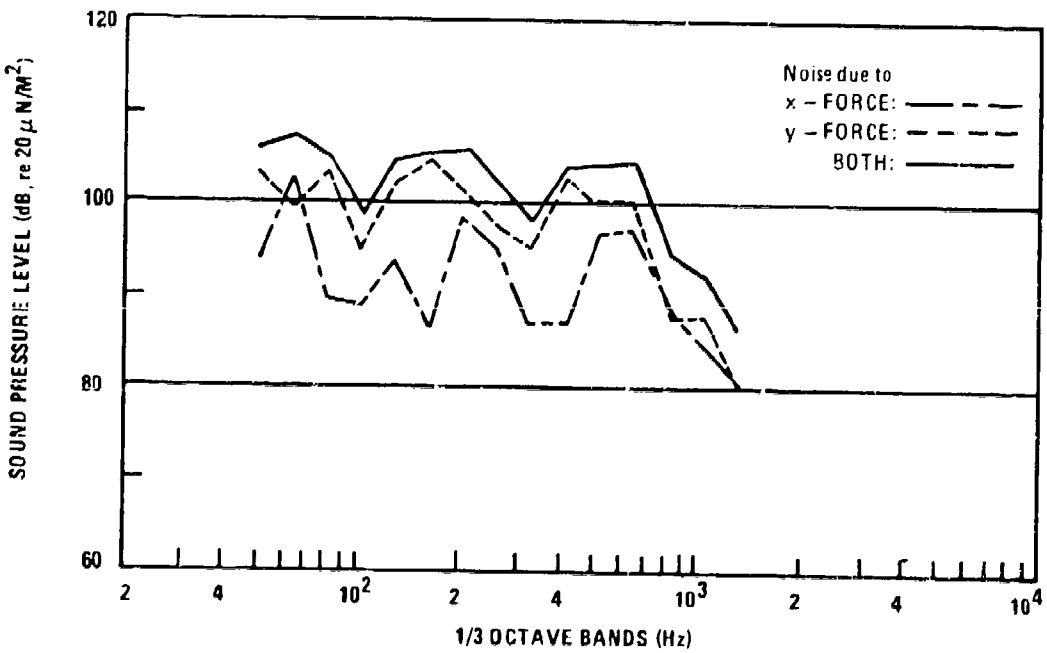

Figure C-9b: Associated Noise Spectra

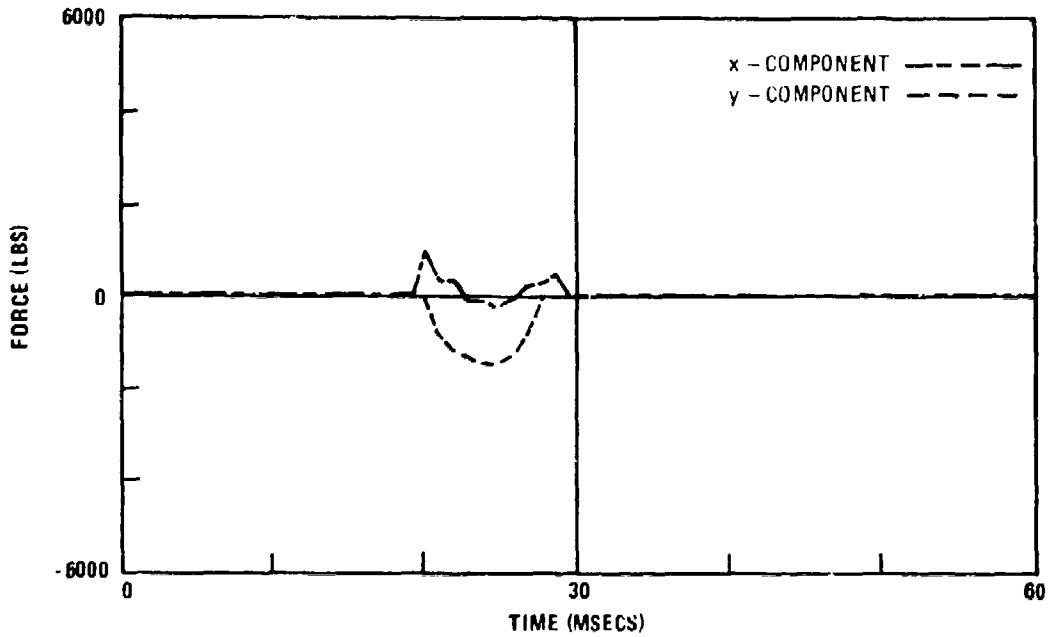

Figure C-10a: Time Histories of Forces Exerted on Wheel by Track Shoe No. 3 (36,000 lb_f/inch)

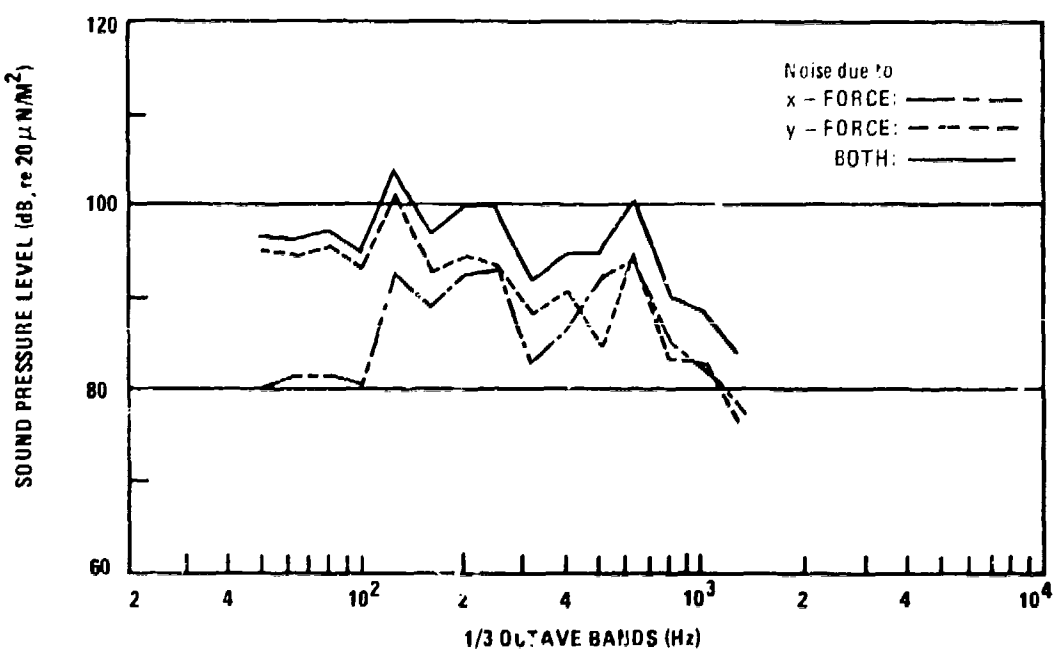

Figure C-10b: Associated Noise Spectra

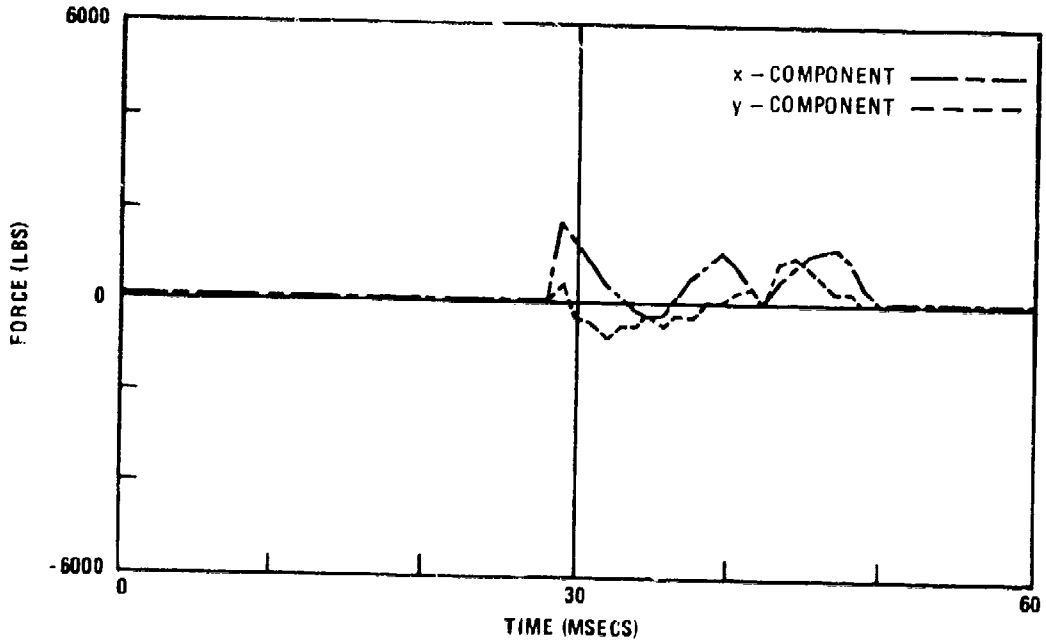

Figure C-11a: Time Histories of Forces Exerted on Wheel by Track Shoe No. 4 (36,000 lb_f/inch)

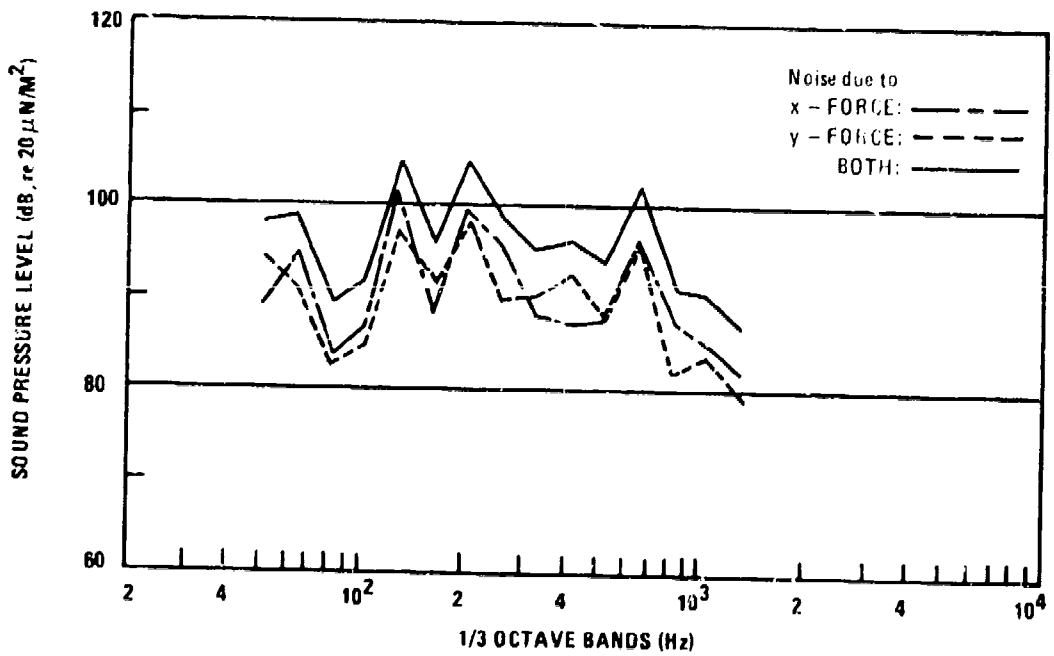

Figure C-11b: Associated Noise Spectra

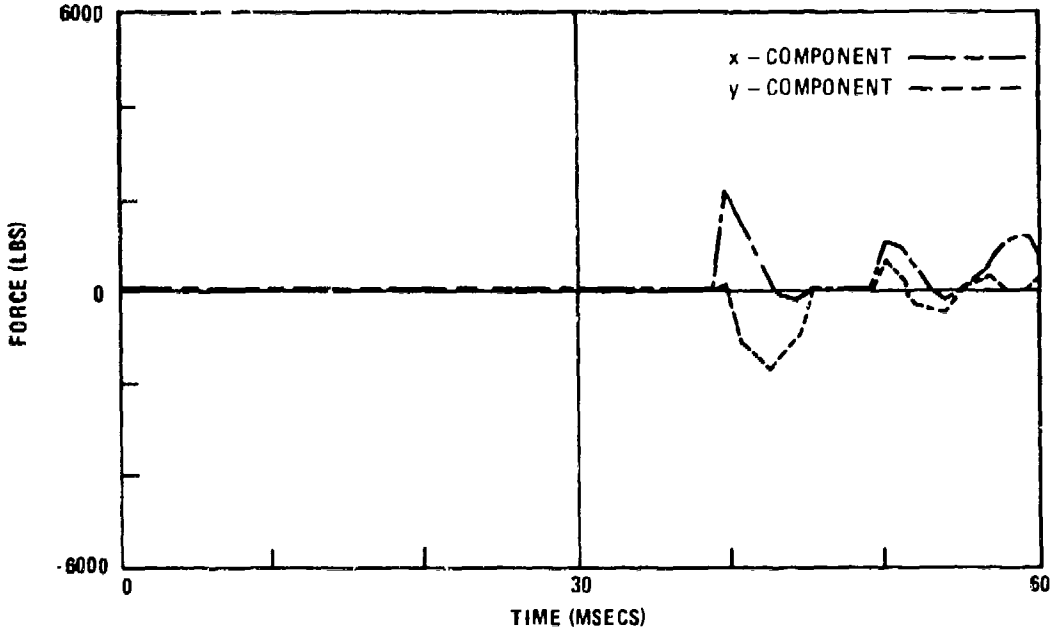

Figure C-12a: Time Histories of Forces Exerted on Wheel by Track Shoe No. 5 (36,000 lb_f/inch)

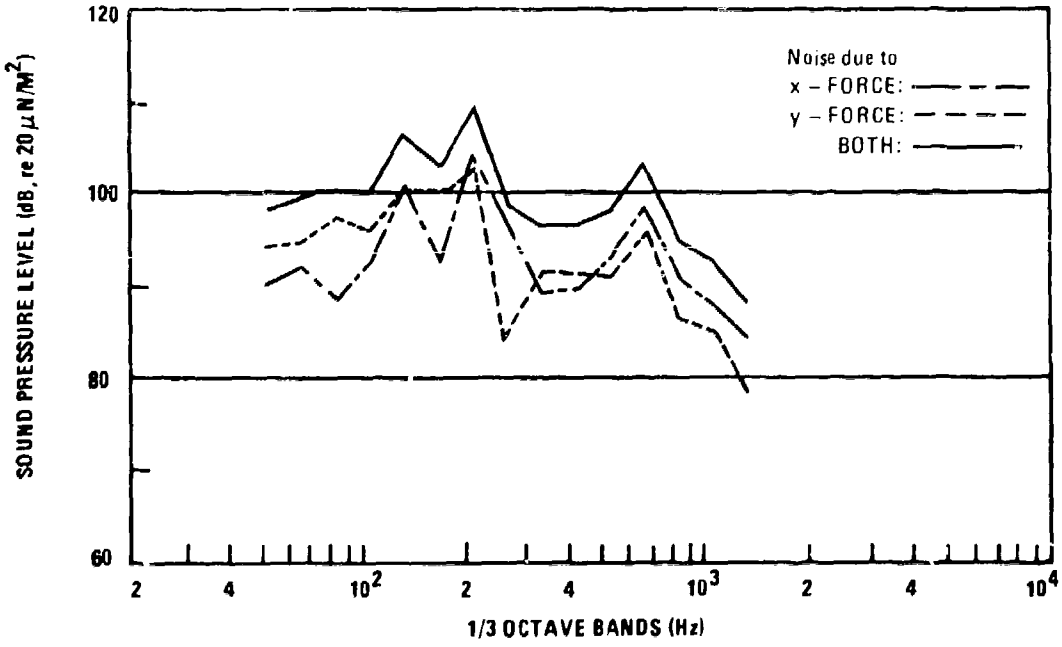

Figure C-12b: Associated Noise Spectra

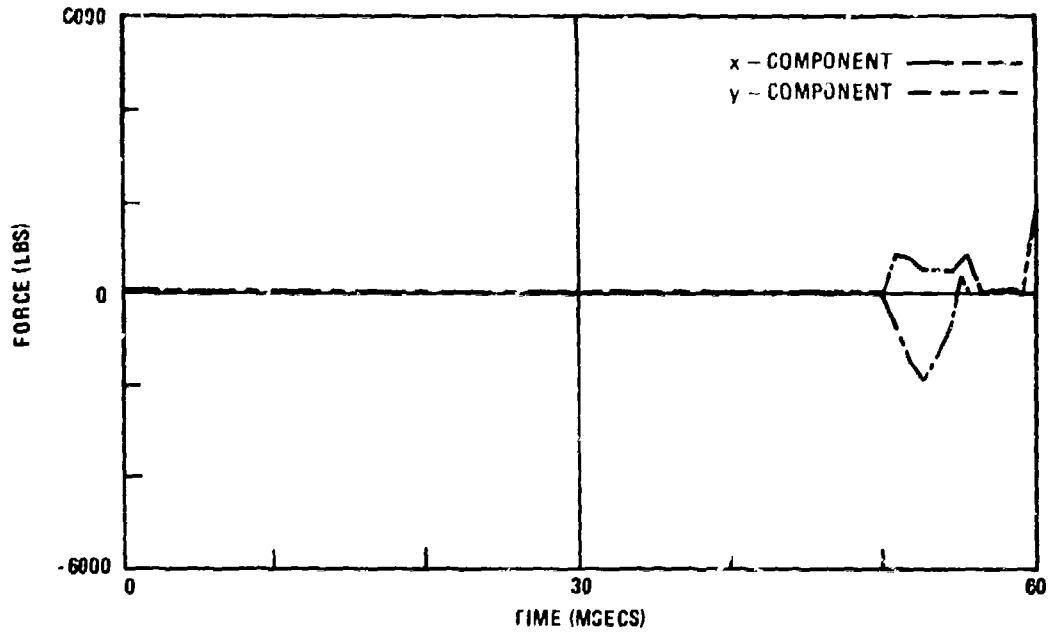

Figure C-13a: Time Histories of Forces Exerted on Wheel by Track Shoe No. 6 (36,000 lb_f/inch)

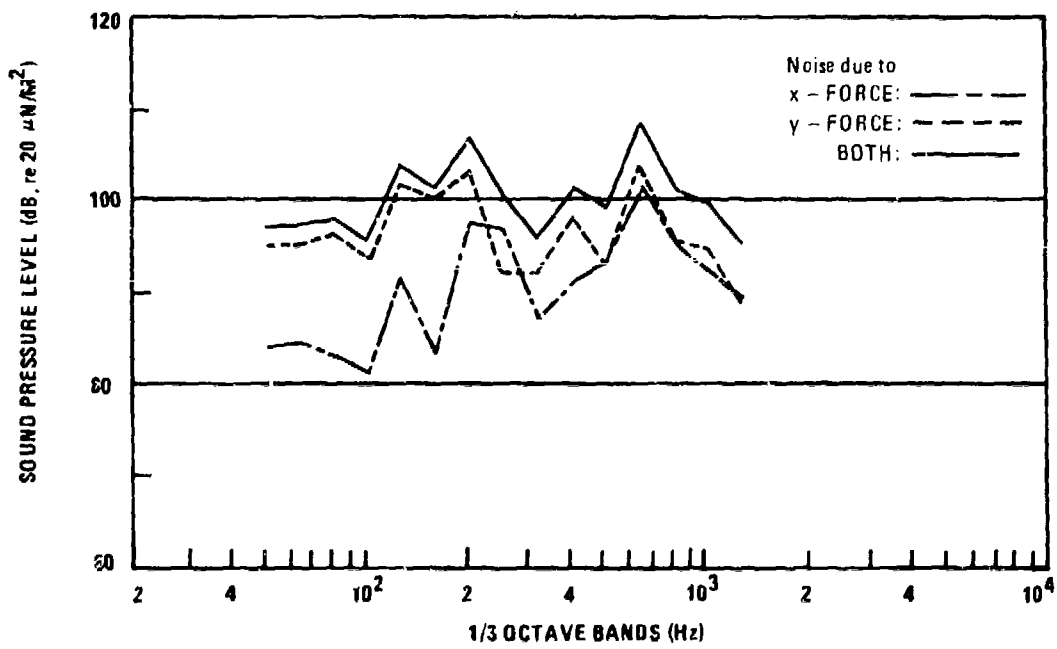

Figure C-13b: Associated Noise Spectra

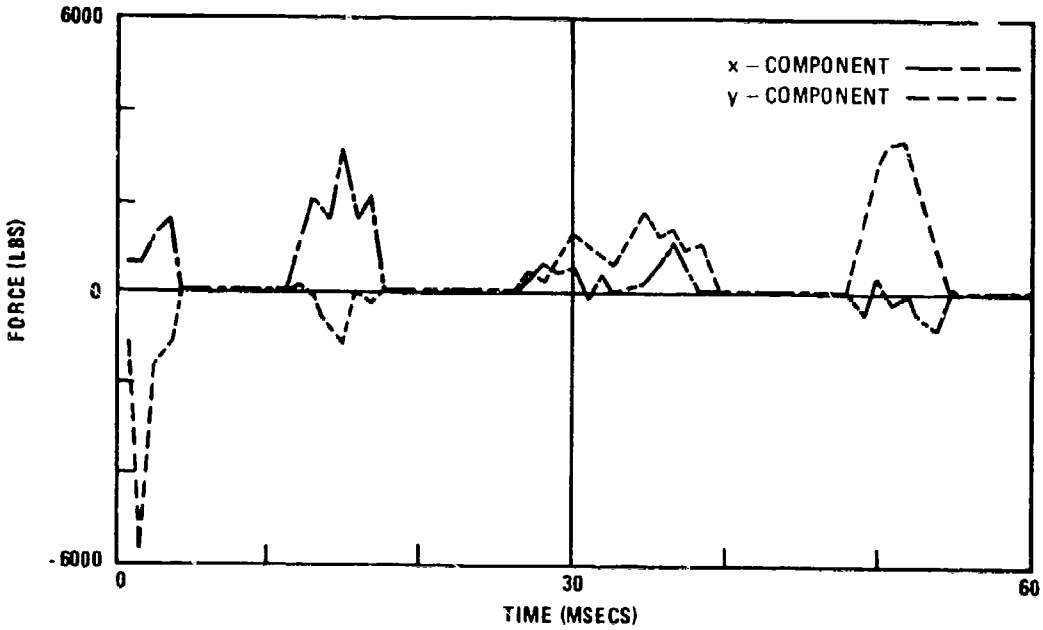

Figure C-14a: Time Histories of Forces Exerted on Wheel by Track Shoe No. 2 (77,000 lb_f/inch)

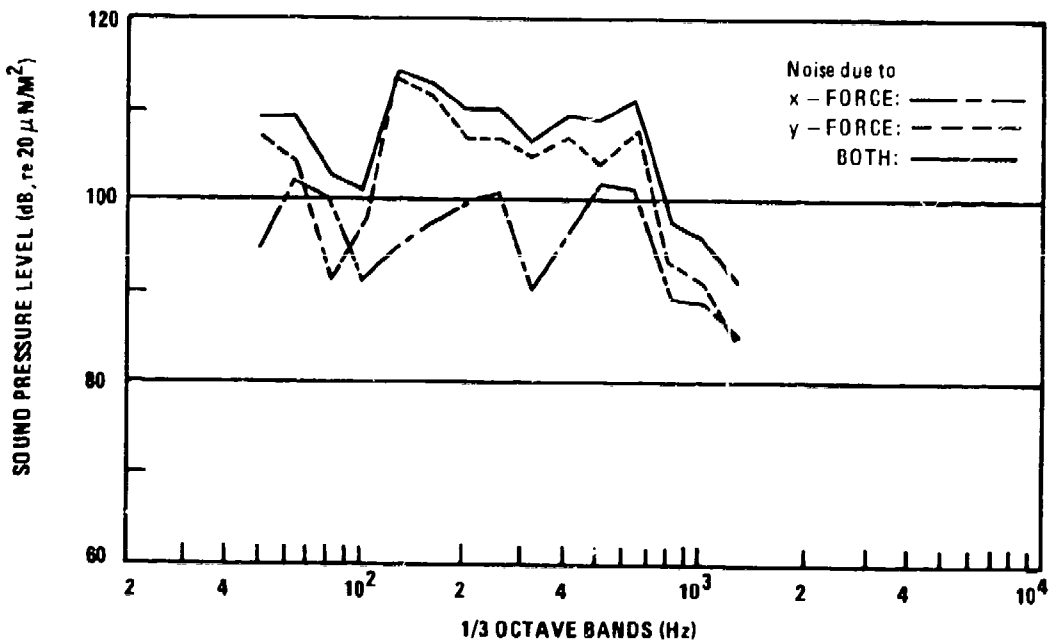

Figure C-14b: Associated Noise Spectra

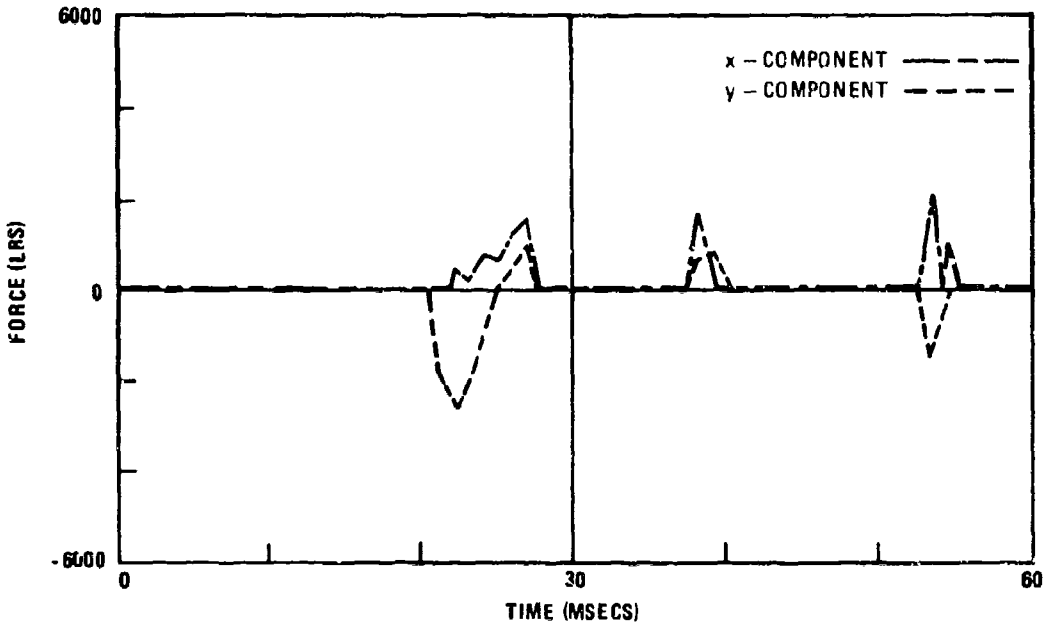

Figure C-15a: Time Histories of Forces Exerted on Wheel by Track Shoe No. 3 (77,000 lb_f/inch)

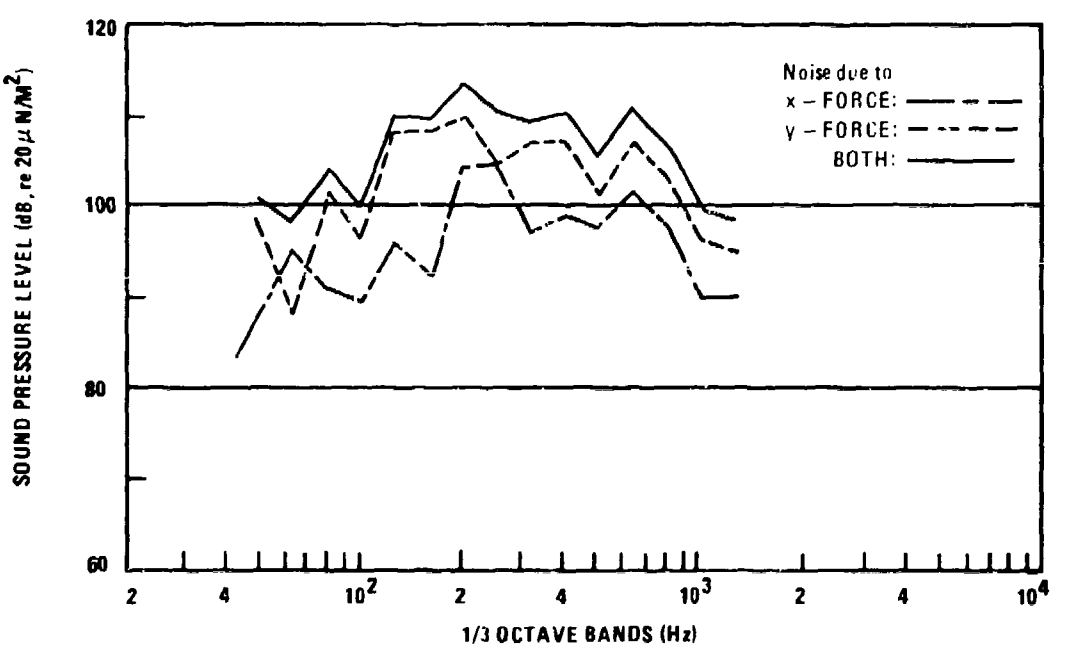

Figure C-15b: Associated Noise Spectra

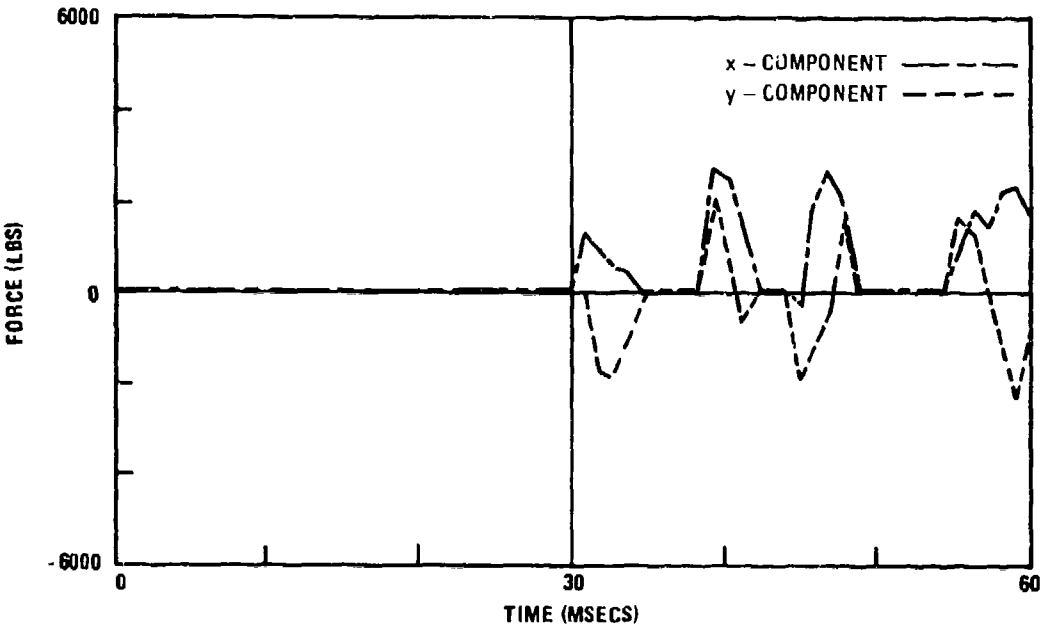

Figure C-16a: Time Histories of Forces Exerted on Wheel by Track Shoe No. 4 (77,000 lb_f/inch)

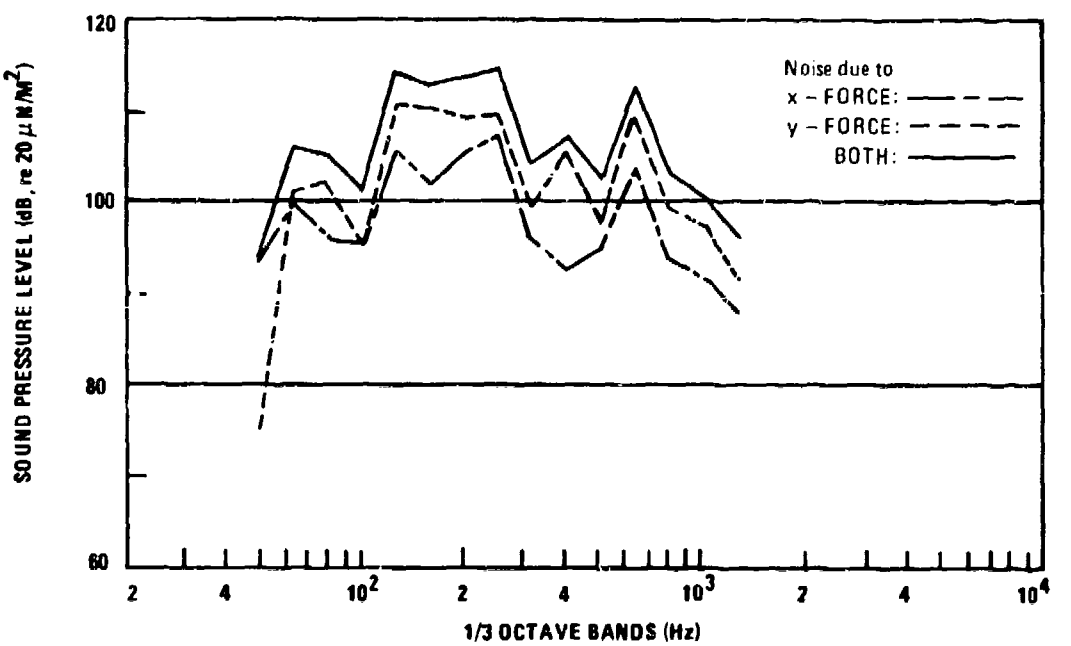

Figure C-16b: Associated Noise Spectra

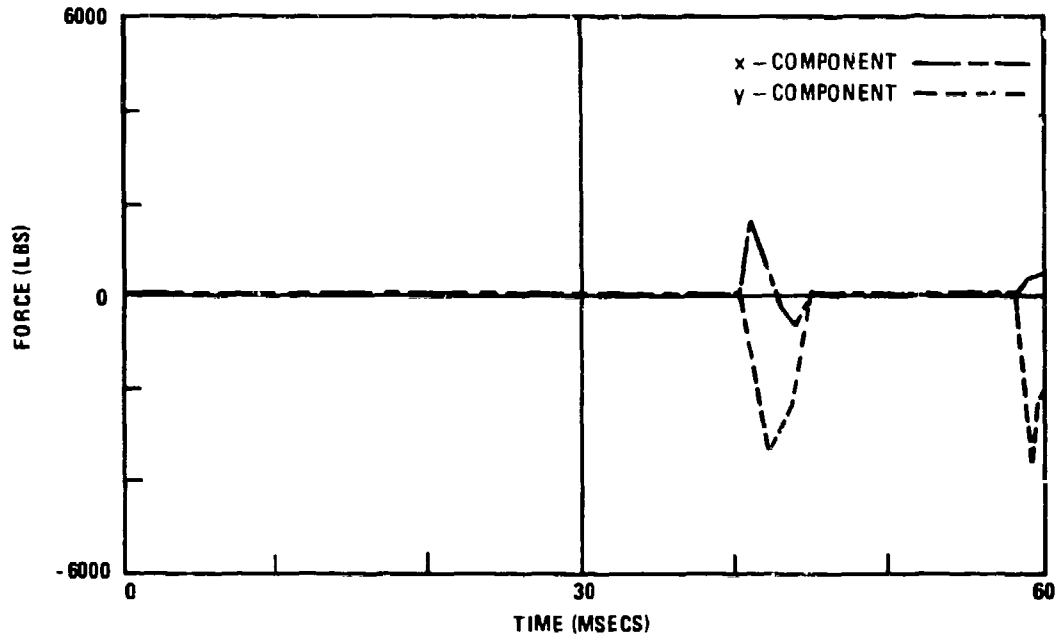

Figure C-17a: Time Histories of Forces Exerted on Wheel by Track Shoe No. 5 (77,000 lb_f/inch)

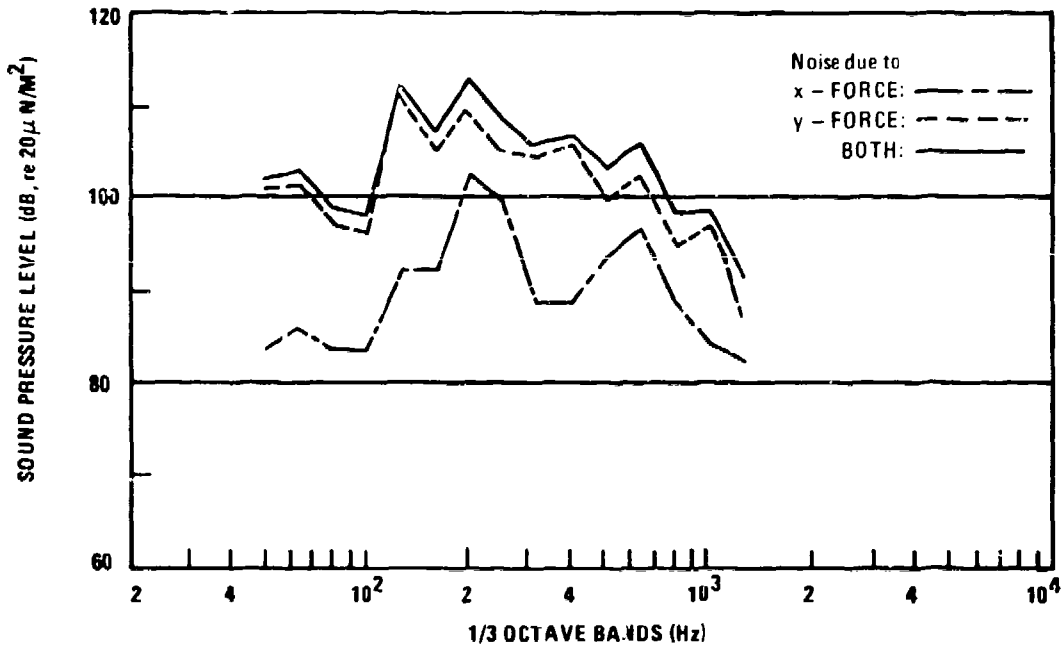

Figure C-17b: Associated Noise Spectra

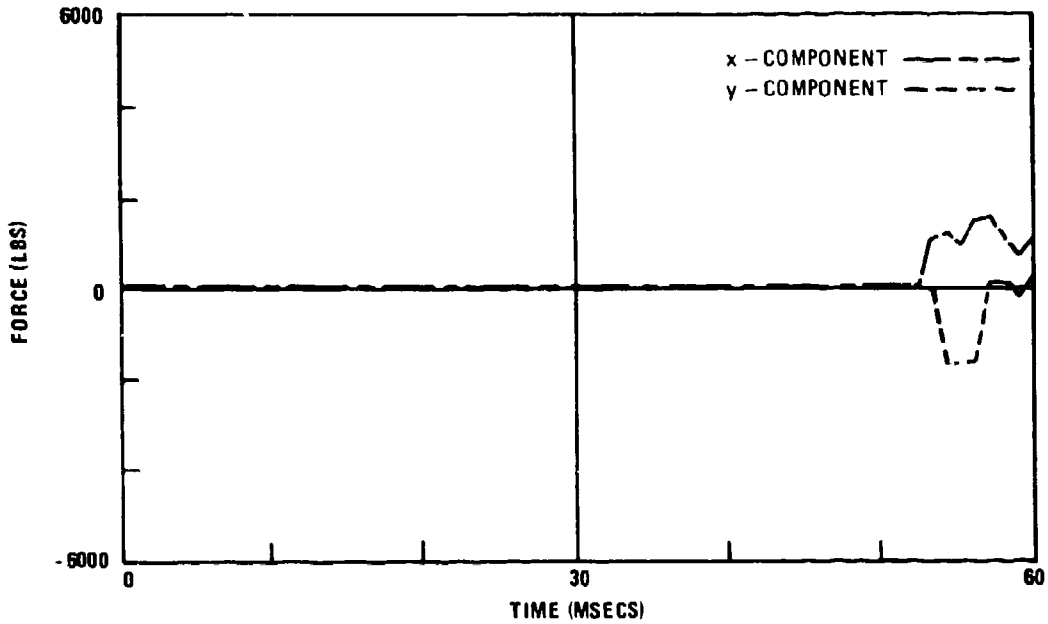

Figure C-18a: Time Histories of Forces Exerted on Wheel by Track Shoe No. 6 (77,000 lb_f/inch)

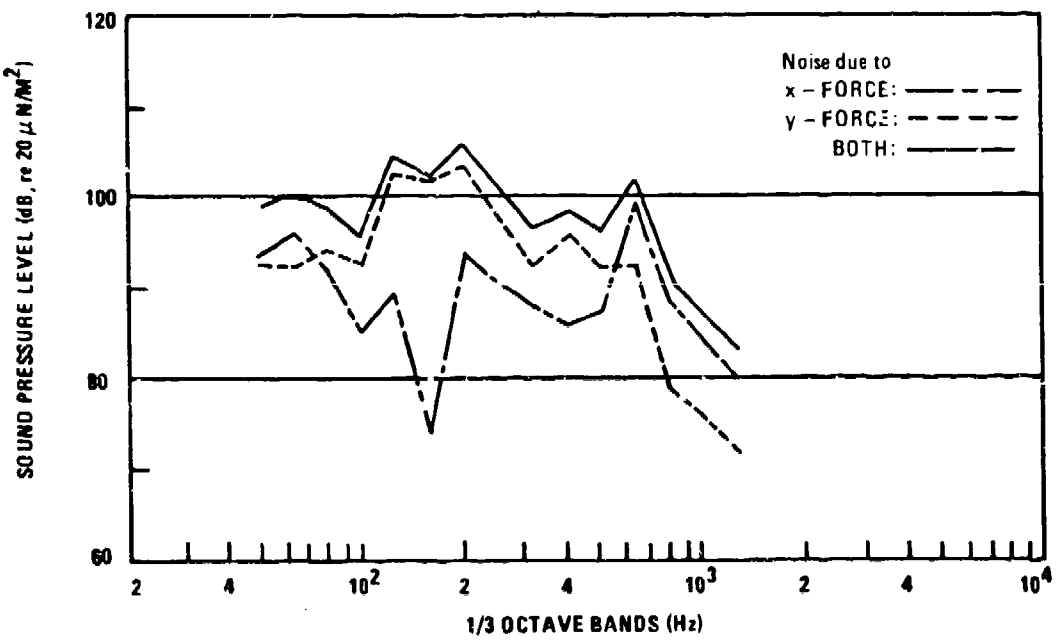

Figure C-18b: Associated Noise Spectra

Discussion of Results

By observing each of Figures C-4a through C-18a, it may be noted that the interaction forces vanish during some time intervals; this occurs when the track shoe "bounces" out of contact with the wheel.

As a track shoe arrives at the wheel, the y-component of the force is negative; i.e., the shoe pushes the wheel downward. Similarly, the y-force becomes predominantly positive when the shoe is on the underside of the wheel.

Inspection of Figures C-4 through C-18 reveals that, in general, none of the shoes achieves steady-state motion within the 60 msec period to which the computation applies.

Because steady-state motion was not achieved in the present analysis, the 1/3 octave band spectra show wide variations between track shoes for each rim compliance. Possible reasons for this variation include:

1. The second track shoe, being attached to the first shoe which is "welded" to the wheel, undergoes motions not typical of subsequent shoes.

2. The third through sixth track shoes exert forces during only the latter portion of the analysis time window because of their lack of contact with the wheel. This would lower vibration force delivered to the wheel.

3. Because of severe bouncing of the track shoes on the wheel, the spectra do not represent steady-state conditions. For example, the third shoe for the 36,000 pound per inch compliance run was in contact with the wheel for only about 10 milliseconds out of a 60 millisecond-long simulation.

4. Although the spectra vary greatly, most have a peak of 630 Hz that may correspond to resonances between track shoes (or shoes and the wheel). This peak may be due to the lack of damping in the present simplified model.

5. The tangential compliance exerts its force as if the track were registered to the wheel. That is, the track shoes will be fixed to locations of the wheel rim that are exactly one track shoe length apart for the uncompressed (zero displacement) compliance, as may be seen by examination of Equations 8, 9, and 10. When the compliant rim is compressed by track tension, the effective circumference is reduced, so that the wheel tends to "get ahead" of the track. However, upon initial contact of a shoe on the wheel, a powerful tangential force is suddenly exerted on each shoe and the wheel which forces the track to abruptly "catch up" to the position specified by Equation 10. This artifact of the present simulation would tend to increase the vibration exerted on the wheels and, therefore, results in exaggerated noise estimates. That the simulated wheel exerts a strong initial jerk on the track is confirmed by the positive "x" force shown upon initial impact, on Figures C-4a through C-18a. In many cases this horizontal jerk exceeds the vertical impact force.

6. The transfer functions are for purely radial forces, rather than for a combined tangential and radial force. In the actual vehicle, a horizontal, purely tangential force component at

the rim will cause both "x" and "y" radial forces to be exerted on the spindle due to the asymmetrical contact of the track on the side of the wheel. The change of sound level estimates due to this force coupling is unknown, but is thought to be small.

The averaged A-weighted sprocket noise predictions for 77,000, 36,000, 23,000 and 3,000 pounds per inch rim compliances which appear on Figure 44 of the main report were derived as follows: First, for track shoes three through six, the noise due to the "x" and "y" forces were summed on an energy basis for each 1/3 octave band to obtain an overall sprocket noise spectrum due to each shoe. Next, these three spectra were summed to obtain the average spectrum for each simulated rim compliance value. Finally, the spectra were A-weighted and summed.

The idler noise predictions were obtained by adjusting each horizontal and vertical third-octave band of sprocket noise. This accounts for the differences between the idler and sprocket force-to-noise transfer functions. The combining of noise due to the "x" and "y" forces and averaging between links was then carried out in the same way as for the sprocket. The validity of this procedure depends on the assumptions that the track engages the idler and the sprocket in a similar manner, that the slight difference in wheel diameters is not significant, and that the sprocket teeth do not affect the engagement dynamics. In Figure 43, the A-weighted sprocket noise level at 77,000 lb/inch is seen to be in excellent agreement with the measured sound level at 60,000 lb/inch. However, the predicted idler noise level at 77,000 lb/inch is 126 dB(A), which is 14 dB above the measured value of 112 dB(A) for the nominally 60,000 pound per inch standard idler. At the present, it is uncertain why this discrepancy is large compared to the excellent sprocket noise estimate. Possible reasons are that the force-to-noise transfer functions are incorrect and that the computer analysis requires further development.

Figures C-19 and C-20 present the predicted idler and sprocket noise spectra.

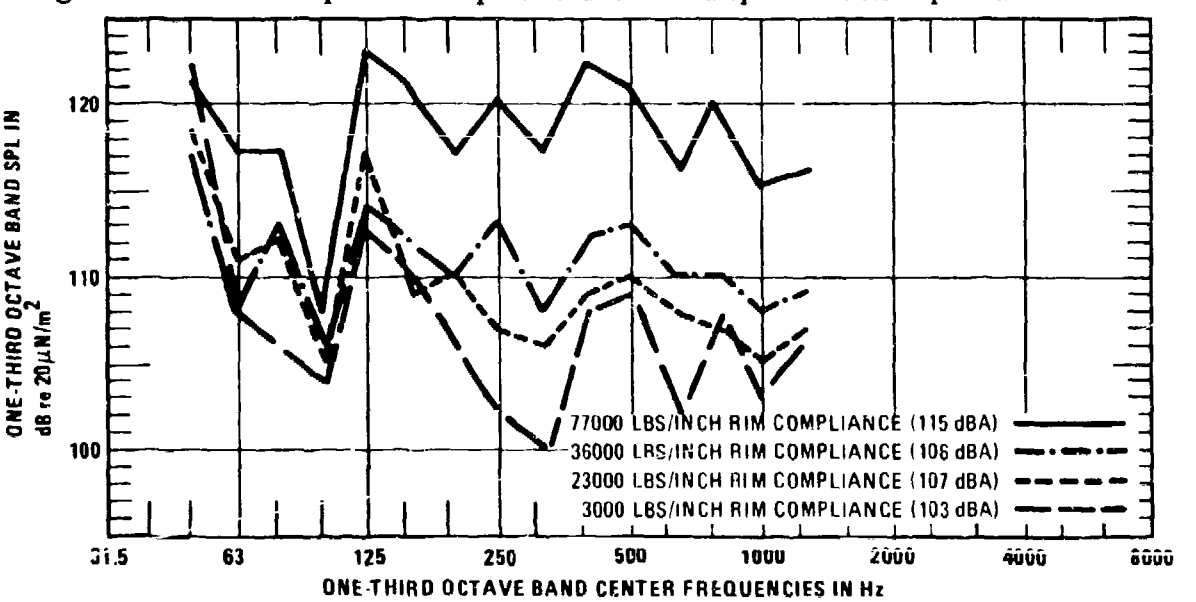

Figure C-19: Computer Estimate of Noise in the Crew Area Due to One Idler Wheel at 30 MPH

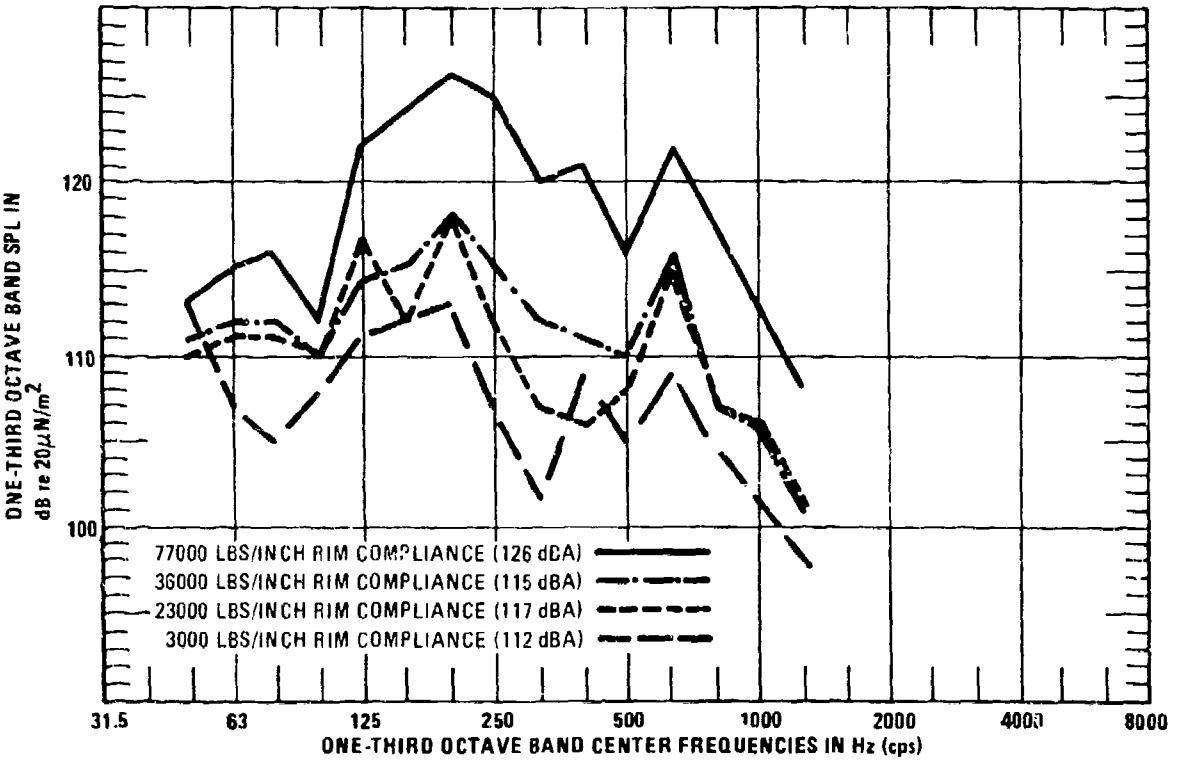

Figure C-20: Computer Estimate of Noise Spectra in the Crew Area Due to One Sprocket Wheel at 30 MPH

Significant trends that may be observed on these figures are that 1) the average noise reduction generally increased with softer rim compliance, 2) some noise reduction occurred for most frequencies, and 3) higher frequencies were reduced more than lower frequencies.

It may be expected that if damping were included in the model, development of steady-state behavior would be accelerated because reflected waves from the far end of the track would be damped. Improved analyses should take account of damping, should consider extended track action on both sides of the wheel, and should include improved descriptions of the track/wheel interaction.

REFERENCES

C-1. K. Symon, Mechanics, Addison Wesley, Chap. 9, 1960.

C-2. G. Fowles, Analytical Mechanics, Holt, Rinehart and Winston, Chap. 11.

C-3. M. Salvatori and M. Baron, Numerical Methods in Engineering, Prentice Hall, 1961, Sec. I and II.

C-4. D. Potter, Computational Physics, Wiley, 1973, Chap. II.

C-5. See Ref. 2, sec. 11.7, pp. 250-255.